# Mixing and In situ Product Removal in Micro-Gioreactors



Xiaonan LI

## Mixing and In-situ Product Removal in micro-bioreactors

#### **PROEFSCHRIFT**

ter verkrijging van de graad van doctor aan de Technische Universiteit Delft, op gezag van de Rector Magnificus, Prof. dr. ir. J. T. Fokkema, voorzitter van het College voor Promoties, in het openbaar te verdedigen op Maandag 8 Juni 2009 om 14:00 uur

door

#### Xiaonan LI

Designer in Bioprocess Engineering geboren te BeiJing, China

Dit proefschrift is goedgekeurd door de promotoren: **Prof. dr. ir. L. A. M. van der Wielen** 

Copromotor: Dr. ir. M. Ottens

#### Samenstelling promotiecommissie:

Rector MagnificusTechnische Universiteit Delft, voorzitterProf.dr.ir.L.A.M.van der Wielen Technische Universiteit Delft, promotorDr. ir. M. OttensTechnische Universiteit Delft, copromotor

**Prof. dr. ir. J.J.Heijnen** Technische Universiteit Delft

**Dr. M.H.M.Eppink** Synthon, Nijmegen

**Dr. ir. H.J.Noorman** DSM Anti-infectives, Delft

**Prof. dr. J.G.E.Gardeniers** Universiteit Twente

**Prof. dr. ir. M.T. Kreutzer** Technische Universiteit Delft

**Prof. dr. P.D.E.M. Verhaert** Technische Universiteit Delft, reservelid

The studies performed in this thesis were performed at the Bioseparation Technology section, Department of Biotechnology, Delft University of Technology. The research was financially supported by the Dutch Science Foundation (NWO) via the ACTS program IBOS (integration of Biosynthesis and Organic Synthesis), with financial contributions from NWO, DSM Anti-Infectives, Organon and Applikon.

ISBN: 978-90-9024339-9

To my mother and father, my families & shengbin

TIan Xing Jian Jun Zi Yi Zi Qiang Bu Xi

### **Contents**

Chapter 1 General introduction	1
Chapter 2  The use of recycle flows to improve mixing in micro bioreactors	29
Chapter 3  Application of direct fluid flow oscillations to improve mixing in micro bioreactors	67
Chapter 4  Quantitative determination of glucose transfer between cocurrent, laminar flowing water streams in H-shaped microchannel	105
Chapter 5 In-situ product removal in micro-bioreactor	129
Chapter 6 Outlook	153
Summary	163
Samenvatting	167
Curriculum vitae	171
Publications	173
Acknowledgements	177

# Chapter 1

**General Introduction** 

#### 1.1 Introduction

In the year 1919, a Hungarian agricultural Kark Ereky first coined the term "biotechnology" to cover the biology and technology as all the lines of work by which products are produced from raw materials with the aid of living organisms. (Bud, 1989; Ereky, 1919) But biotechnology's history is far longer than that. Archaeologists have found indications for the production of wine and soy bean sauce in Egypt and China at millennia BC respectively (Harris, 2007). Moreover, bakers's yeast was used for making bread from Ancient Egypt and at 6000BC in the Middle East people already used cow milk to make cheese. (Wikipedia, 2008a, Wikipedia, 2008b) Of course, nowadays, biotechnology is much more than production of food or beverages and also agricultural processes, biochemical, microbiological engineering and genetic manipulation. Especially for gene technology, it has become possible to modify genes, cells, or other living micro-organism to improve the production of both bulk and fine chemicals, such as fuel, bio based plastics, food flavoring compounds, antibiotics, vitamins, vaccine and therapeutic proteins; this has made biotechnology closely related to a wide range of fields in the modern life.

In all those applications, the cultivation of micro-organisms or cells plays a crucial role within the technologies. As it can be easily imagined, in order to establish the most suitable micro-organism in the optimized environment for a new process, enormous permutation of culture conditions will have to be evaluated to identify critical factors that turn the genes on. Following this, the identity of the proteins produced will have to be determined. (Kostov et al., 2001) Furthermore, for those existing processes, it normally required continuously improvement to remain competitive. The improvements / optimizations on the process are also based on large amount of experiments to reach sufficient data and preferable to be completed in short time. The cost of the development and improvement will take a significant fraction of the total cost of the production, and should be added to the product price to the market. (Harms et al., 2002) Clearly, the ability to culture cells efficiently in controlled environments is crucial to this venture. The use of high-throughput screening technologies is a possible solution; furthermore, the use of microbioreactors for high-throughput screening applications has the potential to both increase the process development rate and to reduce research cost.

#### 1.2 Microbioreactor Technology

#### 1.2.1 Micro-bioreactor definition

A micro-bioreactor is a reactor which combines small working volume and lab-scale (fed-) batch / chemostat bioreactor's working functions with integrated monitoring and controlling features. (Kumar, et. al., 2004) But it is more than a simply scaled-down lab-scale bioreactor; a micro-bioreactor has the unique possibilities comprising relatively fast mixing, sufficient heat transfer, sensitive and efficient reaction control, and simple parallelizing in principle allowing for environmentally friendly screening and production methods. (Ehrfeld et. al. 1999)

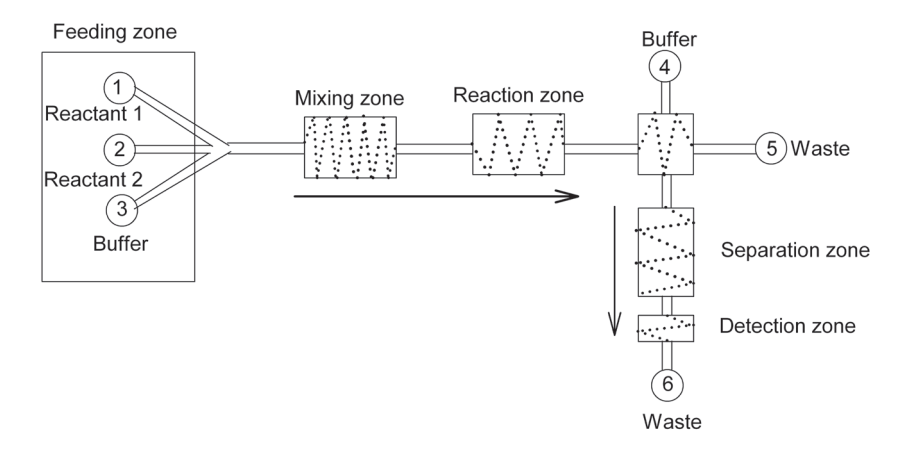


Figure 1-1 Illustration of microfluidic components in a typical lab-on-achip device

4

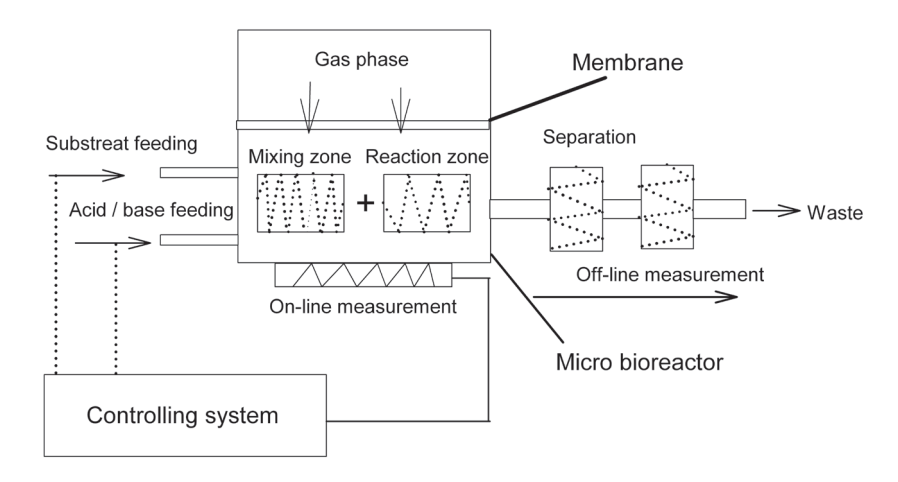


Figure 1-2 Illustration of a (fed)-batch micro-bioreactr integated with mixing, sensing and controlling system

Figure 1-1 presents a schematic illustration of a typical lab-on-a-chip. The system is consists a feeding zone, mixing zone, reaction zone, separation zone and analysis zone, and all five zones are placed in series. Figure 1-2 presents a schematic illustration of a (fed-) batch bioreactor with all necessary functions implemented. The feeding zone is connected with the reaction zone to supply substrates or pH regulation solutions to the rest of parts of the reactor. The mixing zone is placed within the reactor to provide adequate mixing and to enhance liquid / gas mass transfer. The analysis zone includes two parts, on-line measurement and off-line measurement. On-line measurement is an integration of different sensors to online monitoring relevant fermentation parameters like, pH, T, DO etc. Based on the measured value further control on substrates feeding and pH condition would be achieved. The measured values also would be used to analyze the fermentation result afterwards. However, because of the complexities of a fermentation processes, it is difficult to gain all related information from on-line measurement, thus, samples will be taken from reactor and purified in the separation zone and then measured off-line. In certain instance, it is possible to implement a separation zone within the reactor to continuously remove target by-product from the reactor to improve fermentation performance. If the integrated separation zone can selectively and quantitatively remove certain compound from the system, this separation zone also can be used as an online measurement sensor to monitor

the concentration profile of the certain compound.

#### 1.2.2 Micro-bioreactor applications

A micro-bioreactor has the potential to be parallelized and integrated within a high-throughput system. Thus, the arrays of micro-bioreactors would be valuable to gain better quality information both faster and cheaper. (Ratledge, et al., 2006) If the development of a single micro-bioreactor is successful, it is possible to simultaneously screen various microorganism cultivation processes under conditions more similar to the final industrial process for strains selection; (Micheletti et al., 2006) it is possible to simultaneously screen the same microorganism with different feeding strategies / in varies media to optimize growth conditions; (Doig et al., 2005b) it is possible to integrate with a controllable feeding system and separation system to help the development of a new process or improvement of the exiting process; (Roberge et. al., 2005; Chovan et al.,2002) it is possible to be used in other cells cultivation related fields, such as single cell biologic studies, gene mutation studies or metabolic engineering studies (Boettner et al., 2002; Boccazzi et al., 2005b) to save the laborious and time consuming research.

## 1.2.3 Recent developments on miniaturized and parallelized bioreactors for high-throughput cell cultivation

In the last decades, there has been a growing interest in developing minute "laboratories on a chip" and micro-chemical reactors which are able to perform chemical and biological experiments and analysis at a small scale. (Yi et. al., 2003) Many research groups have explored the possibility of developing a micro-bioreactor, which can be used for the cultivation of micro-organism, with working volume of a few millilitres to nanolitres. Several review articles have given a clear overview on this rapidly progressing field of micro-bioreactor development. (Lye et. al. 2003; Kumar, et. al. 2004; Micheletti et. al. 2006; Betts et. al. 2006; Fernandes et.al., 2006; Van Leeuwen, 2008; Titchener-Hooker et al., 2008) In this part of the thesis, we will briefly discuss several interesting results that have been reported in recent literature about the present development results and future possibility on this topic.

The research group of professor Rao in the University of Maryland pioneered the field of micro-bioreactor development with a cuvette-based batch micro-bioreactor for Escherichia coli cultivation with working volume 2 ml. (Kostov et al. 2001) Optical sensors for monitoring pH, the dissolved oxygen concentration (DO) and the optical density (OD) were implemented. Small stirrer and sparger was installed in the bioreactor to improve mixing, however, the liquid side mass transfer coefficient (KLa) value in the micro-bioreactor was reported to be only 27.5 h<sup>-1</sup>. This micro-bioreactor was later be parallelized to a 24-well plate. (Kostov, et al. 2001; Harms, et al. 2004; Harms, et al. 2006)

At the Massachusetts Institute of Technology (MIT) professor Sinskey and Professor Jensen's groups, investigated scaled down bioreactors for Escherichia coli fermentations with working volume 5, 50, 80, 150 µl were reported. Optical sensors for online monitoring pH, dissolved oxygen concentration (DO) and optical density of biomass (OD) were implemented in the reactor. For the smallest micro-bioreactor with working volume 5 µl and 50 µl, reactor height 300 µm. Oxygen supply was only based on diffusion via a PDMS membrane, which resulted a k<sub>i</sub>a value around 60 h<sup>-1</sup>. No mixing unit was implemented. Reactors were operated as batch reactors. Glucose, acetate, formate and lactate profiles were measured off-line. Then Zhang et al. (2003, 2005, 2006a, 2006b and 2007) increase the working volume of a similar micro-bioreactor up to 80 μl and 150 μl for accommodating better sampling possibilities and integrated a magnetic stirrer bar into the reactor to give a better fluid mixing and better gas / liquid mass transfer capability. PH condition in the reactor was controlled. Reactors were operated as fed batch reactor (Zhang, et al. 2003), batch reactor (Zhang, et al. 2006a; Szita, et al. 2005) and Chemostat (Zhang, et al. 2006b and 2007). With vigorous stirring created by small magnetic stirrer at 800 rpm, KLa value increased to 75 h<sup>-1</sup>. Zhang et al. also utilized an array of four 80 μl fed-batch and continuous microbioreactor for E coli growth.

At the University College London (UCL) the research group of professor Baganz developed three different microplates (24-, 96- and 384-wells) with working volume 65  $\mu$ l and 1,182  $\mu$ l to grow Bacillus subtilis. All these batch bioreactor arrays have a same diameter equal to the diameter of a single well of a standard 24-well plate. Air sparging mixing technique was tested in a prototype reactor with working volume 2 ml, good mixing results were obtained with KLa value up to 220 h<sup>-1</sup>. Optical sensors for pH, DO and optical

density were used but only for a larger reactor (6 ml, 7 ml) with stirrer mixing and shaken mixing. (Doig et al. 2005a; Doig et al., 2005b; Doig et al. 2005c)

The smallest bioreactor in the literature was developed by professor Quake's group at the California institute of Technology. (Balagadde et al. 2005a; Balagadde et al. 2005b) They demonstrated a 16 nl micro-chemostat on a chip to monitor a long-term bacteria growth. The reactor was comprised of a circular tube with integrated peristaltic pumps and a series of micromechanical valves to add medium, remove waste and recover the cells. However, due to limitation of the current analytical technology development, it is too small to be sampled and to be measured. Thus, the usage of the reactor is limited.

Various groups and companies have developed different micro-bioreactor arrays with larger working volume up to hundreds mililitres. (Reis, et al., 2006; Weuster-Botz, et al. 2002; Weuster-Botz, et al. 2005; Knorr, et al. 2007; Van Leeuwen 2008) Here, we will not introduce them one by one. Just to sum it up, there is a rapid progress in development and commercialization on miniaturized bioreactors. Most of fed-batch microbioreactors have the working volume between tens to hundreds milliliters. Smaller scale (microliter) reactors are mainly operated as batch reactor. Optical sensors for pH, DO and OD are the most commonly used sensors for online monitoring. However, most of the current successful applications on optical sensors were around pH 7 for E. coli cultivation. The lower pH condition, like, pH 4 - 5, is not in the working range of the optodes. (Van Leeuwen, 2008) Kuznetsova et al. have established the idea of applying of ultrasonic piezoceramic devices as biosensors in microscale, but no testing result combined with micro-organism cultivation was reported. (Kuznetsova, et al., 2007) Integrated electronic sensors for pH, DO, temperature and biomass concentration was reported by Krommenhoek et al. (Krommenhoek, 2007; Krommenhoek et al., 2008) Van Leeuwen et al. tested the integrated electronic sensors with a fed-batch micro-bioreactor (150 μl) for cultivation of Saccharomyces cerevisae. (Krommenhoek, 2007; Van Leeuwen, 2008) Furthermore, shaking and stirring are the most commonly used mixing methods for micro-bioreactors. However, the oxygen transfer ability is still a bottleneck for high-concentration micro-organism cultivation, especially for reactors with working volumes under hundreds microliters. Thus, much work remains to be done on the development of mixing method for a micro-bioreactor, and there are opportunities for other developments related with micro-bioreactors, e.g. the development of integrated in-situ

product recovery (ISPR) method, the development of integrated pumps and valves, the development of analytical tools for small amount of samples, still need to be further explored.

#### 1.2.4 Recent development in micro-mixing technology

Mixing is an important component in a microfluidic system for a variety of applications, For instance, biological processes such as cell activation, enzyme reactions and protein folding commonly involve reactions which require the mixing of reactants for initiation and fast processing; (Pennemann et al., 2004; Urban et al., 2006) some chemical reactions require rapidly homogenized solution of varies reagents to ensure maximum productivity; (Holladay et al. 2004; Wilms et al. 2008) a long-term high concentration micro-organism cultivation requires vigorous mixing to increase the mass transfer between liquid / gas phases to avoid insufficient oxygen supply and the switching between aerobic / anaerobic metabolisms. The importance of micro-mixing technologies started to be recognized in recent years and several research groups are focusing on this area. In this part of the thesis, the development of the micro-mixer is briefly reviewed and discussed to give a comprehensive view on the current micro-mixing method development, the trends and the problem areas of combining the mixing method to micro-bioreactor.

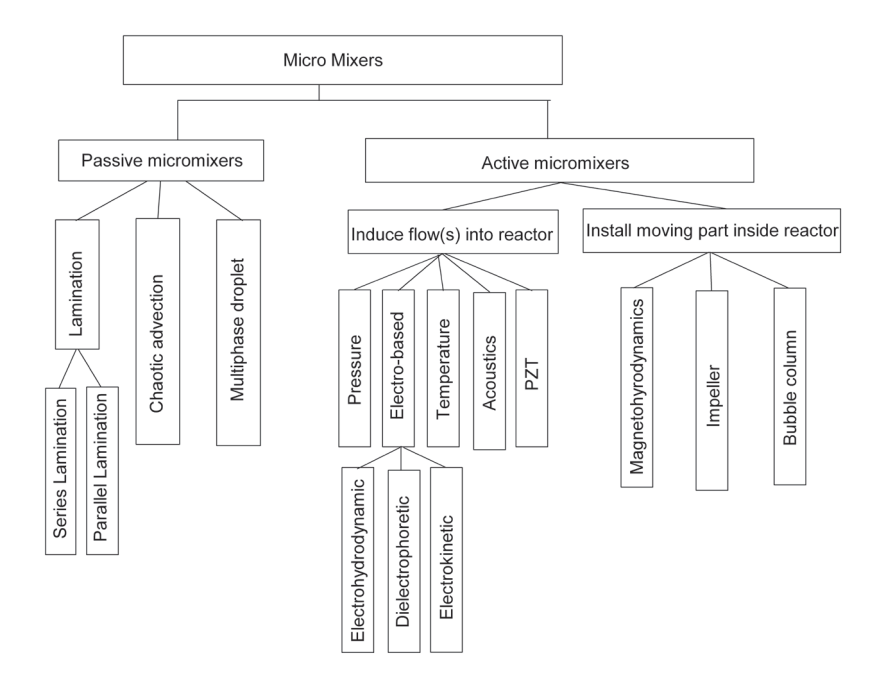


Figure 1-3 Categorization of Micro mixers

In general, micromixers can be categorized as passive micromixers and active micromixers as shown in Figure 1-3. Passive micromixers are the mixers that do not require external energy input except the mechanism used to drive fluid flow at a constant rate while the mixing mechanism relies on diffusion or advection. Passive micromixers can be further categorized as Lamination (series and parallel), chaotic advection and multiphase droplets. Active micromixers use external energy to create mixing, the active micromixers can be categorized as induced flow(s) driven by external sources and installed moving parts inside the reactor. The active micromixers also can be categorized by the types of external energy such as pressure, electrobased, temperature, acoustics, piezoelectric lead-zirconate-titanate (PZT) and magnetohyrodynamics. (Kakuta et al., 2001; Benz et al. 2001; Nguyen et al., 2005; Hessel et al., 2005)

Because of the simple concept, the passive micromixer was one of the first microfluidic devices which were reported by many research groups. Passive micromixer mainly relies on molecular diffusion and advection. Thus, in order to achieve better mixing, passive micromixers normally increase the contact area between different fluids and decrease the diffusion path between different fluids to improve molecular diffusion. Chaotic advection can occur either by complicating the micro channel structure or placing microstructured objects within the micro channel to create two-dimensional unsteady velocity fields or by three-dimensional unsteady velocity with or without time-dependence.

The basic design for a passive micromixer is a long micro channel with two inlets to its geometry; these designs are often called the T-mixer and Y-mixer. For parallel lamination mixers, is to split the inlet streams into multiple streams and then reunifying them to allowing faster molecular diffusion, for example, Bessoth et al. reported a parallel lamination mixer with 32 streams that can achieve full mixing in 15 ms. (Bessoth et al. 1999; Hinsmann et al., 2001; Kölbl et al., 2008) For series lamination mixers, also called split and recombine mixer (SAR), basically three steps are required, flow splitting, flow recombination and flow rearrangement to create multi-streams. (Schwesinger et al., 1996; Liu et al. 2000; Löwe et al., 2000; Yamaguchi et al., 2004) The basic idea of chaotic convection mixers is the modification of the channel shape for splitting, stretching, folding and breaking of the flow. The first publications on chaotic advection by micromixers rely on placing microsturectured objects within the flow passage on one side of the microchannels. (Stroock et al., 2002a; 2002b) By this means, flow circulations are generated which lead to an exponential increase of specific interface, hence to accelerate mixing. After that, more works have been done in this area to design the micromixers to be used for varies applications under different ranges of Reynolds number. (Jen et al., 2003; Kim et al., 2003; Chung et al., 2004; Melin et al., 2004; Hong et al., 2004; Schönfeld et al., 2004; Aubin et al., 2005; Howell et al., 2005; Kim et al., 2005) Another solution to improve the mixing for passive micromixers is to form droplets of the mixed liquid. The surface tension between the two phases and the movement of the droplet causes an internal fluid field and make mixing inside the droplet possible. (Paik et al., 2003; Tice, et al., 2003)

All reviewed passive micromixers can achieve good mixing in short time without an external actuator needed. However, the complex structure of the micro channel increases the manufacturing and construction cost and causes problems on cleaning. Furthermore, the dimensions of the micro channel have

significant influence on the mixing performance; the limited volume of the micro channel (nanoliter) increases the difficulty to create sufficient mixing for a microreactor with working volume of hundreds microliter. Therefore, for the development of a micro-bioreactor with a working volume of hundreds microliter, more attention is given to active micromixing technologies.

Active micromixers do require an external power source to create force fields, either directly working on the fluids or working on the integrated moving components, to induce advection or even turbulence in the micro device. The integration of the external power resource and the corresponding components in a microfluidic system is both challenging and expensive. However, using active micromixers for mixing in small volumes may have advantages over applying complying complex device manufacturing and construction techniques, as it has more flexibility to work on various scale devices and it is easier to be computer controlled and adjusted. Recent results about the development of active micromixers have been reported in the literatures. (Nguyen et al., 2005; Hessel et al., 2005)

The most commonly used mixing methods on milliliter scale operations are shake flasks, (Klein et al., 2005; Micheletti et al., 2006; Dasgip, 2008) magnetic stirrers (Kostov, et al. 2001) and impellers (Harms, et al. 2004; Weuster-Botz, et al. 2002; Weuster-Botz, et al. 2005). The use of a bubble column for microorganism cultivation was reported by Doig et al., 2005a, 2005b and 2005c) The most straightforward way to develop a suitable mixing method for a small bioreactor with working volume tens to hundreds microliters is to directly scale down the present mixing device. Zhang et al. developed microbioreactor (80 μl) with integrated magnetic stirrer as the mixing device; Presense developed various microbioreactors with working volume 100-200 μl, using shake flasks to provide mixing. (Zhang et al., 2003; 2006a; 2006b; 2007; Presense, 2008) However, Van Leeuwen showed that unless under really violent mixing conditions, (shaking frequencies >1000rpm or stirrer speed >1000rpm) the mixing in the micro-scale devices (hundreds microliter) is not strong enough to provide sufficient oxygen mass transfer for high-density cultivation. That is due to the fact that forces, like surface tension, which normally can be neglected for larger scale liquid mixing, become important in miniaturized system. (Hermann et al., 2003; Van Leeuwen et al. 2008)

More active micromixers were developed based on different external

disturbance effects. Deshmukh et al. reported a T-mixer with pressure disturbance. An integrated planar micropump connects with one of the inlets of the T-mixer, drives and stops the flow in the mixing channel to divide the liquid into serial segments and make the mixing process independent of convection. (Deshmukh et al., 2001; Glasgow et al., 2003) Based on the same idea, but using a more complex structure (serial T-mixers), Niu and Lee demonstrated an active micromixer using pressure as driven force to generate chaotic mixing in micro channel. (Niu et al., 2003) With partly similar design, instead of pressure sources, electrohydrodynamic disturbance, (Tsouris et al., 2003; EI Moctar et al., 2003) dielectrophoretic disturbance (Deval et al., 2002), electrokinetic disturbance (Lettieri et al., 2000) and temperature disturbance (Siddheshwar et al., 1998; Tsai et al., 2002) were used to generate chaotic advection along the micro channel. Active micromixer also can be used for a system larger than microfluidic channel. For instance, Liu et al. demonstrated successful mixing in a micro-chamber (300 µm depth, 15 mm diameter) with shaking air bubbles as actuator. Air bubbles were energized by an acoustic field. (Liu et al., 2002; 2003) Several other actuators for inducing mixing in a micro-chamber were reported in recent literature, including, ultrasonic wave induction (Monnier et al., 1999), pneumatically actuator (Lee et al., 2006), magnetostrictive thin film, (Quandt et al., 1996) piezoelectric lead-zirconatetitanate actuator (PZT) (Zhen et al., 2001) and pressure driven hydrodynamic actuator. (Tabeling, et. al., 2004; Li et al., 2008a; 2008b)

Different micormixing methods are applicable for different cases; there is no mixing method that can be used for every applications. For instance, electro-based mixing methods are easy to be controlled and parallelized but normally require certain ions concentration in the solution to accomplish sufficient advection; static mixers give rapid mixing but always need complex structures and are difficult to be integrated in a batch reactor; magnetic stirrer bar and shaking flasks are widely used in varies scales of experiments, but for micro-scale (microlitres or less) become problematic, when sensors are introduced and it becomes hard to provide sufficient oxygen mass transfer; bubble columns can solve the oxygen mass transfer problem but give rise to the question about liquid evaporation; ultrasonic waves may kill the cell, PZT requires large surface area around the reactor to create enough shaking; temperature actuator (Rayleigh-Bénard convection) does not need a large area for heating or cooling the surface but the large temperature difference may influence the behavior of the micro-organism; hydrodynamic actuators seem

good for bio-applications but always suffer from the dead-zone.. Therefore, experiments need to be done in order to validate the most suitable mixing method for a certain application. Moreover, computational fluidic dynamic (CFD) simulation has been proved and pervasively used as an important tool to accelerate and simplify the design of the micro-device.

## 1.3 COMPUTATIONAL FLUID DYNAMICS (CFD) SIMULATION

Computational fluid dynamics (CFD) was originally developed from the pioneer accomplishment of scientists such as Richardson (1910) and Courant, Friedrichs and Lewy (1928), who in their work to procure insight into fluid motion instigated the development of powerful numerical techniques that have advanced the numerical description of all types of fluid flow (Shang et al., 2004; Norton et al., 2006) In the last two decades coupled with the rapid development of computer performance, vast improvements in numerical algorithms the CFD modeling techniques were achieved. CFD is now growing into a powerful and pervasive tool in many industries, with each solution representing a rich tapestry of mathematical physics, numerical methods, user interfaces and state of the art visualization techniques. (Xia et al., 2002)

Several commercial software packages, like CFX, FLUENT, COMSOL and PHOENICS, are available. Many researchers have used those softwares to design or to predict the fluid dynamic behavior with a complex geometry on a micro device. The Navier-Stokes equations, which describe how the velocity, pressure, temperature and density of a moving fluid are related and include the effects of viscosity on the flow, are shown in Equation 1 (a, b) and are the preferable option for solving fluid-based applications in many cases, like reactor design and improvement. (Hutmacher & Singh, 2008; Kelly, 2008)

$$\rho \frac{\partial U}{\partial t} - \nabla \cdot \left[ \eta \cdot \left( \nabla U + (\nabla U)^T \right) \right] + \rho U \cdot \nabla U + \nabla P = F$$
 Equation 1 a

$$\nabla \cdot U = 0$$
 Equation 1 b

In the above equations,  $\eta$  denotes the dynamic viscosity of the solution (kg m<sup>-1</sup> s<sup>-1</sup>), U denotes the velocity vector (m s<sup>-1</sup>),  $\rho$  denotes the density (kg m<sup>-3</sup>), P is the pressure (Pa), F denotes the selected volume force field (i.e. gravity), which influences the velocity field, (N m<sup>-3</sup>).

Friedrich reported that the Navier-Stokes equations can be solved directly for laminar flows, however, for the current state of computational capability is difficult to resolve the fluid motion in the Kolmogorov microscales associated with turbulent flow regimes. (Fredrich et al., 2001) For most of micro-devices, the fluid on the device is in low Reynolds number range (<100), mixing in a micro fluidic system is typically dominated by diffusion rather than turbulence, hence, the N-S equations can be directly used in CFD simulations.

#### 1.4 AIM OF THE THESIS

In 2003, a large cluster project was formed between DSM, Organon, Applikon and two university groups (TU Delft and University of Twente), under the ACTS and IBOS program. The aim of this cluster project was to develop a system consisting of parallel bioreactors of 30 to 200 µl working volume for the cultivation of micro-organisms under well controlled industrially relevant condition (T, pH, DO etc.), and operated as fed-batch reactor in long term (>200h). This platform has the potential to be used for high throughput screening applications for gene identification or the related small scale protein fermentation to increase the protein production process development rate and to reduce the research cost.

The development of the platform starts with the design of a single micro-reactor; the single micro-reactor is the integration of well developed sensing system, control system, mixing system and other accessories, like, pumps, valves, adaptors, vessels etc.; all involved components play important roles. Some components are commercial available, but many components are not available or not suitable for our application.

The work described in this thesis aims at development of a suitable mixing method, which can provide sufficient mixing in a micro-reactor to satisfy the

need of micro-organism fermentation. Furthermore, microfluidic components are important to facilitate substrate feeding as well as by product removing. An ISPR concept was experimentally demonstrated in this thesis to distinguish a wider scope of micro-reactor applications.

#### 1.5 STRATEGY AND SCOPE OF THE THESIS

The research aim is to develop a fed batch micro-bireactor for cultivation of microorganism. This pre-defines, though not strictly, the development of mixing method and ISPR method in this study to be easily integrated to a micro-reactor and be suitable for cell cultivation. Instead of directly using a growing-cell system in a complete micro-bioreactor that has all the complexities of aseptic experimentation, dye solution distribution (none cell) was used to experimentally test the mixing behavior of selected methods, lactic acid extraction (none cell) was used to test ISPR possibility, resting cells were used to test the settling issue and CFD simulation was applied to verify the scenarios of cell growth. Once the working concepts have been established with all individual parts without cells or resting cells, cultivation of the cells will be included in an integrated microreactor.

A general introduction explaining the scope and the research aim of the project has been given in chapter 1. In this chapter we also briefly reviewed the development of the micro-reactor in recent years, especially for the development of micro-mixing technologies.

As discussed previously, one of the main reasons to apply micro systems technology is that compared with traditional reaction (fermentation) technologies, a superior, rapid and sufficient mixing can easily be achieved using micro technologies, especially for those microfluidic devices, which integrated with passive micro structures, with working volume tens of nanoliters. The superior mixing characteristics of micro-reactors leads to more efficient mass and heat transfer, which otherwise may be a bottleneck in certain processes. Chapter 2 and chapter 3 describe the development and testing of different micromixing methods. In chapter 2, recycle flow mixing (RFM) method was presented. By continuously moving liquid solution from high oxygen concentration area to low oxygen concentration area via multiple

fluxes, the system obtains maximum oxygen transfer, which is considered as the bottleneck for high cell density fermentation. Meanwhile, the recycled flows create vigorous convection in the micro-reactor and obtain good mixing. The mixing performance was experimentally verified. The impact of various oxygen transfer abilities on high cell density fermentation was estimated by CFD simulations. The mixing performance of RFM method is dependent on the strength of the recycle fluxes, therefore, a strong internal micro-pump plays essential role in the system.

To avoid the dependence on the micro-pump development, an alternative micro-mixing method is presented in chapter 3. Oscillation flows, which are created by a central actuator, induce vigorous convection in the micro-reactor(s) to obtain good mixing. The mixing performance within a single reactor was estimated by CFD calculations and validated experimentally. The oscillation mixing method has the potential to be easily integrated with parallel reactors. This concept has been proven experimentally using a 96-wells micro titer plate and one oscillation pump. Additional experiments have been done with oscillation mixing method to test the influence of the mixing methods on cells viability and influence of the oscillation mixing method on cells suspension.

The characteristics of microfluidic channels for mass transfer were explored in chapter 4. When two liquid streams join into one microchannel with diameter around 150  $\mu$ m, both streams will behave as laminar flows and run parallel to each other with a stable interface in between. If for certain components there are concentration differences between two streams, over the interface, components can transfer from one stream to another via diffusion. In this chapter the quantitative transfer of glucose between two cocurrent streams was estimated by CFD and experimentally verified. A microchannel has a large surface to volume ratio; therefore, within a short time significant amount of glucose can be transferred from one stream to another.

Chapter 5 focuses on demonstrating the feasibility of applying a suitable ISPR method on micro-scale bioreactor. Lactic acid was selected as the target chemical. Extraction was selected as the separation method. By pushing a selected extractant (trioctylamine / decanol / dodecane) through a hydrophobic micro hollow fiber, lactic acid is extracted from the aqueous phase into organic phase, and then removed from the microreactor. The micro hollow fiber has

the sole task to be the barrier to isolate microorganism from organic phase. The extraction ability was estimated by model and then validated experimentally.

Finally, a general outlook on the different aspects and possibilities of development of mixing and ISPR for a micro bioreactor is given in chapter 6.

#### References

- Aubin, J., D.F. Fletcher, and C. Xuereb (2005) Design of micromixers using CFD modeling, Chemical engineering science, 60, 2503-2516
- Balagaddé, Frederick K., Lingchong You, Carl L. Hansen, Frances H. Arnold, Stephen R. Quake, (2005a) Long-Term Monitoring of Bacteria Undergoing Programmed Population Control in a Microchemostat, Science, 309 (5731) 137-140
- Balagaddé, Frederick K., Carl L. Hansen, E. Kartalov and Stephen R. Quake, (2005b) Microfluidc chemostat, WO 2005/069980
- Benz, K., K.-P. Jäckel, K.-J. Regenauer, J. Schiewe, K. Drese, W. Ehrfeld, V. Hessel, and H. Löwe, (2001) Utilization of micromixers for extraction processes, Chemical engineering Technology, 24 (1) 11-17
- Bessoth, F.G., A.J. de Mello and A. Manz, (1999) Microstructure for efficient continuous flow mixing, Anal. Commun., 36, 213-215
- Betts, J.I. and Baganz F. (2006) Miniature bioreactors: current practices and future opportunities Microbio cell Fact 5 (21) 1-14
- Boccazzi, P., A.Y. Chen, K.F. Jensen, N. Szita, A. Zanzotto and Z. Zhang, (2005a) Apparatus and methods for simultaneous operation of miniaturized reactors. WO 2005/097969.
- Boccazzi, P., A. Zanzotto, N. Szita, S. Bhattacharya, K.F. Jensen and A. J. Sinskey, (2005b) Gene expression analysis of Escherichia Coli grown in miniaturized bioreactor platforms for high-throughput analysis of growth and genomic data, Appl. Microbiol. Biotech., 68 (4) 518-532
- Boettner, M., B. Prinz, C. Holz, U. Stah, and C. Lang, (2002) High-throughput screening for expression of heterologous proteins in the yeast Pichia pastoris, Journal Biotechnol., 99, 51-62
- Bud R. (1989) Biotechnology Nature 337, (10)
- Chován, T. and András Guttman, (2002) Microfabricated devices in biotechnology and

- biochemical processing, Trends in Biotechnology, 20 (3) 116-122
- Chung, Y.-C., Y.-L. Hsu, C.-P. Jen, M.-C. Lu and Y.C. Lin, (2004) Design of passive mixers utilizing microfluidic self-circulation in the mixing chamber
- Dasgip A.G., Jülich, Germany, http://www.deagip.de, (2008)
- Deshmukh, A.A., D. Liepmann and A.P. Pisano, (2001) Characterization of a micromixing, pumping, and valving system, Proc. Transducer'01, 11th Int. Cofe. On Solid-State sensors and actuators, Munich, Germany, 779-782
- Deval, J., P. Tabeling and C.M. Ho, (2002) A dielectrophoretic chaotic mixer, Proc. MEMS'02, 15th IEEE Int., Micro electromechanical system, Las Vegas, Nevada, 36-39
- Doig, Steven D., Samuel C. R. Pickering, Gary J. Lye, Frank Baganz, (2005a), Modeling surface aeration rates in shaken microtitre plates using dimensionless groups, Chemical Engineering Science, 60, 2741-2750
- Doig, Steven D., Anh Diep and Frank Baganz, (2005b) Characterization of a novel miniaturized bubble column bioreactor for high throughput cell cultivation, Biochemical Engineering Journal, 23 (2) 97-105
- Doig, Steven D., Ortiz-Ochoa K., Ward J.M. and Frank Baganz, (2005c) Characterization of oxygen transfer in miniature and lab-scale bubble column bioreactors and comparison of microbial growth performance based on constant kLa , Biotechnology Progress, 21 (4) 1175-1182
- EI Moctar, A.O., N. Aubry and J. Batton, (2003) Electrohydrodynamic microfluidic mixer, Lab on a chip, 3, 273-280
- Ereky K. (1919) Biotechnologie der Fleisch-, Fettund Milcherzeugung im landwirtschaftlichen Grossbetrieb, Berlin: Paul Parey
- Ehrfeld W., Klaus Golbig, Volker Hessel, Holger Lowe and Thomas Richter, (1999).

  Characterization of Mixing in Micro mixers by a Test Reaction: Single Mixing
  Units and Mixer Arrays, Ind. Eng. Chem. Res. 38, 1075-1082

- Fernandes, P. and J.M.S. Cabral, (2006) Microlitre/milliliter shaken bioreactors in fermentative and biotransformation processes a review, Biocatalysis and Biotransformation, 24 (4) 237-252
- Friedrich, R., T.J. Hutti, M. Manhart and C. Wagner, (2001) Direct numerical simulation of incompreible turbulent flows, Computers and fluids, 30, 555-579
- Glasgow, I. and N. Aubry, (2003) Enhancement of microfluidic mixing using time pulsing, Lab on a chip, 3, 114-120
- Harms P., Y. Kostov, and Govind Rao, (2002) Bioprocess monitoring Curr. Opin. Biotechnol., 13 (2) 124-127
- Harms, P., (2004) Parallel miniature bioreactors in twenty-four well plate. Ph.D, Thesis, University of Maryland, 3
- Harms P., Y. Kostov, J.A. French, M. Soliman, M. Anjanappa, A. Ram, and G. Rao (2006)

  Design and performance of a 24-station high throughput microbioreactor

  Biotechnology and Bioengineering, 93 (1) 6-13
- Harris D. (2007) Transcriptomics and quantitative physiology of  $\beta$ -lactam-producing Penicillium chrysogenum, Ph.D. Thesis
- Hellel, V., H. Löwe and F. Schönfeld, (2005) Micromixers a review on passice and active mixing principles, Chemical engineering science, 60, 2479-2501
- Hermann, R., M. Lehmann and J. Büchs, (2003) Characterization of gas-liquid mass transfer phenomena in microtiter plates, Biotechnology and bioengineering, 81 (2) 178-186
- Hinsmann, P., J. Frank, P. Svasek, M. Harasek and B. Lendl, (2001) Design, simulation and application of a new micromixing device for time resolved infrared sprctroscopy of chemical reaction sin solution, Lab on a chip, 1, 16-21
- Holladay, J.D., Yong Wang, and Evan Jones, (2004) Review of developments in portable hydrogen production using microreactor technology, Chemical Review, 104, 4767-4790

- Hong C.C., Choi, J.W., Ahn, C.H., (2004). A novel in-plane passive microfluidic mixer with modified Tesla structures, Lab on a Chip, 4, 109 –113
- Howell, P.B., D.R. Mott, S. Fertig, C.R. Kaplan, J. P. Golden, E.S. Oran and F.S. Ligler, (2005) A microfluidic mixer with grooves placed on the top and bottom of the channel, Lab on a chip, 5, 524-530

http://en.wikipedia.org/wiki/cheese, (2008a)

http://en.wikipedia.org/wiki/baker's yeast (2008b)

- Hutmacher, D.W. and H. Singh, (2008) Computational fluid dynamics for improved bioreactor design and 3D culture, Trends in Biotechnology, 26 (4) 166-172
- Jen et al., (2003) Design and simulation of the micromixer with chaotic advection in twisted microchannel, Lab on a chip, 3, 77-81
- Kakuta, M., F.G. Bessoth and A. Manz, (2001) Microfabricated devices for fluid mixing and their application for chemical synthesis, Chem. Rec., 1, 395-405
- Kelly, W.J., (2008) Using computational fluid dynamics to characterize and imnprove bioreactor performance, Biotechnol. Appl. Biochem., 49, 225-238
- Kirner T., J. Albert, M. Gunther, G. Mayer, K. Reinhackel and J. M. Kohler, (2003).

  Static micro mixers for modular chip reactor arrangements in two-step reactions and photochemical activated processes, Book of Abstracts: IMRET 7th International Conference on Micro reaction Technology, Lausanne, Switzerland 101-105
- Kim, D.S., S.W. Lee, T.H. Kwon and S.S. Lee, (2003) Barrier embedded chaotic micromixer, IEEE, The Sixteenth Annual International Conference on Micro Electro Mechanical Systems, Kyoto, Japan, 19–23
- Kim, D.S., S.H. Lee, T.H. Kwon and C.H. Ahn, (2005) A serpentine laminating micromixer combining splitting/recombination and advection, Lab on a chip, 5, 739-747
- Knorr, B., H. Schlieker, H.P. Hohmann and D. Weuster-Botz, (2007) Scale-down and

- parallel operation of the riboflavin production process with Bacillus subtilis, Biochemical Engineering Journal, 33 (3) 263-274
- Kölbl, A., M. Kraut and K. Schubert, (2008) The iodide iodate method to characterize microstructured mixing devices, AICHE Journal, 54 (3) 639-645
- Kostov, Y., Peter Harms, Lisa Randers-Eichhorn and Govind Rao, (2001) Low-Cost Microbioreactor for High-Throughput Bioprocessing, Biotechnology and Bioengineering, 72 (3) 346-352
- Krommenhoek, E.E., Michiel van Leeuwen, Han Gardeniers, Walter M. van Gulik, Albert van den Berg, Xiaonan Li, Marcel Ottens, Luuk A.M. van der Wielen, Joseph J. Heijnen, (2008), Lab-scale fermentation tests of micro chip with integrated electrochemical sensors for pH, temperature, dissolved oxygen and viable biomass concentration, Biotechnology and Bioengineering, 99 (4) 884–892
- Krommenhoek, Erik, (2007), Integrated electrochemical sensor array for on-line monitoring micro bioreactors, PhD thesis University Twente
- Kumar S., C. Wittmann, and E. Heizale, (2004) Minibioreactors, Biotechnology letter, 26 (1) 1-10
- Kuzenetsova, L.A., and W. Terence Coakley, (2007) Application of ultrasound streaming and radiation force in biosensors, Biosensors and bioelectronics, 22, 1567-1577
- Lee, H.L.T., P. Boccazzi, R.J. Ram and A.J. Sinskey, (2006) Microbioreactor arrays with integrated mixers and fluid injectors for high-throughput experimentation with pH and dissolved oxygen control, Lab on a chip, 6 (9) 1229-1235
- Lettieri, G.L., et al., (2000)Consequences of opposing electrokinetically and pressreinduced flows in microchannels of varying geometries, Proc. Micro total analysis systems, Enschede, NL, 351-354
- Li, X, G. van der Steen, G.W.K. van Dedem, L.A.M. van der Wielen, M. van Leeuwen, W.M. van Gulik, J.J. Heijnen, E.E. Krommenhoek, J.G.E. Gardeniers, A. van den Berg and M. Ottens, (2008a), Improving mixing in micro bioreactors,

- accepted for Chem Eng. Sci. doi:10.1016/j.ces.2008.02.036
- Li, X., L.A.M. van der Wielen, G. van der Steen, G.W.K. van Dedem, van M. Leeuwen, W.M. van Gulik, J.J. Heijnen, J.G.E. Gardeniers, E.E. Krommenhoek, A. van den Berg,, M. Ottens, (2008b). The application of direct oscillations to improve mixing in micro bioreactors, AICHE, submitted for publication
- Liu, R.H., Stremler, M.A., Sharp, K.V., Olsen, M.G., Santiago, J.G., Adrian, R.J., Aref, H., Beebe, D. J., (2000). Passive Mixing in a Three-Dimensional Serpentine Micro-channel, Journal of Micro-electromechanical Systems, 9 (2) 190-197
- Liu, R.H., et al., (2002) Bubble-induced acoustic micromixing, Lab on a chip, 2, 151-157
- Liu, R.H., et al., (2003) Hybridization enhancement using cavitation microstreaming, Analytical Chemistry, 75 (8) 1911-1917
- Löwe, H., et al. (2000) Micromixing technology, Fourth international conference on microreaction technology, IMERT 4, Atlanta, USA, AICHE topical proceedings, 31-47
- Lye, G.J., P. Ayazi-Shamlou, F. Baganz, P.A. Dalby and J.M. Woodley (2003) Accelerated design of bioconversion processes using automated microscale processing techniques, Trends Biotechnology, 21 (1) 29-37
- Melin, J., G. Gimenez, N. Roxhed, W. van der Wijgaart and G. Stemme, (2004) A fast passive and planar liquid sample micromixer, Lab on a chip, 4, 214-219
- Micheletti, M. and G.J. Lye, (2006) Microscale bioprocess optimization Curr. Opin. Biotech. 17 (6) 611-618
- Monnier, H., Willhelm, A.–M., Delmas, H., (1999). Influence of ultrasound on mixing on the molecular scale for water and viscous liquids. Ultrasonics Sonochemistry, 6, 67-74
- Niu, X.Z. and Y.K. Lee, (2003) Efficient spatial-temporal chaotic mixing in microchannels, J. micromech. Microeng., 13, 454-462

- Norton, T., and D.-W. Sun, (2006) Computational fluid dynamics (CFD) an effective and efficient design and analysis tool for the food industry: A review, Trends in food science & technology, 17, 600-620
- Paik, P., V.K. Parmula and R.B. Fair, (2003) Rapid droplet mixers for digital microfluidic system, Lab on a chip, 3, 253-259
- Pennemann, H., P. Watts, S.J. Haswell, V. Hessel and H. Löwe, (2004) Benchmarking of microreactor applications, Organic process research & development, 8, 422-439
- Presens Precision Sensing, Regensburg, Germany. http://www.presens.de, 2008
- Quandt, E., and Klaus Seemann, K., (1996). Magnetostrictive Thin Film Microflow Devices. Micro System Technologies 96, VDE-Verlag GmbH, 451-456
- Reis, N., C.N. Goncalves, A.A. Vicente and J.A. Teixeira, (2006) Proof of concept of a novel micro-bioreactor for fast development of industrial bioprocesses. Biotechnology and Bioengineering, 95 (4) 744-753
- Roberge, Dominique M., Laurent Ducry, Nikolaus Bieler, Philippe Cretton and Bertin Zimmermann, (2005) Microreactor Technolgy: A Revolution for the Fie Chemical and Pharmaceutical Industries, Chem. Eng. Technol., 28 (3) 318-323
- Schönfeld, F., V. Hessel and C. Hofmann, (2004) An optimized split-and-recombine micro mixer with uniform 'chaotic' mixing, Lab on a chip, 4 65-69
- Schwesinger, N., Frank, T., Wurmus, H., (1996). A modular microfluid system with an integrated micromixer. Journal of Micromechanics and Microengineering, 6, 99-102
- Shang, J.S., (2004) Three decades of accomplishments in computational fluid dynamics, Progress in aerospace sciences, 40, 173-197
- Siddheshwar, P.G., Pranesh, S., (1998). Effect of a non-uniform basic temperature gradient on Rayeigh-Benard Convection in a micropolar fluid. International Journal of Engineering Science, 36, 1183-1196

- Stroock, A.D. et al., (2002a) Chaotic mixing in microchannels, Science, 295 (1) 647-651
- Stroock, A.D. et al., (2002b) Patterning flows using grooved surfaces. Analytical Chemistry, 74 (20) 5306-5312
- Szita, N., P. Boccazzi, Z. Zhang, P. Boyle, A.J. Sinskey and K.F. Jensen, (2005) Development of a multiplexed microbioreactor system for high-throughput bioprocessing, Lab on a Chip, 5 (8) 819-826
- Tice, J.D., A.D. Lyon, and R.F. Ismagilov, (2003) Effects of viscosity on droplet formation and mixing in microfluidic channels, Anal. Chim. Acta., 507, 73-77
- Titchener-Hooker, N.J., P. Dunnill, M. Hoare, (2008) Micro Biochemical Engineering to accelerate the Design of Industrial-Scale Downstream Processes for Biopharmaceutical Proteins, Biotechnology and Bioengineering, 100 (3) 473-487
- Tsai, J.H. and L. Lin, (2002) Active microfluidic mixer and gas bubble filter driven by thermal bubble pump, Sensors Actuators A, 97-98, 665-671
- Tsouris, C., Culbertson, C.T., Depaoli, D.W., Jacobson, S.C., de Almeida, V.F., Ramsey, J.M., (2003). Electrohydrodynamic Mixing in Microchannels, AIChE Journal 49, 8, 2181-2186
- Urban, P.L., D.M. Goodall and N.C. Bruce, (2006) Enzymatic microreactors in chemical analysis and kinetic studies, Biotechnology Advances, 24 (1) 42-57
- Van Leeuwen, M. (2008) Development of a bioreactor with integrated on-line sensing for batch and fed-batch cultivation on a  $100\mu l$ -scale, Ph.D. Thesis, Technical University Delft
- Weuster-Botz, D., R. Puskeiler, A. Kusterer, K. Kaufmann, G.T. John and M. Arnold, (2005) Methods and milliliter scale devices for high-throughput bioprocess design, Bioprocess Biosystem Engineering, 28 (2) 109-119
- Weuster-Botz, D., S. Stevens and A. Hawrylenko, (2002) Parallel-operated stirred-columns for microbial process development, Biochemical Engineering

- Journal, 11 (1) 69-72.
- Wilms, D., Johannes Klos and Holger Frey, (2008) Microstructured reactors for polymer synthesis: A renaissance of continuous flow processes for Tailor-Made macromolecules, Macromolecular Chemistry and Physics, 209, 343-356
- Xia, B., and D.-W. Sun, (2002) Applications fo computational fluid dynamics (CFD) in the food industryL a review. Computers and Electronics in Agriculture, 34, 5-24
- Yamaguchi, Y., K. Ogino, K. Yamashita and H. Maeda, (2004) Rapid micromixing based on multilayer laminar flows, Journal of chemical engineering of Japan, 37 (10) 1265-1270
- Yi, Mingqiang and Haim H. Bau, (2003), The kinematics of bend-induced mixing in micro-conduits, International Journal of Heat and Fluid Flow, Vol. 24 645-656
- Zanzotto, Andrea, Klavs F. Jensen, A.J. Sinskey, M.A. Schmidt, P.E. Laibinis, R.J. Ram and Nicolas Szita, (2003), Microfermentors for rapid screening and analysis of biochemical processes. WO 2003/093406.
- Zanzotto, Andrea, Nicolas Szita, Paolo Boccazzi, Philip Lessard, Anthony J. Sinskey, Klavs F. Jensen, (2004), Membrane-Aerated microbioreactor for High-Throughput Bioprocessing, Biotechnology and Bioengineering, 87 (2), 243-254
- Zengerle, R., W. Geiger, M. Richter, J. Ulrich, S. Kluge, A. Richter, (1994), Application of Micro Diaphragm pumps in microfluid systems, Proc. Actuator '94 Bremen, 25-29
- Zhang, Z., N. Szita, P. Boccazzi, A. J. Sinskey and K.F. Jensen, (2003) Monitoring and control of cell growth in fed-batch microbioreactors, 7TH International Conference on Miniaturized Chemical and Biochemical Analysis Systems, California, USA
- Zhang, Zhiyu, Gerardo Perozziello, Nicolas. Szita, Paolo Boccazzi, Anthony J. Sinskey, Oliver Geschke, and Klavs F. Jensen. (2005), Microbioreactor "Cassette" with

- integrated fluidic and optical plugs for high-throughput bioprocess. Micro-TAS 2005
- Zhang, Z., N. Szita, P. Boccazzi, A. J. Sinskey and K.F. Jensen, (2006a) A well-mixed, polymer-based microbioreactor with integrated optical measurements, Biotechnology and Bioengineering, 93 (2) 286-296
- Zhang, Zhiyu, Paolo Boccazzi, Hyun-Goo Choi, Anthony J.Sinskey and Klavs F. Jensen, (2006b) Microchemostat microbial continuous culture in a polymer-based, instrumented microbioreactor, Lab on a Chip, 6 (7) 906-913
- Zhang, Zhiyu, Paolo Boccazzi, Hyun-Goo Choi, Anthony J.Sinskey and Klavs F. Jensen, (2007) Microbioreactor for continuous cell cultivation, WO 2007/038572
- Zhen Y., Sohei Matsumoto, Hiroshi goto, Mikio Matsumoto, Ryutaro Maeda, (2001).

  Ultrasonic micromixer for mixfofluidic systems, Sensors and Actuators, A
  Vol. 93, 266-272

# Chapter 2

## The use of recycle flows to improve mixing in micro bioreactors

This chapter is published as X. Li, G. van der Steen, G.W.K. van Dedem, L.A.M. van der Wielen, M. van Leeuwen, W.M. van Gulik, J.J. Heijnen, E.E. Krommenhoek, J.G.E. Gardeniers, A. van den Berg, M. Ottens, *Improving mixing in microbioreactors, Chem. Eng. Sci.*, 63 (2008) 3036-3046

## **Abstract**

This chapter describes a possible active mixing method for a  $30\mu$ l microbioreactor that was designed, simulated and tested. Pressure based recycle flow was investigated in a cylindrical micro-reactor for mixing efficiency. Based on the computational fluid dynamics (CFD) simulation results and the requirements of the application. the recycle flow mixing method proved to be suitable as a method to induce sufficient mixing in the micro bioreactor. This was verified experimentally using image analysis of dye distribution behavior.

## 2.1 INTRODUCTION

Fermentation plays a critical role in the gene identification and the related protein production. The method of choice to produce proteins is by cloning and expression in a suitable host at optimized broth conditions and fermentation conditions in a bioreactor. Clearly, to have optimized protein production conditions identified, large amount of experiments is needed to establish these critical factors. (Kostov et al., 2001)

The use of microbioreactors has the potential to both increase the process development rate and to reduce research cost. Therefore, in the last decades, there has been a growing interest in developing minute "laboratories on a chip" and micro-chemical reactors which are able to perform chemical and biological experiments and analysis at a small scale. (Yi et al., 2003; Pennemann et al., 2004). A number of mini- and micro-bioreactors has been described in the literature. For instance, Kostov et al. (2001) described a 24-well plate with 2 ml micobioreactors, which can be used to study the cultivation of Escherichia coli. Zanzotto et al. (2004) developed a batch microbioreactor with volume 5-50 µl also for Escherichia coli fermentations. Zhang et al. (2003, 2005) utilized an array of four 80µl fed-batch and continuous microbioreactor for E coli growth. Balagadde et al. (2005) demonstrated a 16nl microchemostat on a chip to monitor a long-term bacteria growth. Doig et al. (2005) used three different microplates (24-, 96- and 384-wells) with working volume 65 µl and 1,182 µl to grow Bacillus subtilis. Many other groups have developed different milliliter scale bioreactor arrays.

One of parameters of a successful fermentation is the mode of operation, which can be batch, fed-batch or continuous. Because of the best controllability and the most efficient biomass growth, fed-batch is mostly the preferred choice in many cases. Thus, the development of a fed-batch microbioreactor is one of the most interesting research areas in the field.

In fed batch mode the transfer of oxygen, as an important substrate, is always the bottleneck for biomass growth in many fermentation processes, particularly for the high biomass concentration processes. The oxygen is fed from gas phase to liquid phase. Therefore, increasing the interfacial area or enlarging the concentration gradient around the area, can increase the mass transfer of oxygen, furthermore, it can help the system to handle a larger

amount of biomass. On a normal lab-scale experiment, vigorous mixing is normally applied to create the maximum concentration gradient around the interfacial area. On a microliter scale, it is also necessary to find a suitable mixing method for a fed-batch experiment to have sufficient gas-liquid mass transfer.

The most common mixing methods on milliliter scale operations are shake flasks, magnetic stirrers and impellers. However, mixing in a micro fluidic system is typically dominated by diffusion rather than turbulence, due to the low Reynolds numbers (<100) on a micro-scale. Mixing by diffusion only is time-consuming and inefficient. Improved mixing normally relies on two principles: first increasing the interfacial area between the liquids to achieve fast mixing via diffusion; second creating a more 'turbulent flow' on a small scale. Based on the first principle, different types of micromixers have been developed that only require structured microchannels to increase the interfacial area. Examples are utilizing surface tension effects to create a timedependent flow pattern inside a multi-sample liquid plug as this plug moves through a chamber (Melin et al, 2004); repeated dividing and merging of fluids (Kim et al, 2003; Kirner et al, 2003); and varying the 3D structure to enhance the convection around bends (Hong et al, 2004; Liu et al, 2000; Schwesinger et al, 1995; Ehrfeld et al, 1999). The most straightforward method to create some form of 'turbulence' on a small scale is to enhance energy input, introduced into the flow from an external source. Several actuators have recently been implemented, including, ultrasonic wave induction (Monnier et al; 1999; Zhen et al, 2001), magnetic stirring (Zhang et al, 2003) and piezoelectric leadzirconate-titanate actuators (PZT) (Zhen et al, 2001). Those recent micro-size mixers are normally larger than hundreds microlitre, and for a very small size reactor (<1 µl) no extra mixing method is needed, because diffusion is normally more than enough to match the mass transfer requirement. There is no suitable mixing method for reaction volumes between hundred to ten micro liters.

In this chapter we will demonstrate, on the basis of computational fluid dynamics (CFD) simulations as well as by experimental validation, the possibilities of two mixing strategies, i.e. Rayleigh-Bénard convection and recycle flow mixing in a micro reactor. Both methods have potential to be applied within a large volume range and can be easily applied for multiple reactor system. The simulations were performed using the CFD program FEMLAB

3.1(COMSOL, Sweden), using the Navier-Stokes equation for incompressible fluids and the Convection and Diffusion equations. The reactor was designed based on the simulations with a double-layered geometry to enhance the mass transfer by diffusion. Actual mixing experiments were carried out using time-resolved image analysis of a tracer dye distribution in the microreactor. In what follows, we first briefly describe the model used in the simulation before presenting the simulation results. Subsequently, we describe the experimental system, the experimental results, and the comparison between experiments and simulations, and end with a discussion of the results and conclusions.

#### 2.2 THEORY

## 2.2.1 Rayleigh-Bénard convection

Rayleigh-Bénard convection (RBC) is a well-known phenomenon and has been frequently reported in literature. (e.g., Thorne et al., 2003, Pradeep et al., 1997, Berge et al., 1976) The simplest case exhibiting RBC is to confine a fluid between two horizontal plates with a distance d, each plate maintained at a fixed temperature, with the upper plate's temperature lower than the bottom plate, at a temperature difference T. When the temperature difference  $\Delta$  T is small, due to the effect of viscous forces circulation is inhibited; so, although there is an upward buoyancy force on the hotter, less-dense fluid near the bottom plate, the fluid remains stable at the bottom plate with heat being conducted diffusively upward. If the temperature difference between plates is sufficiently increased, the buoyancy of the fluid becomes gradually stronger. In that case, at a certain  $\Delta$  T, it will be large enough to overcome the viscous forces, and the fluid will start to circulate. This phenomenon can be characterized by the following model (Hinze et. al., 1975, Thorne et. al., 2003):

$$Ra = \frac{\alpha g \Delta T h^3}{\nu X} = \frac{g C_P \rho_f^2 \beta h^3 \Delta T}{\mu_f \lambda_f}$$
 Equation 2-1

where Ra is the dimensionless Rayleigh number, characterizing the stability of a shallow horizontal layer of a pure fluid confined between two horizontal plates at certain temperature difference.  $\Delta$  T is the temperature difference

between plates; h denotes the distance between plates, typically the height of the reactor, in our case; g is gravitational acceleration;  $C_p$  is specific heat capacity;  $\rho_f$  is density at average film temperature;  $\beta$  is coefficient of expansion of gas;  $\lambda_f$  is the heat conductivity at average film temperature;  $\mu_f$  is the dynamic viscosity at film temperature;  $\alpha$  is the thermal expansion coefficient for volume;  $\upsilon$  is  $\mu_f$  divided by density and X is known as thermal diffusivity and the value equal to  $\lambda_f$  divided by heat capacity at film temperature and density  $\rho$ . With low aspect ratio geometries (h/d< 1, where d is the diameter of the reactor) and a small temperature gradients, a linear stability analysis can be performed on the momentum and energy conservation equations yielding a critical Rayleigh number for the onset of flow, Racrit, in the vicinity of 1700. (Krishnan, 2004)

## 2.2.2 Recycle flow mixing

As mentioned in the introduction, one of the bottlenecks for micro-scale high cell density fermentation is insufficient oxygen supply. In order to increase the oxygen supply we can either increase the interfacial area or enlarge the oxygen concentration gradient over the interfacial area. Introduction of tiny gas bubbles into the liquid phase or changing the reactor geometry are the most common used strategies to increase the interfacial area for a millilitre or a larger volume reactor. Compared with those reactors, a microlitre size reactor has the advantage of a higher surface to volume ratio. Therefore, even with a regular shape, which means the diameter to height (D/H) ratio is in the range of 2 to 4, in a microlitre reactor it is still possible to obtain a large specific gas-liquid (G/L) interfacial area. For an open microlitre reactor, the impact of the evaporation has to be considered, and consequently, the usage of the tiny gas bubbles has to be limited.

Enlarging the oxygen concentration gradient over the interfacial area can further improve the mass transfer between the gas and the liquid phase. Using a vigorous mixing to keep the oxygen concentration around the interfacial area in the liquid phase equal to the average concentration in the reactor is the normal way to the improve mass transfer in a large scale reactor. However, in a microlitre scale device, it is difficult to produce a turbulent flow, and vigorous mixing. Notwithstanding the fact that we can only have a relatively weak mixing in the microreactor, it is still possible to obtain a good G/L mass

transfer by using the concept of recycle flow mixing (RFM).

The notion of RFM is to transfer the oxygen rich solution from the membrane side to the other parts of the reactor, especially far away from the membrane area. On one hand this concept can accelerate the oxygen transfer rate; on the other hand the added kinetics energy of the recycle flow improves the convection in the system.

The necessary energy is introduced by using a micropump unit. The selection of an efficient pumping method has a large impact on the overall mixing performance. Several micropumps have been developed and reported by various research groups based on various principles for the actuator and valve units. For example, electro-osmotic flow (EOF), syringe pumping and diaphragm pumping. EOF pushes the solution by electrokinetically-driven ion movement by high voltage supplies. A syringe uses pressure-driven flow to move the solution. A diaphragm pump uses an actuation diaphragm to generate a stroke volume and causes alternate under- and overpressure in a pump chamber. The actuation diaphragm can be driven by different actuation principles, e.g. piezoelectric actuation (Van Lintel, 1988; Woias et al, 1998;), thermopneumatic (Van der Pol et al, 1990), electromagnetic (Quandt and Seeman,1996) or electrostatic actuation (Zengerle et al, 1994; Guijt, 2003; Johnson et al, 2002; Tsouris et al, 2003).

## 2.3 DESIGN AND SIMULATION

To achieve good mixing, many micromixers have complex structures to increase the diffusion area or to enhance convective radial diffusion (Taylor dispersion) in a micro-channel. Such unique passive structures may limit the use of the mixer, especially in a multi-phase system. The complex structure may also cause cell attachment on the wall and other unwanted effects. Therefore, to avoid such a complex structure, a simple micro-reactor was used as the base case in the mixing method validation.

## 2.3.1 Rayleigh-Bénard convection (RBC)

The basic geometry of the device in the simulation is shown in Figure 2-1

(a) and (b). Briefly, it is a simple cubical micro-reactor with a temperature control system on the top and the on the bottom of the reactor. On the top of the reactor there is a membrane to segregate the liquid phase in the reactor and the continuous gas phase. A hot source, with temperature  $T_1$  is installed in the bottom of the micro-well, the temperature of the gas phase is controlled to a temperature  $T_2$ . To investigate the RBC in the micro-system, FEMLAB 3.1 was used for computational fluidic dynamic (CFD) analysis. The physical properties of water were applied in the simulation. To simplify the simulation, a 2D simulation was selected instead of a 3D simulation. The geometry of the reactor was set to be a rectangle with length 5mm and height 1mm as given in Figure 2-2. The model uses the Incompressible Navier-Stokes equations and the Convection and conduction equation. The model equations are formulated below:

$$\rho \frac{\partial U}{\partial t} - \nabla \cdot \left[ \eta \cdot \left( \nabla U + (\nabla U)^T \right) + \rho U \cdot \nabla U + \nabla P = F \right]$$
 Equation 2-2 a

$$\nabla \cdot U = 0$$
 Equation 2-2 b

$$\delta_{ts} \cdot \rho \cdot C_p \cdot \frac{\partial T}{\partial t} + \nabla \cdot (-k \cdot \nabla T) = Q - \rho \cdot C_p \cdot U \cdot \nabla T$$
 Equation 2-3

In the above equations,  $\delta_{ts}$  denotes the time scaling coefficient (-), U denotes the velocity vector (m s<sup>-1</sup>),  $\rho$  denotes the density (kg m<sup>-3</sup>), T is the temperature (K), Q denotes the heat source (J), u denotes the velocity vector (m s<sup>-1</sup>),  $C_p$  denotes the heat capacity of the solution (J kg<sup>-1</sup> K<sup>-1</sup>). F denotes the select volume force field, which influences the velocity field, such as gravity (N m<sup>-3</sup>). In this case F is the buoyancy difference of the liquid between different temperatures as shown in Equation 2-4. The expression within the brackets represents the flux vector, where the first term describes the transport by diffusion and the second represents the convective flux.

$$F = \alpha \cdot \mathbf{g} \cdot \rho \cdot (\mathbf{T}_1 - \mathbf{T}_2)$$
 Equation 2-4

where  $\alpha$  is the thermal expansion coefficient for volume; g is the gravity acceleration. Boundary 3 was set as the cold plate with temperature  $T_2$ . Boundary 5 was set as the hot plate with temperature  $T_1$ . Other boundaries were set as Thermal insulation boundaries. The system was considered as an

isolated system. Thus, all other boundaries were set as no slip boundaries in Incompressible Navier-Stokes equations. A stationary nonlinear solver was used to determine the velocity field in the reactor.

## 2.3.2 Recycle flow mixing

3D and 2D model geometries and corresponding simulations were created and executed using FEMLAB 3.1. The overall geometry was consisted by three connected cylinders. The top one was set with height 0.1 mm and diameter 5mm. The middle one was with height 0.4 mm and diameter 0.6 mm. The last one was put on the bottom with diameter 5mm and height 1 mm. Two (four) outlet channels, which were connected with the top rectangle, were put symmetrically in 2D (3D) simulation as shown in Figure 2-1(c) and (d). All outlet channels were of 0.1 mm width and set with a constant linear flow rate. Similar to the outlet channels, two (four) inlet channels were placed at the bottom of the third rectangle with width of 0.2 mm.

The model uses the Incompressible Navier-Stokes equations (Equation 2-2) and the Convection and Diffusion equation. The later equation is formulated below:

$$\frac{\partial c_i}{\partial t} + \nabla \cdot (-D_i \nabla c_i + c_i U) = R_i$$
 Equation 2-5

In the above equations, U denotes the velocity vector (m s<sup>-1</sup>),  $c_i$  denotes the concentration of chemical i in solution (kg m<sup>-3</sup>),  $D_i$  denotes its diffusion coefficient, and  $R_i$  denotes the reaction term (kg s<sup>-1</sup> m<sup>-3</sup>). The expression within brackets in Equation 2-5 represents the flux vector, where the first term describes the transport by diffusion and the second represents the convective flux. In the simulations the physical and thermodynamic properties of the solution were set to the data of water at 298 K. The meshing used in the 2D simulations was triangular and in the 3D simulations tetrahedral and around the boundaries triangular.

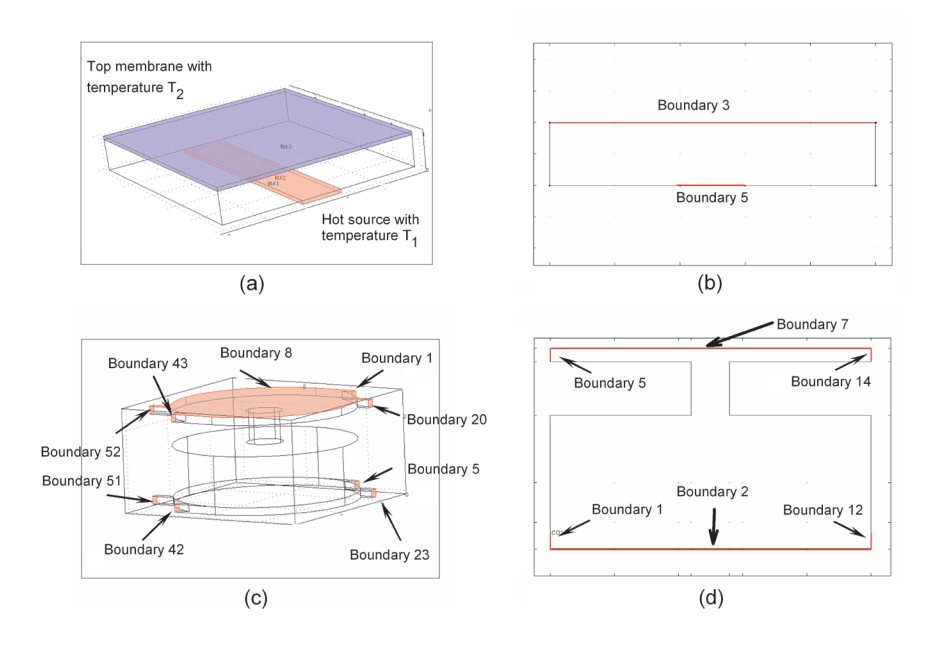


Figure 2-1 (a) 3D simulation geometry for RB convection method; (b) 2D simulation geometry for RB convection method; (c) 3D simulation geometry for recycle flow mixing method; (d) 2D simulation geometry for recycle flow mixing method

## 2.3.3 2D transient simulation of oxygen transfer and biomass growth

As mentioned in the theory, the concept of RFM is to continuously remove the oxygen rich solution from the G/L interfacial area, which is on the top of the reactor, and mixed with other parts of the reactor. To simplify the simulation, initially a 2D simulation was selected instead of a 3D simulation (Figure 2-1 (c)). The oxygen transfer and biomass growth are the most interesting factors to be studied. The side view geometry of the reactor was used in the simulation as shown in Figure 2-1(d). Although 2D simulations may be different from 3D simulation, it is still indicative for oxygen transfer limitation and other important factors.

The Incompressible-Navier-Stokes equation and Convection and Diffusion equation (Equation 2-2 and Equation 2-5) were simultaneously used in the simulations. The biomass growth and substrates consumption followed the equations as given below:

$$R_{biomass} = \mu^{\max} \cdot \frac{c_s}{k_m + c_s} \cdot c_{biomass}$$
 
$$R_s = -\mu_s \cdot c_{biomass}$$
 Equation 2-6

 $R_{\rm O} = -\mu_{\rm O} \cdot c_{biomass}$ 

Where R denotes the reaction rate in kg m<sup>-3</sup> s<sup>-1</sup>,  $\mu^{max}$  denotes the maximum growth rate of yeast (s<sup>-1</sup>),  $\mu_s$  denotes the consumption rate of glucose (kg<sub>s</sub> kg<sub>biomass</sub><sup>-1</sup> s<sup>-1</sup>),  $\mu_o$  denotes the consumption rate of oxygen (kg<sub>o</sub> kg<sub>biomass</sub><sup>-1</sup> s<sup>-1</sup>), k<sub>m</sub> denotes the specific growth rate of biomass (kg m<sup>-3</sup>), c<sub>s</sub> denotes the glucose concentration (kg m<sup>-3</sup>), c<sub>biomass</sub> denotes the concentration of biomass (kg m<sup>-3</sup>). Values of  $\mu^{max}$  and k<sub>m</sub> used in the calculation are  $\mu^{max}$  = 8.33\*10<sup>-5</sup> s<sup>-1</sup> and k<sub>m</sub> = 0.064 (kg m<sup>-3</sup>), respectively and are typical values found in these fermentations (e.g., Valentinotti et al, 2003; Han and Floros, 1998). Values of  $\mu_s$  and  $\mu_o$  are

then  $5.5*10^{-4}$  (kg<sub>s</sub> kg<sub>biomass</sub><sup>-1</sup> s<sup>-1</sup>) and  $2.31*10^{-4}$  (kg<sub>s</sub> kg<sub>biomass</sub><sup>-1</sup> s<sup>-1</sup>), respectively.

The initial biomass concentration was  $0.5 \text{ g } l^{-1}$ , and the biomass growth rate was determined by the specific growth rate, when substrates, oxygen and glucose, are not limited. The oxygen was introduced to the reactor via the top membrane by diffusion, the glucose was injected into the reactor with a constant inward flux from the bottom boundary of the geometry. Because of the existing convection in the reactor, induced by the recycle flow, the specific diffusivity of glucose is neglected but the general diffusion coefficient in the water was used to instead.

Integrated biomass, oxygen and glucose concentrations were used for the total outlet flux, biomass growth in the recycle channel was considered, and therefore, oxygen and glucose were consumed continuously during the transferring period. The mass transfer time was dependent on the length of the cycle channels, which was 2cm, and the linear flow rate, which was set to the outlet boundary. At a certain moment, biomass growth in the recycle channels may stop due to the lack of substrates. The biomass, oxygen and glucose concentration at the inlet ports were calculated based on the integrated result of substrates from outlet ports and biomass growth in the channels. Since

the typical flow in those micro channels results in a low Reynolds number generally less than 100, the flow is strictly laminar. The overall biomass growth description for this period is as given:

$$c_{biomass}^{inlet} = \begin{cases} c_{biomass}^{outlet} \cdot e^{\mu \cdot t} \cdot \left( if \ c_s^{outlet} > c_s^{com} \ and \cdot c_O^{outlet} > c_O^{com} \right) \\ + \left( \frac{c_s^{outlet}}{\mu_s} + c_{biomass}^{outlet} \right) \cdot \left( if \ c_s^{outlet} < c_s^{com} \ and \cdot \frac{c_s^{outlet}}{\mu_s} < \frac{c_O^{outlet}}{\mu_o} \right) \\ + \left( \frac{c_O^{outlet}}{\mu_o} + c_{biomass}^{outlet} \right) \cdot \left( if \ c_O^{outlet} < c_O^{com} \ and \cdot \frac{c_s^{outlet}}{\mu_s} > \frac{c_O^{outlet}}{\mu_o} \right) \end{cases}$$

Equation 2-7

$$\mu = \mu_{\text{max}} \cdot \frac{c_s^{\text{outlet}}}{k_m + c_s^{\text{outlet}}}$$
Equation 2-8

The oxygen and glucose concentrations on boundary1 were set as:

$$c_g^{outlet} = \mu_s \cdot \left(c_{biomass}^{outlet} - c_{biomass}^{inlet}\right)$$
 Equation 2-9

$$c_O^{outlet} = \mu_o \cdot \left(c_{biomass}^{outlet} - c_{biomass}^{inlet}\right)$$
 Equation 2-10

where,  $c_{o}^{\text{outlet}}$  denotes the average oxygen concentration on outlet boundary,  $c_{o}^{\text{com}}$  denotes the predicted minimum oxygen requirement during transfer.  $c_{s}^{\text{com}}$  denotes the predicted minimum glucose requirement during transfer.  $\mu_{s}$  and  $\mu_{o}$  are specific consumption rate of oxygen and glucose in kg glucose (oxygen) / kg biomass / s. The above equations cover all three situations, including non-substrate limitation, glucose limitation, and oxygen limitation.  $c_{s}^{\text{outlet}}$  denotes the average concentration of glucose on outlet.  $c_{s}^{\text{inlet}}$  denotes the calculated biomass concentration.

As shown in Figure 2-1(d), the oxygen diffuses into the reactor through boundary 7, and it was set with an oxygen concentration of 0.037 kg m<sup>-3</sup>, which is the solubility of oxygen under normal conditions with pure oxygen gas pass-through. The glucose diffuses into the reactor via boundary 2, the glucose concentration was set as 3 kg m<sup>-3</sup>, which is high enough for biomass growth. In practice, the solution leaves via boundaries 5 and 14 as the starting point of the recycle flow and those two boundaries were both set convective flux. The recycle flows go back into the system through boundaries 1 and 12. The concentration of oxygen, biomass and glucose on boundary 1 and 12 could be calculated from the component concentrations at boundary 5 and 14 based on above equations.

The impact of different recycles flow rates on the oxygen transfer capability and the mixing behavior of the reactor were assessed based on the simulation results. Over 20,000 seconds of time fermentation process was simulated. Thus, a complete oxygen concentration profile in the liquid phase, including accumulation, maintaining, and consuming, is obtained from the simulation.

#### 2.3.4 3D transient simulation

A 3D simulation with the described geometry was carried on as shown in Figure 2-1(c). Oxygen diffuses into the reactor through boundary 8, and it was set again to an oxygen concentration of 0.037 kg m³. The solution will leave via boundaries 1, 20, 43 and 52 as the starting points of the recycle flows, those boundaries were set as convective flux. The recycled flows will go back into the system through boundaries 5, 23, 42 and 51. Oxygen is continuously recycled. Due to the fact that the total oxygen flux remains in equilibrium throughout the system, the concentration of oxygen at the boundaries could be calculated from the oxygen concentration at the bottom boundaries. The mass transfer of oxygen during recycle flow mixing was assessed with a transient simulation of recycle flow mixing, the concentration of the oxygen in the reactor gives an indication of the mixing behavior in time.

#### 2.3.5 Residence time distribution

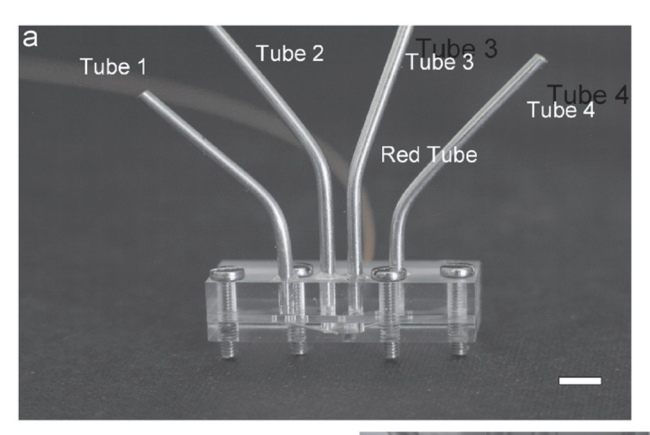
Another way to determine the mixing behavior in the  $\mu$ -bioreactor is via the residence time distribution of a pulse injected in the system. The mixing of

a system can be described by a tanks-in-series model, as shown in Figure 2-15. For a realistic reactor, the mixing lies between the CSTR (continuous stirred tank reactor) and the PFR (plug flow reactor) extremes. In the ideal PFR, the continuous phase flows as a plug through the reactor, there is no mixing or, no axial dispersion. So, the mixing in our  $\mu$ -bioreactor can be represented by the mixing of a cascade of CSTRs. Depending on the number of tanks n in the series, it behaves as an ideal mixer for  $n \rightarrow 1$  or an ideal PFR for  $n \rightarrow \infty$ . A larger n number indicates less ideal mixing.

## 2.4 EXPERIMENTAL SECTION

## 2.4.1 Materials and reagents

All reagents were analytical grade. Rhodamine B powder was supplied by SIGMA (Steinheim, Germany). (NH<sub>4</sub>)<sub>2</sub>SO<sub>4</sub>, KH<sub>2</sub>PO<sub>4</sub> and MgSO<sub>4</sub>-7H<sub>2</sub>O were purchased from Baker Analyzed reagent (Deventer, The Netherlands). All solutions were prepared with double distilled water and passed through a 0.22 μm cellulose acetate filter (Molshelm, France). 2.5 g (NH<sub>4</sub>)<sub>2</sub>SO<sub>4</sub>, 1.5 g KH<sub>2</sub>PO<sub>4</sub> and 0.51 g MgSO<sub>4</sub>-7H<sub>2</sub>O were dissolved into 50 ml deionized water to prepare the pH 4 buffer solution. 1mM Rhodamine B solution was prepared by dissolving 1.2 g *Rhodamine B* powder into 30 ml buffer solution.



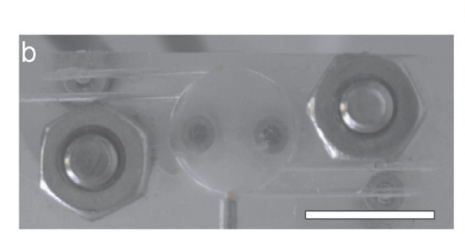




Figure 2-2 Micro reactor: (a) overall picture of the microreactor; (b) bottom view of the microreactor; (c) side view of the microreactor. The white bar indicates 5mm length

#### 2.4.2 Micro bioreactor

Photographs of the micro reactor are shown in Figure 2-2. The reactor consisted of three parts. i.e. the lid layer, the interfacial area layer and the reactor layer. All three layers were made of poly(dimethylsiloxane) PDMS. For the reactor layer, the main reactor volume was drilled out by using a 5mm diameter bore drilled on a PDMS plate. Using a 0.1mm bore, several side channels with a diameter of 100-120  $\mu$ m were drilled in the reactor plate. Red PEEK (polyetheretherketone) polymer tubing was connected to the bottom port of the reactor. Four metal tubes were fixed to the lid layer. Tube 1 and tube 4 were connected to the side channels of the reactor. Tubes 2 and 3 were placed above the central reactor axis. For the interfacial layer, two holes were drilled though the 1mm PDMS plate. The top hole with a diameter 5 mm, a height 100-150  $\mu$ m, the bottom hole with a diameter 200  $\mu$ m and a height 850-900  $\mu$ m. The micro reactor had a diameter of 5 mm, a height of 1.5 mm and a volume of 30  $\mu$ l. The side channels had a diameter of approximately 300-

 $500\mu m$ . The backside port diameter was  $800\text{-}1200~\mu m$ . The internal diameter of tubes was  $1000~\mu m$ . The three layers were placed on top of each other and secured with four screws.

## 2.4.3 Experimental setup and procedure

A Leica DFC 280 digital camera (Heerbrugg, Germany), Rheodyne MXTM Automated Switching Valves (USA), KD-scientific S-101 syringe pump (USA), Several different sized Hamilton syringes (USA), a Labview control program and a Leica Qwin image control and analysis program were used in this work.

A semi-continuous recycle flow mixing setup is shown in Figure 2-3. A syringe pump was used as the driving force to create recycle flows. Four transparent PEEK tubes were connected to the metal tubes and an automatic valve to complete two recycle cycles. Two 100 µl syringes were placed oppositely on the push-pull syringe pump. Two needle adaptors were fixed on the port and the automated valve. The initial position of the automated valve was at position 1. To characterize the actual mixing in the micro-reactor, 1.5 µl of a solution of Rodamine red B dye in DI water was injected into the reactor via valve port 6. Subsequently, by continuously running the push-pull syringe pump, connected to the automatic valve port 8 and 2, the dye was dispersed in the reactor. The syringe pump displaced a fixed volume (2µl) at a fixed pumping rate. The valve synchronized its switching step (from position 1 to position 2 and then switched back to position 1) same as the pump. The digital camera was used to record the mixing performance on video by measuring the change in color distribution in the reactor and in the transparent PEEK tubes. Thus, at the beginning of the experiment only the injected dye spot showed up as a red spot in the tube 2. During the recycle, the dye was dispersed in the overall reactor system including reactor and recycle tubes. One of the driving forces for dye dispersion is the dye concentration gradient (diffusion), but more importantly, the dye's dispersion was caused by the recycled convection flow. At the end of the experiment, the color in the reactor was the same everywhere, indicating that the dye was homogeneously distributed in the reactor. The color density of the images was measured and it showed that mixing was achieved after a certain time.

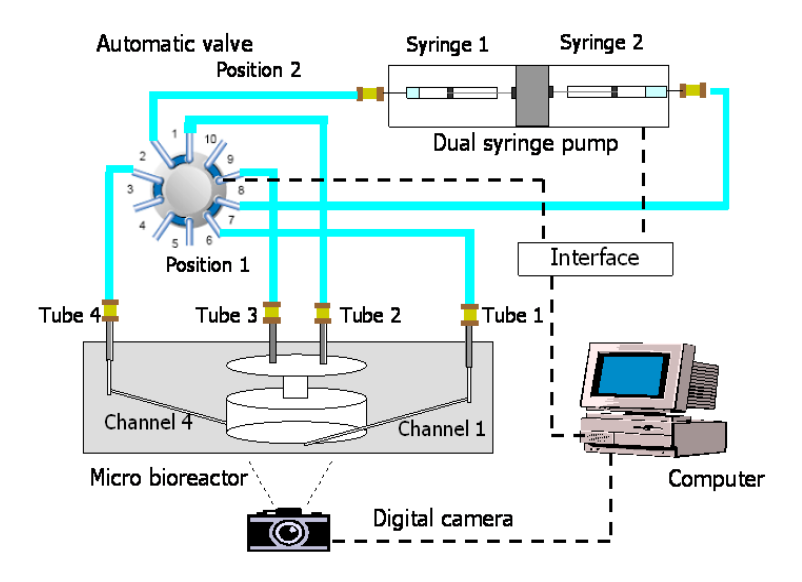


Figure 2-3 Schematic diagram of the recycle mixing experimental setup

Reconnecting the experimental set-up, by removing the reactor and connecting tube 1 to tube 3 and tube 2 to tube 4 allowed accessing the mixing contribution of the tubes. 1.5  $\mu$ l of a solution of Rodamine red B dye in DI water was injected via the automated valve port 6. By following the same experiment procedure as described, mixing in the tubes was determined by measuring the color density of the images in the tubes.

## 2.4.4 Data processing

The mixing performance of the recycle flows in the reactor can be quantitatively analyzed from the recorded pictures. However, unlike in a static mixer, which uses outlet concentration against flow rate ratio to indicate the mixing performance, the quantitative analysis in this case uses the color density in several small areas in the reactor and in the transparent recycle tubes. Because the color intensity is directly related to the *Rhodamine B* concentration, the constant color densities at the end of the experiments indicate a steady state dye concentration and full dispersion. Other factors, which were obtained from the images analysis, like, Mean grey level and Standard deviation in the reactor area were used to describe the mixing in the

reactor zone.

## 2.5 RESULTS

#### 2.5.1 Simulation result

## Rayleigh-Bénard convection

The only requirement to induce Rayleigh-Bénard convection is creating a temperature difference between two surfaces as described previously. Temperatures and the position of the hot resource were parameters that needed to be decided upon in this simulation model. As shown in Figure 2-1, instead of using two paralleled flat surfaces, which were applied in most recent research, a flat cold surface was set on the top of the reactor and a narrow square surface on the bottom of the reactor was set as the hot area. Following this arrangement, two complete fluidic cycles were build up in the reactor. It is a rather simple mechanism for generating a continuous flow field. Unfortunately, there is a significant disadvantage for this strategy to be applied to the fed-batch fermentation, which is the relatively weak convection, as indicated in Figure 2-4, with temperature difference 1 °C, which is the maximum acceptable temperature difference within fermentation. An average linear flow rate 2×10<sup>-6</sup> m s<sup>-1</sup> was achieved, under that flow rate, with the saturated oxygen concentration 0.037 kg m<sup>-3</sup>. The maximum oxygen transfer rate was 4\*10<sup>-10</sup> g s<sup>-1</sup>, furthermore, this amount of oxygen can only support biomass concentration 0.69 kg m<sup>-3</sup> in this 25 µl reactor. To obtain a higher biomass concentration, for instance, 20 g l<sup>-1</sup>, the volume of the reactor has to be reduced to 0.9 µl. Based on the simulation results, the Rayleigh-Bénard convection method seems not to be a viable option. Therefore, we chose the recycle flow method for further experimental investigation.

## Recycle flow mixing

In Figure 2-5 the results are shown for a linear flow velocity of 0.001 m/s. The oxygen is distributed to the entire reactor within 30 s, which is much faster than the time needed (1000s) in the diffusion only process, as shown in Figure 2-6. This is because of the presence of the convective flow, which

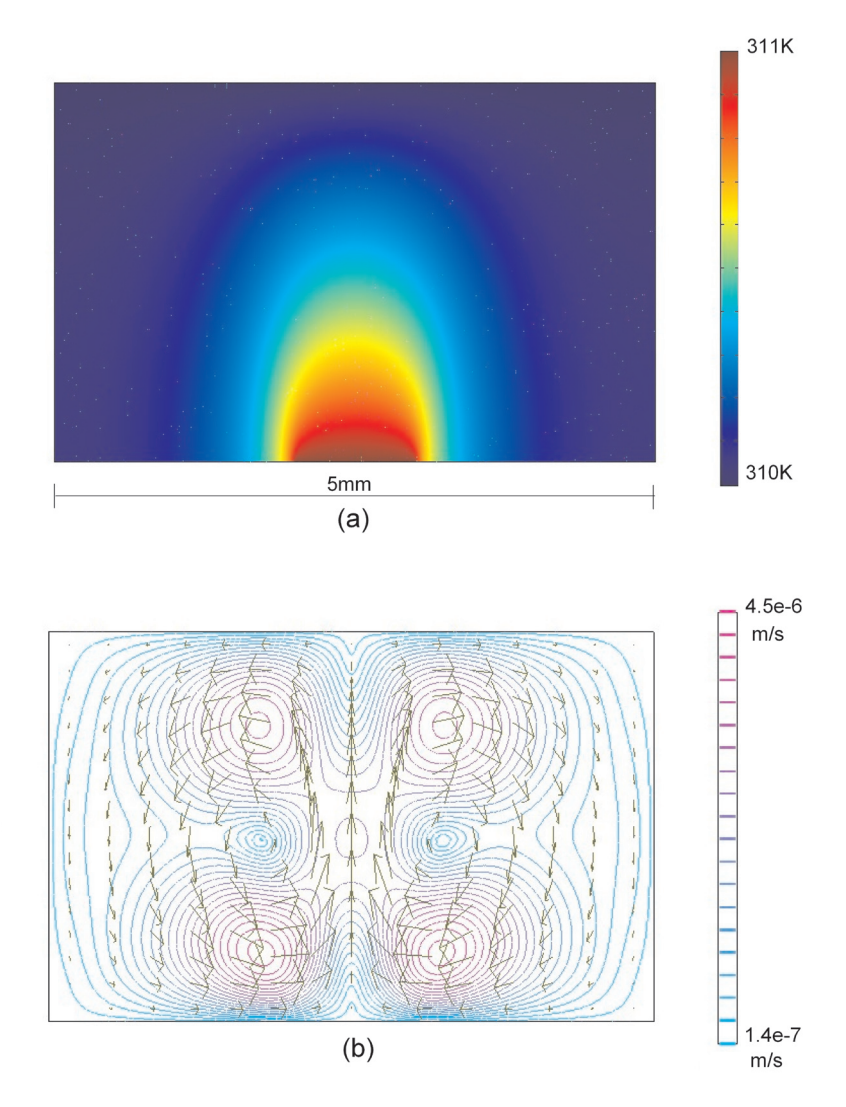


Figure 2-4 Simulation result for Rayleigh-Bénard convection with temperature difference 1°C: (a) temperature profile; (b) velocity profile

helps the mass transfer of oxygen. However, as shown in Figure 2-6, the flow in the reactor was not evenly distributed, although, most of the reactor was covered by a similar velocity field, the middle part of the reactor bottom and corners of the reactor shoulder were covered by a smaller velocity field. Those places constitute the bottleneck for the oxygen transfer. The influence

of oxygen transfer limitation can be indicated by simulating biomass growth fermentation. Two substrates, glucose and oxygen were introduced into the microreactor via diffusion as explained in the design and simulation section. High glucose concentration was used in the simulation to make sure the oxygen transfer was the rate limiting step. Figure 2-7 indicates the oxygen concentration with time changing at the middle point of the reactor bottom (Figure 2-5 (c)). Within 30 s, the oxygen concentration already reached to a sufficient level (>10% oxygen solubility), and remained in that oxygen sufficient level for more than 28,000 s, then, the oxygen concentration reduced to zero at time 30,000 s. The oxygen concentration decrease is because the biomass concentration reached a critical level, which required more oxygen than the recycle mixing method can supply. Figure 2-8 indicates the critical concentration of biomass and the oxygen transfer time under different recycle flow rates. Clearly, a stronger recycle flow leads to higher oxygen transfer ability and a better mixing. Under a stronger recycle flow, a larger Reynolds number in the interfacial layer is obtained. Furthermore, based on Equation 2-11 and Equation 2-12, it is clear that a larger oxygen mass transfer coefficient is obtained. 2D simulations shows that by using recycle flow mixing, the oxygen transfer ability has a significant improvement, the mixing in the reactor is sufficient, moreover, under a high recycle flow rate the mixing can be further improved. Figure 2-9 indicates the oxygen concentration profile with varying recycle flow at a simulation time 10,000 s. Obviously, the recycle fluid flow has a large impact on the ratio between the diffusion domain and the convection domain.

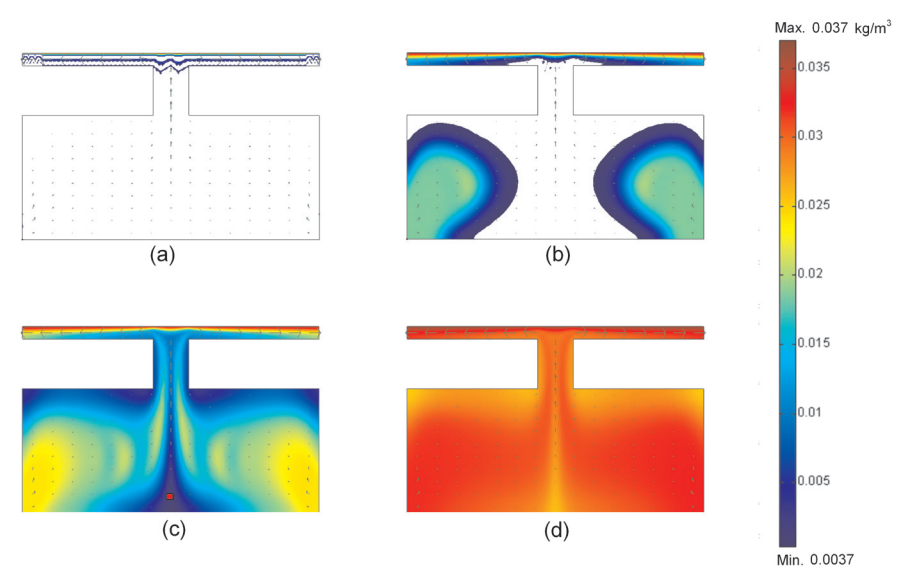


Figure 2-5 Simulation result for oxygen transfer in the liquid phase via recycle flow at time: (a) 0 s; (b) 10 s; (c) 28 s; (d) 100 s. The white area indicates insufficient oxygen concentration in the liquid to sustain growth (< 0.10  $C_{02'}$ <sub>L, sat</sub>).

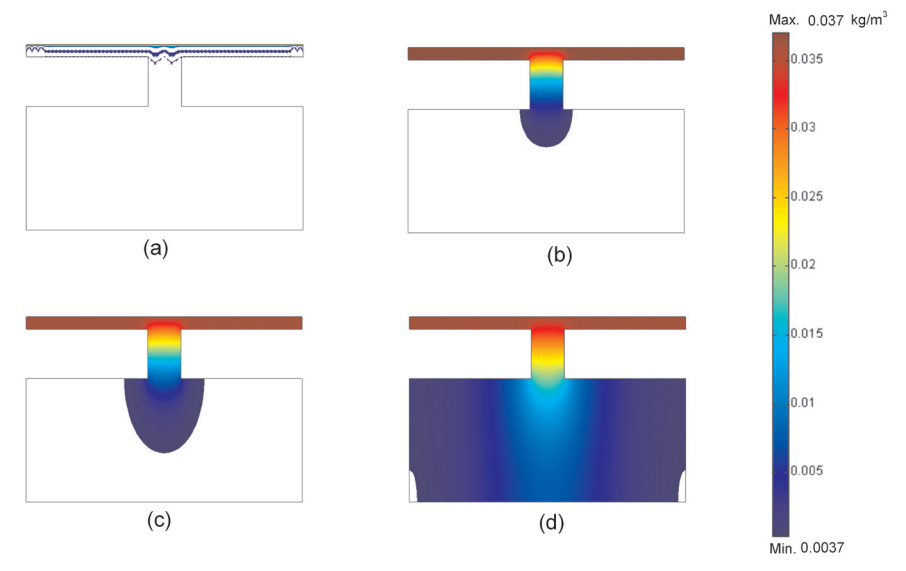


Figure 2-6 Simulation result for oxygen transfer in the liquid phase via diffusion only at time: (a) 0 s; (b) 50 s; (c) 100 s; (d) 1000 s. The white area indicates insufficient oxygen concentration in the liquid to sustain growth (<  $0.10\ C_{O.2.L.sat}$ ).

Maximum oxygen mass transfer in a micro device, which is integrated with RFM method as described previously, is determined based on the mass transfer coefficient k. The value of k can be calculated based on the following equation:

$$k = \frac{Sh \cdot D}{d}$$
 Equation 2-11

Where k denotes mass transfer coefficient (m s<sup>-1</sup>), Sh denotes Sherwood number (-), D denotes the diffusion coefficient of oxygen in water (m<sup>2</sup> s<sup>-1</sup>), d denotes the thickness of the interfacial area (m).

In a microlitre scale device, it is difficult of obtain a turbulent flow, which means Reyonlds number normally has a small value (<100). Furthermore, the gas phase and the liquid phase in the device can be treated as two parallel plates. Therefore, Sherwood number is determined based on the equation:

$$Sh = 0.322 \cdot \text{Re}^{\frac{1}{2}} \cdot Sc^{\frac{1}{3}}$$
 Equation 2-12

Where Re denotes the Reynolds number(-), Sc denotes Schmidt number (-).

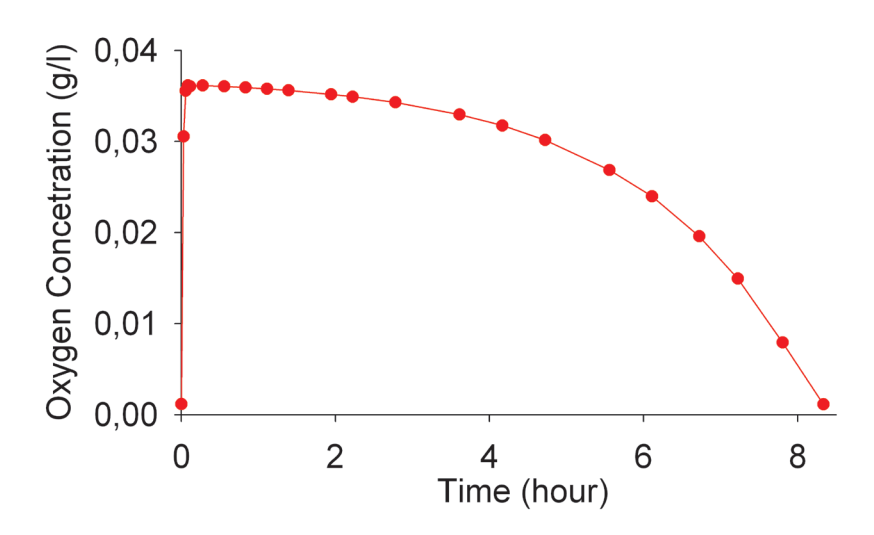


Figure 2-7 Oxygen concentration at spot (x: 0.0028; y:0.0001) in complete process simulation.

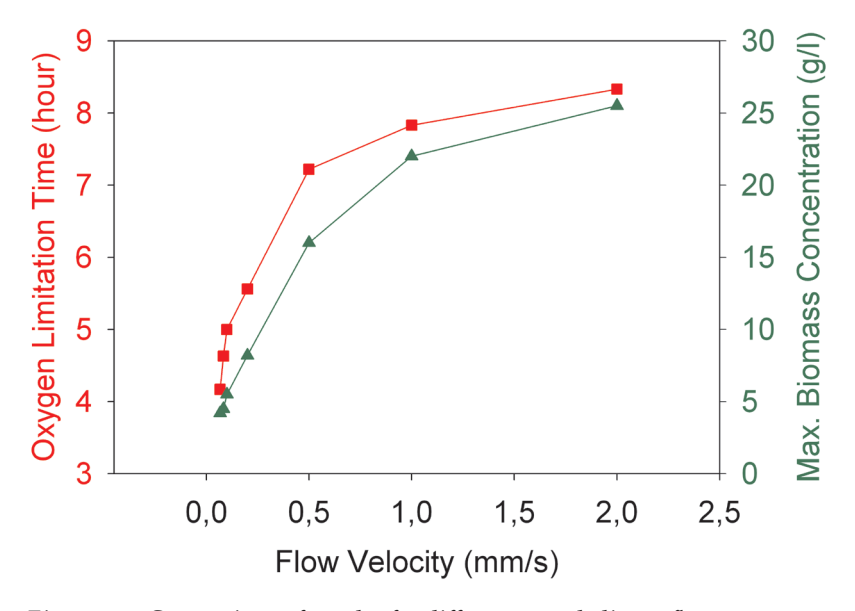


Figure 2-8 Comparison of results for different recycle linear flow rates vs. Max. biomass concentration (triangle); vs. oxygen limitation time (square)

Based on the geometry of these 2D simulations, when recycle flow rate is 0.001 m s<sup>-1</sup>, Reynolds (Re) number at the layer is around 5. Schmidt (Sc) number is around 500. Sherwood (Sh) number is determined from Equation 2-12, has a value of 5.88. Mass transfer coefficient is calculated from Equation 2-11, is  $1.18\times10^{-4}$  m s<sup>-1</sup>. The specific area to volume ratio of the prototype reactor, which is 196.25 m<sup>-1</sup>. Therefore, k<sub>i</sub>a value is around 0.023 s<sup>-1</sup>, which is in the same order of magnitude as the k<sub>i</sub>a value of a regular stirred tank (van 't Riet and Tramper, 1991). It indicates that the mass transfer ability and mixing efficiency between a micro scale device, which is integrated with recycle flow mixing, and a large scale stirrer tank is comparable.

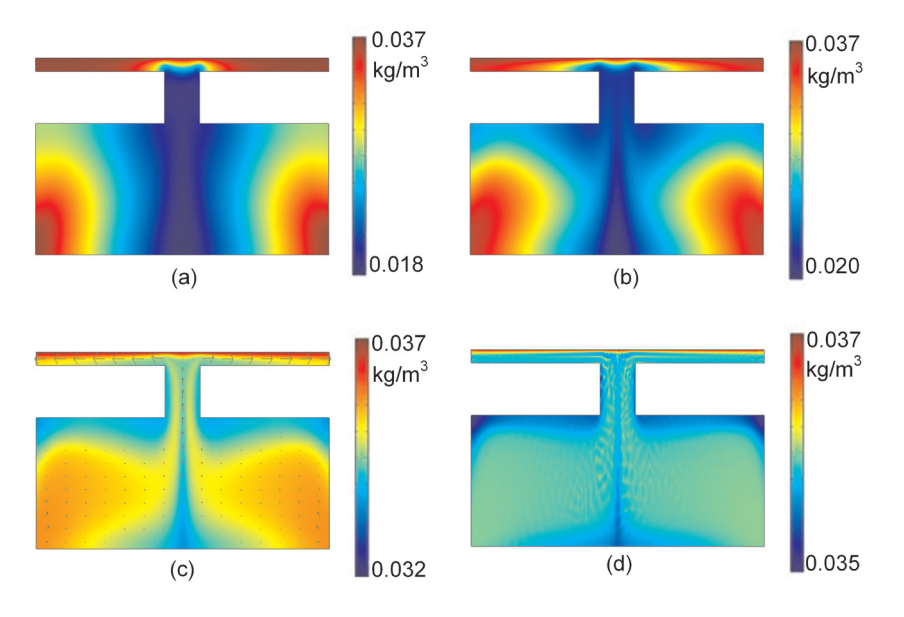


Figure 2-9 Oxygen concentration profile with different recycle flow rate at time 10000 s, with linear recycle flow rate: (a) 0.066 mm  $s^{-1}$ ; (b) 0.2 mm  $s^{-1}$ ; (c) 1 mm  $s^{-1}$  and 10 mm  $s^{-1}$ 

As mentioned in the simulation procedure, four recycle channels were used in the 3D simulation, and the linear flow rate was set to 0.02 mm s<sup>-1</sup>. Because of the lower energy input compared to the 2D simulation, the oxygen transfer time was increase to 300 s, but it was still better than the diffusion only based mass transfer. The position of dead zone areas was also different from 2D simulation. The dead zone areas were located at the side of reactor shown in Figure 2-10. There are two ways to solve the dead zone area problem. The first is to add more recycle channels on both sides of the reactor, especially beside the dead zone area. The second is to use a wider channel instead of the currently used 120  $\mu m$  ones.

From the simulations several problems were identified. First, oxygen transfer is the bottleneck for high biomass concentration fermentations even in a microliter scale reactor. Second, recycled flow helps oxygen transfer and mixing in the reactor, and the strength of the recycle flow has a direct impact on the oxygen transfer ability. A relatively high biomass concentration can be obtained even with a small recycle flow. Third, unevenly distributed

convective flow induce the presence of a dead zone area, however, by using a more complexly structured reactor, the size of dead zone areas can be decreased. Furthermore, since no significant influence of the dead zone area was found during the simulation, and the improvement of the reactor

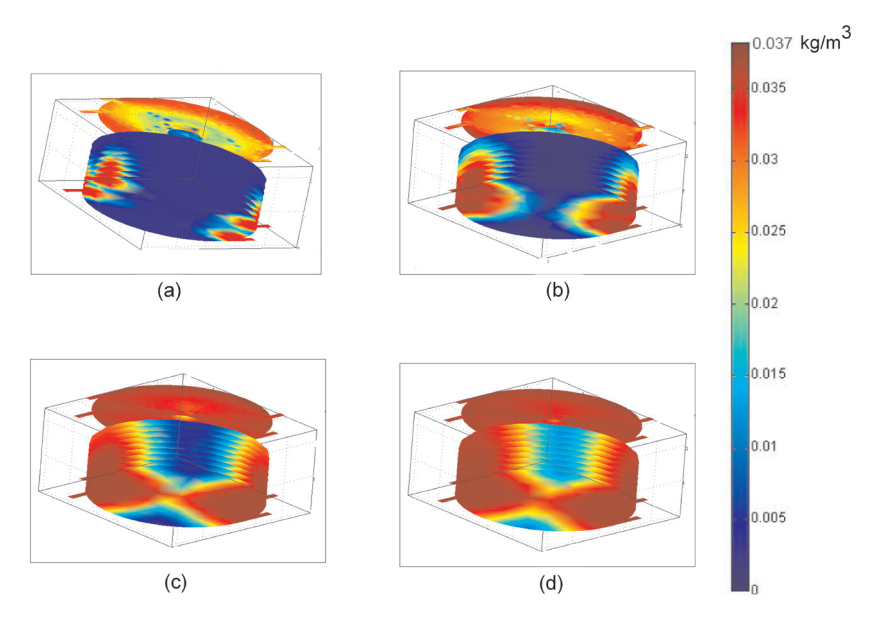


Figure 2-10 Oxygen concentration profile in recycle process at time: (a) 30s; (b) 100s; (c) 300s; (d) 500 s.

geometry will increase the production cost and may lead to other problems, like, positioning of sensors, blocking the channel, cleaning of the reactor etc. Therefore, the simplest cylindrically shaped reactor was the choice for the design of the experimental micro bioreactor.

## 2.5.2 Experiments results

Figure 2-11 shows the experimental results with a recycle flow rate 20  $\mu$ l min<sup>-1</sup> (cycle time approximately 400 s cycle<sup>-1</sup>). The grey level in channel 1 and channel 4 were monitored, the correlation between grey level and time was used to characterize the mixing. The mixing time was defined as the time for the grey level to reach steady state. Because of the small dimensions of recycle channels, the measured grey level from the 2D pictures directly indicates the concentration of the dye solution in the channel.

Figure 2-12 (a) indicates the correlation between the grey level and the time, after two peaks, which were shown in the plot, the measured grey level in channel 1 reached to a steady state. The first peak indicates the initial injected dye solution. During flow recycling, dye solution was distributed, and a much smaller peak was shown in Figure 2-12 (a) after the first cycle. At the same time a similar size peak was observed in the channel 4 curve. After the first cycle, the dye solution was evenly distributed in the upper part of the reactor. Figure 2-12 (a) also shows the average grey level (curve) at the center of the reactor and the standard deviation (SD) (curve) within the same area. The grey level curve of the reactor center in Figure 2-12(a) indicated a mixing time (around 800 s), which is as same as the determined mixing time from other two curves. Thus, the mixing time can be directly determined based on the grey level in the reactor area and is not influenced by the thickness of the reactor. After well mixing, the dye was evenly distributed in the device as shown in Figure 2-11, remaining grey level differences in Figure 2-12 (a) were caused by the background differences in the pictures.

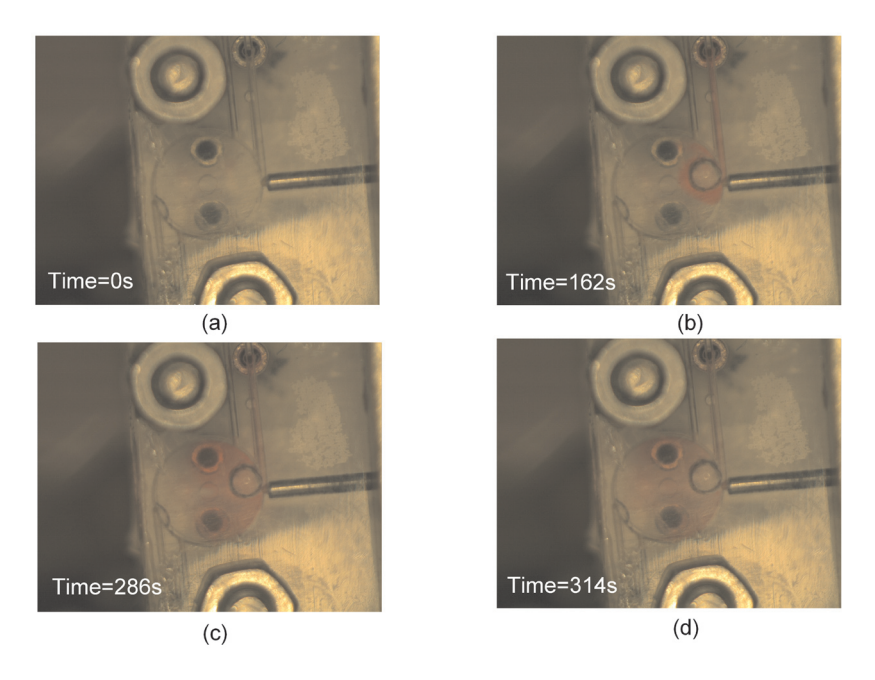


Figure 2-11 Experimental results for recycle flow rate 20  $\mu$ l/min. Dye intensity distribution at: (a) 0 s; (b) 162 s; (c) 286 s; (d) 314 s

The SD curve shows that after the first cycle of the dye solution (first peak), the dye was rapidly distributed in the center part of the reactor. As shown in Figure 2-12 (a) the first peak in the SD curve indicated a large color difference at that time period. That difference is caused by the introduced dye from channel 1. Since one recycled flow only influences the convection within half of the reactor (as shown in Figure 2-5), the SD curve followed the grey level trace of channel 1. After that, because of the small switching step, dye distribution was within the diffusion layer, colored solution was nearly equally distributed into two channels. That is the peak observed in both channel 1 and channel 4. During the second peak period and the time after it, SD curve is constantly low to a value 1; it shows that the mixing happens within both half-sides of the reactor which were both too fast to be recognized from the SD curve.

The total volume of the experimental system (V) is around 90 µl (reactor 30 μl; four metal tubes and side channels 20-25 μl; recycle tubes adaptors and dead volume of valve 40-45 µl). Mixing happens in the reactor part as well as in the channels, tubes and joints of adaptors and valves. The mixing mechanism is different at different positions. For instance, along tubes, shear force and diffusion take the dominant place; in the reactor zone and in adaptors dead volume, convective flow is the most important mechanism; and within the syringe connected tubes, two-directional Taylor dispersion has a significant contribution on mixing (Hong et al, 2004; Beard, 2001). The impact of long recycle tubes, adaptors and the valve were studied experimentally, Figure 2-12 shows the experimental mixing results with various recycle flow rates (20, 60 μl/min) for a reactor-excluded system. Five clear peaks appear in the 20 μl/min experiment. Only 3 clear peaks can be identified in the 60 μl/min experiment. Because the height of the peaks is proportional to the concentration of the dye solution, it is clear that every cycle the dye concentration is smaller and the dye disturbed area is larger. Continuously decreasing peaks indicate the mixing behavior within the tube; the better the mixing is, the larger the peak decrease will be, and the lower the number of peaks' will be. Comparing different flow rate experiments shows that a flow rate of 60 µl/min resulted in steady state at 300s, while a flow rate of 20 µl/min steady state was reached after 1200 s. Faster mixing was achieved because of the smaller cycle time and the more vigorous convection in the joint area.

Comparing Figure 2-12(a) and 2-13, both with a recycle flow rate 20 µl

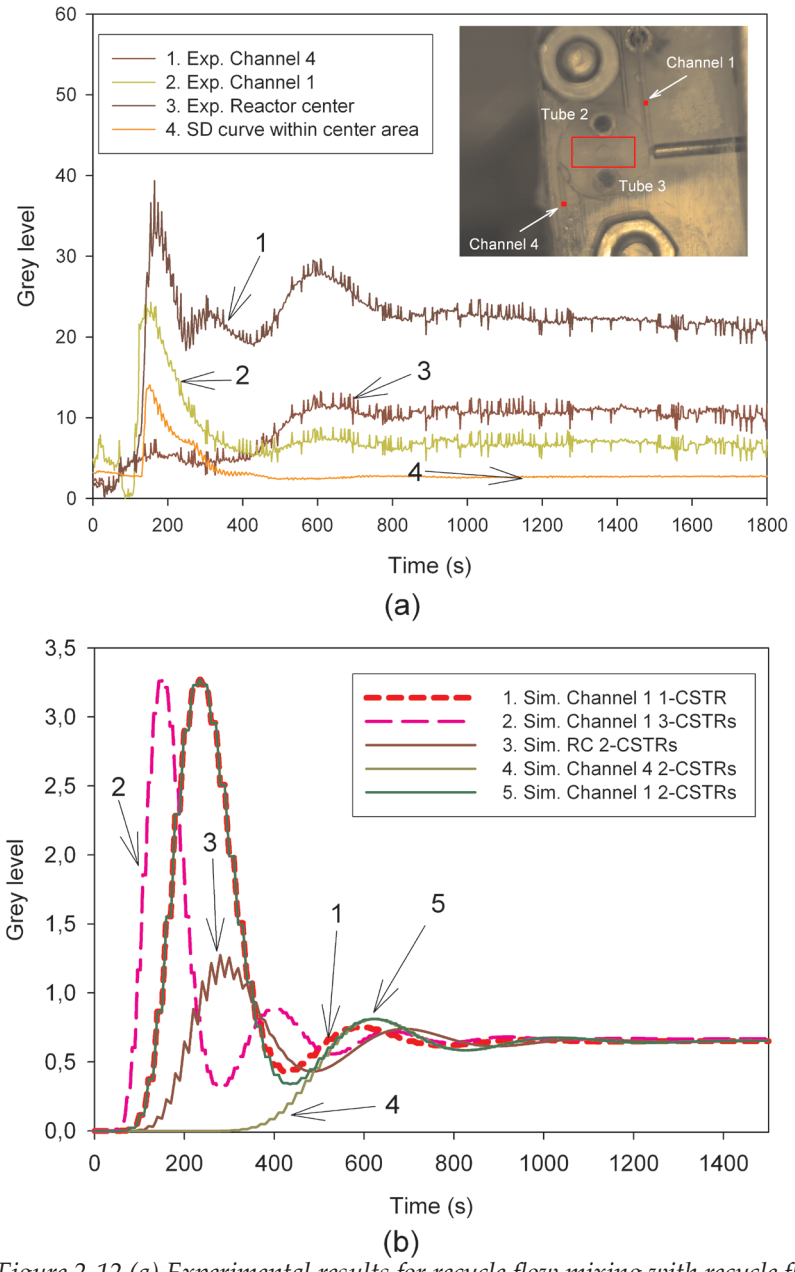


Figure 2-12 (a) Experimental results for recycle flow mixing with recycle flow rate 20  $\mu$ l/min at various position; (b) simulation fitting curve at 20  $\mu$ l/min for 1 CSTR, 2 CSTRs in series and 3 CSTRs in series

min<sup>-1</sup>, the total volume of the experimental set-up in Figure 2-12 (90  $\mu$ l) was 2-3 times larger than the volume of the set-up in Figure 2-13 (40  $\mu$ l). However, the mixing time in Figure 2-12 is smaller. It is a clear indication that the reactor improves mixing. To study the mixing performance of this RFM method, it is necessary to investigate the mixing within the large side-volume and the mixing within the rector separately.

Because the mixing in a realistic reactor can be represented by the mixing of a cascade of CSTRs, the large side-volume, includes the volume of recycle tubes, valves and adaptors and syringes, could be treated as a whole mixing unit, and this unit could be converted as a series of same size CSTR with total

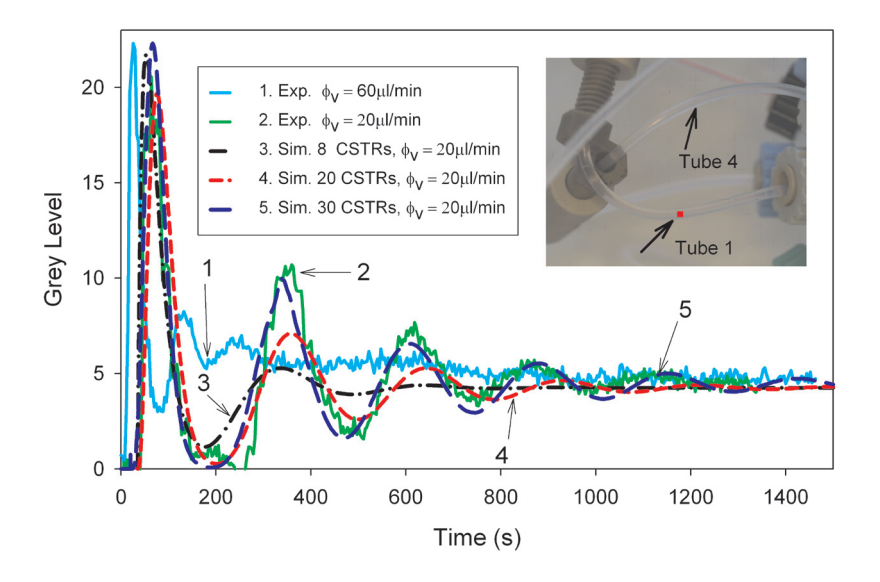


Figure 2-13 Experimental results for recycle flow mixing in tube only system with recycle flow rate 20  $\mu$ l/min, 60  $\mu$ l/min; simulation fitting curve at 20  $\mu$ l/min for 8 CSTRs in series, 20 CSTRs in series and 30 CSTRs in series

reactors number n, total volume 42  $\mu$ l. As shown in Figure 2-14 (a), the outflow of the  $n^{th}$  CSTR is the inflow the first CSTR. The inflow has the flow rate 10  $\mu$ l/min, which is the average recycling flow rate in Figure 2-13, because the semi-continuous flow, which was created by oscillation syringe pump, occurred during experiment.

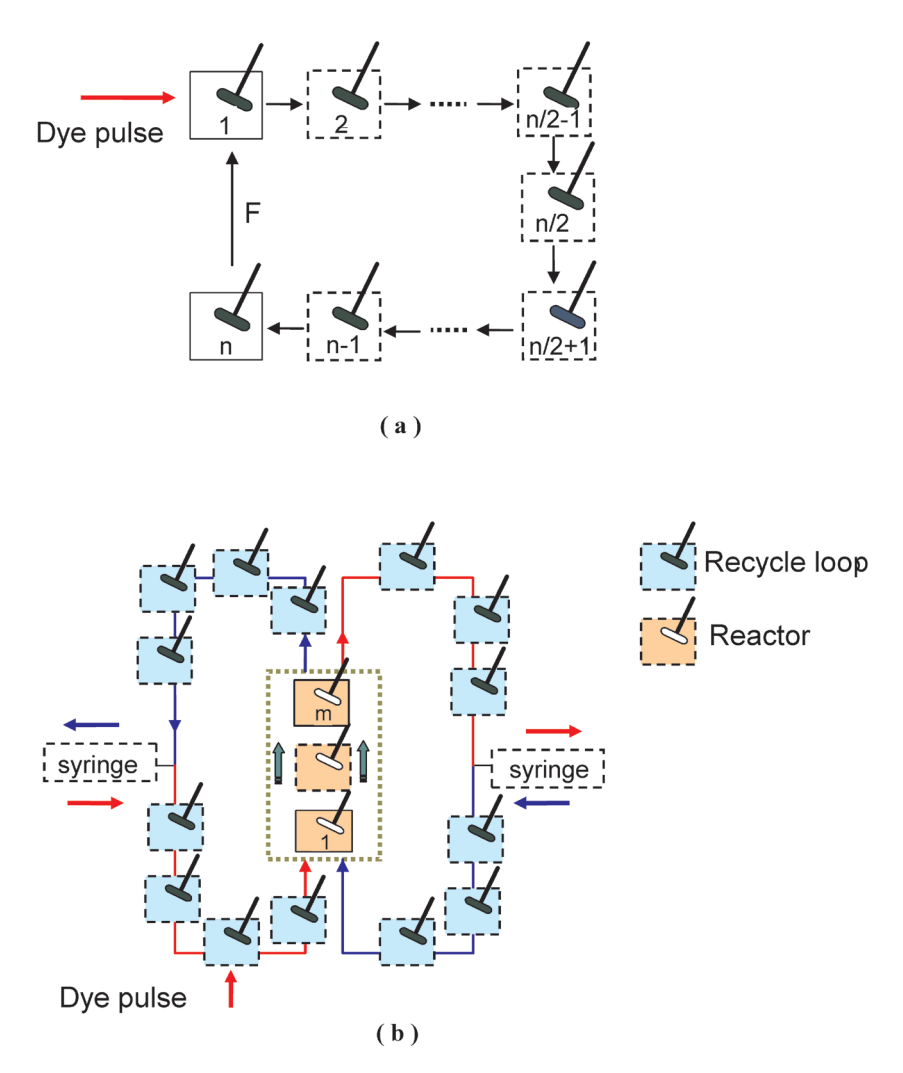


Figure 2-14 Schematic representation of mixing in series of CSTR; (a) CSTRs representing recycle loop system; (b) CSTRs representing reactor included system

Figure 2-13 shows the fitting of simulated curves to the experimental curve; it indicates that the mixing behavior of tube only system is close to the mixing behavior of 30 CSTRs in series. Thus, the mixing in the tubes is quite weak, resembling a plug-flow reactor. Using thirty 1.5  $\mu l$  continuously stirred-tank reactors to represent the recycle loop as shown in Figure 2-14 (b), syringe pumping was included in the simulation, flow rate for the reactor part was continuous, for recycle tubes were semi-continuous. Red cycle and blue cycle

run one after another. Total volume for the reactor part was 50  $\mu$ l, which includes reactor and four metal tubes. The number of series CSTRs m was determined from Figure 2-12 (b). Based on the shape of the grey level curve, m was between 2 to 3. If m  $\rightarrow$  1, it indicates that the mixing behavior in the reactor part is close to an ideal mixed reactor. For m around 2 to 3, it indicates a good mixing in the microreactor, especially after the four metal tubes (Figure 2-2), having a mixing behaviour more close to a PFR than CSTR, were taken into account.

Table 1 Impact of recycle flow rate and recycle volume on well mixing time based on simulated result

	Recycle flow rate (µl/min)	Recycle volume / total volume (%)	Well mixing time (s)
	200	70,00%	140
Variable	100	70,00%	230
Recycle flow rate	60	70,00%	320
	20	70,00%	800
	20	70,00%	800
Variable	20	50,00%	600
Recycle volume	20	30,00%	240
	20	10,00%	120

Although, as shown in Figure 2-12, for the  $20~\mu l$  min<sup>-1</sup> recycle flow rate the mixing time is around 800s, which is rather slow compared with other mixing methods, like e.g. oscillation mixing (Li et al, 2008), using a higher recycle flow rate or reduce the recycle volume can significantly decrease the mixing time in the overall system as shown in Table 1. Table 1 shows the correlations of various recycle flow rates and various recycle volume percentage against well mixing time. The results are calculated based on the simulation of Figure 2-14(b).

## 2.6 CONCLUSIONS

In this chapter, a simple active mixing method for a micro-bioreactor using a pressure-based recycle flow was designed, simulated and tested. Using pressure-driven recycle flow mixing it appears that both diffusion and convection contribute to the mixing, however, with a large recycle flow rate the contribution from convection predominates. In this paper, a syringe pump was used as the actuator to create recycle flow. The experimental results show a reasonably good match with the calculated results. The mixing behavior in the prototype reactor is close to an ideally mixed system. Furthermore, because tubes and adaptors were used to connect syringe pump, reactor and valves, the total volume of the system is larger than the reactor volume, leaving room for a more integrated system that can be applied in future to achieve even better mixing.

Finally, from additional simulations it follows that temperature difference based Rayleigh-Bénard convection cannot provide sufficient mixing in a micro bioreactor due to constraints on the maximal applicable temperature difference that can be sustained by the microorganisms.

## Acknowledgements

This work is part of the ACTS-IBOS programme (IBOS 053.63.009), which is funded by the Dutch Science Foundation (NWO), DSM Anti-Infectives BV, Diosynth/Organon and Applikon BV

## **Notation**

```
a = specific area to volume ratio, m<sup>-1</sup>
```

A = specific area,  $m^2$ 

c<sub>i</sub> = concentration of chemical i in solution, kg m<sup>-3</sup>

 $C_p$  = heat capacity, J kg<sup>-1</sup> K<sup>-1</sup>

d = thickness of the interfacial area, m

D<sub>i</sub> = diffusion coefficient, m<sup>2</sup> s<sup>-1</sup>

E = kinetic energy of the injected fluid, J

F = volume force field,  $N m^{-3}$ 

g = gravitational acceleration, m s<sup>-2</sup>

h = distance between plates, m

k = mass transfer coefficient, m  $s^{-1}$ 

 $k_m$  = specific growth rate, kg m<sup>-3</sup>

P = pressure, Pa

Q = heat resources, J

Ra = Rayleigh number, -

Re = Reynolds number, -

 $R_i$  = reaction term for species i, kg s<sup>-1</sup> m<sup>-3</sup>

Sh = Sherwood number, -

Sc = Schmidt number, -

t = time, s

T = temperature, K

U = velocity vector, m s<sup>-1</sup>

V = total volume of the device, m<sup>3</sup>

X = thermal diffusivity,  $m^2 s^{-1}$ 

#### Greek letters

 $\alpha$  = thermal expansion coefficient for volume,

 $\beta$  = coefficient of expansion of gas,

 $\phi_{\rm v}$  = volumetric flowrate, m<sup>3</sup> s<sup>-1</sup>

 $\mu^{max}$  = maximum growth rate of yeast, s<sup>-1</sup>

μ = consumption (growth) rate of certain species, s<sup>-1</sup>

 $\eta$  = dynamic viscosity, kg m<sup>-1</sup> s<sup>-1</sup>

 $\lambda$  = heat conductivity, W m<sup>-1</sup> K<sup>-1</sup>

v = kinematic viscosity, m<sup>2</sup> s<sup>-1</sup>

 $\rho$  = density, kg m<sup>-3</sup>

## Subscripts

S = substrate (glucose)

O = oxygen

L = liquid phase

## References

- Balagaddé, F.K., You, L., Hansen, C.L., Arnold, F.H., Quake, S.R., (2005). Long-Term Monitoring of Bacteria Undergoing Programmed Population Control in a Microchemostat. Science, 309, 137-140
- Beard D.A., (2001). Taylor Dispersion of a solute in a Microfluidic Channel. Journal of Applied Physics, 89, 4667
- Berge, P., Dubois, M., (1976). Time Dependent Velocity in Rayeigh-Benard Convection: A Transition to Turbulence, Optics Communications, 19, 129-133
- Doig, S.D., Pickering, S.C.R., Lye, G.L., Baganz, F., (2005). Modelling surface aeration rates in shaken microtitre plates using dimensionless groups, Chemical Engineering Science, 60, 2741-2750
- Ehrfeld, W., Golbig, K, Hessel, V., Lowe H., Richter, T., (1999). Characterization of Mixing in Micro mixers by a Test Reaction: Single Mixing Units and Mixer Arrays, Industrial Engineering Chemistry Research, 38, 1075-1082
- Guijt, R.M. (2003), Development of a  $\mu TAS$  for real-time monitoring of fermentations. PhD thesis, Delft
- Han, J.H., Floros, J.D., (1998). Modeling the Growth Inhibition Kinetics of Baker's Yeast by Potassium Sorbate using Statistical Approaches. Journal of Food Science, 63(1), 12-14

- Hinze, J.O. (1975), McGRAW Hill series in mechanical engineering: turbulence, McGraw-Hill, Inc., USA.
- Hinze, J. O. (1975), McGRAW Hill series in mechanical engineering: turbulence, USA, McGraw-Hill, Inc.
- Hofland, G.W., Berkhoff, M.R., Witkamp, G.J., van der Wielen, L.A.M., (2003).
  Dynamics of Isoelectric Precipitation of Casein Using Sulfuric Acid, AIChE Journal, 49(8), 2211-2223
- Hong C.C., Choi, J.W., Ahn, C.H., (2004). A novel in-plane passive microfluidic mixer with modified Tesla structures, Lab on a Chip, 4, 109 –113
- Melin, J., Giménez, G., Roxhed, N., van der Wijngaart, W., Stemme, G., (2004). A fast passive and planar liquid sample micromixer, Lab on a Chip, 4, 214-219
- Johnson, T.J., Locascio, L.E., (2002). Characterization and optimization of slanted well designs for microfluidic mixing under electroosmotic flow. Lab on a Chip, 2, 135-140
- Kim, D.S., Lee, S.W., Kwon, T.H., Lee, S.S., (2003). Barrier embedded chaotic micromixer. IEEE, The Sixteenth Annual International Conference on Micro Electro Mechanical Systems, Kyoto, Japan, 19–23
- Kirner, T., Albert, J., Gunther, M., Mayer, G., Reinhackel, K., Kohler, J.M., (2003).

  Static micro mixers for modular chip reactor arrangements in two-step reactions and photochemical activated processes. Book of Abstracts: IMRET 7th International Conference on Micro reaction Technology, Lausanne, Switzerland 101-105
- Kostov, T., Harms, P., Randers-Eichhorn, L., Rao, G., (2001). Low-Cost Microbioreactor for High-Throughput Bioprocessing, Biotechnology and Bioengineering, 72 (3) 346-352
- Krishnan, M., Agrawal, N., Burns, M.A., Ugaz, V.M., (2004). Reactions Fluidics in Miniaturized Natural Convection Systems. Analytical Chemistry, 76, 6254-6265

- Li, X., van der Wielen, L.A.M., van der Steen, G., van Dedem, G.W.K., van Leeuwen, M., van Gulik, W.M., Heijnen, J.J., Gardeniers, J.G.E., Krommenhoek, E.E., van den Berg, A., Ottens, M., (2007). The application of direct oscillations to improve mixing in micro bioreactors, Biotechnology and Bioengineering, submitted for publication
- Liu, R.H., Stremler, M.A., Sharp, K.V., Olsen, M.G., Santiago, J.G., Adrian, R.J., Aref, H., Beebe, D. J., (2000). Passive Mixing in a Three-Dimensional Serpentine Micro-channel, Journal of Micro-electromechanical Systems, 9 (2) 190-197
- Melin, J., G. Gimenez, N. Roxhed, W. van der Wijgaart and G. Stemme, (2004) A fast passive and planar liquid sample micromixer, Lab on a chip, 4, 214-219
- Monnier, H., Willhelm, A.–M., Delmas, H., (1999). Influence of ultrasound on mixing on the molecular scale for water and viscous liquids. Ultrasonics Sonochemistry, 6, 67-74
- Monnier, H., Willhelm, A.–M., Delmas, H., (1999). The influence of ultrasound on micromixing in a semi-batch reactor. Chemical Engineering Science, 54, 2953-2961
- Pennemann, H., Hessel, V., Lowe, H., (2004). Chemical microprocess technology-from laboratory-scale to production. Chemical Engineering Science, 59, 4789-4794
- Pradeep, G, Siddheshwar, and S. Pranesh (1998). Effect of a non-uniform basic temperature gradient on Rayeigh-Benard Convection in a micropolar fluid, International Journal of Engineering Science, Vol., 36, 1183-1196
- Siddheshwar, P.G., Pranesh, S., (1998). Effect of a non-uniform basic temperature gradient on Rayeigh-Benard Convection in a micropolar fluid. International Journal of Engineering Science, 36, 1183-1196
- Quandt, E., Seemann, K., (1996). Magnetostrictive Thin Film Microflow Devices. Micro System Technologies 96, VDE-Verlag GmbH, 451-456
- Schwesinger, N., Frank, T., Wurmus, H., (1996). A modular microfluid system with an integrated micromixer. Journal of Micromechanics and Microengineering, 6, 99-102

- Rani, S.A., Pitts, B., Stewart, P.S., (2005). Rapid Diffusion of Fluorescent Tracers into Staphylococcus epidermidis Biofilms Visualized by Time Lapse Microscopy. Antimicrobial Agents and Chemotherapy, 49, 2, 728-732
  - Thorne, K., (2003), Chapter 17: Convection Caltech, Pasadena CA 91125
- Tsouris, C., Culbertson, C.T., Depaoli, D.W., Jacobson, S.C., de Almeida, V.F., Ramsey, J.M., (2003). Electrohydrodynamic Mixing in Microchannels, AIChE Journal 49, 8, 2181-2186
- Valentinotti, S., Srinivasan, B., Holmberg, U., Bonvin, D., Cannizzaro, C., Rhiel, M., von Stockar, U., (2003). Optimal operation of fed-batch fermentation via adaptive control of overflow metabolite. Control Engineering Practice, 11, 665-674
- Van De Pol, F.C.M., Van Lintel, H.T.G., Elwenspoek, M., Fluitman, J.H.J., (1990). A thermopneumatic Micropump Based on Micro-engineering Techniques, Sensors and Actuators A. Physical, A21-23, 198-202
- Van Lintel, H.T.G., (1988). A Piezoelectric Micropump Based on Micromachining of Silicon, Sensors and Actuators, 15, 153-167
- Van't Riet, K, Tramper, J., (1991), Basic Bioreactor Design, 254
- Woias, P., Linnemann, R., Richter, M., Leistner, A., Hillerich, B., (1998). A silicon micropump with a high bubble tolerance and self-priming capability. D. Jed Harrison (ed.) Proceedings of the @TAS '98 Workshop, Banff, 383-386
- Yi, M., Bau, H.H., (2003). The kinematics of bend-induced mixing in micro-conduits, International Journal of Heat and Fluid Flow, 24, 645-656
- Zanzotto, A., Szita, N., Boccazzi, P., Lessard, P., Sinskey, A.J., Jensen, K.F., (2004).

  Membrane-Aerated microbioreactor for High-Throughput Bioprocessing.

  Biotechnology and Bioengineering, 87 (2), 243-254
- Zengerle, R., Geiger, W., Richter, M., Ulrich, J., Kluge, S., Richter, A., (1994). Application of Micro Diaphragm pumps in microfluidic systems, Proceedings Actuator '94 Bremen, 25-29

- Zhang, Z., Szita, N., Boccazzi, P., Sinskey, A.J., Jensen, K.F., (2003). Monitoring and control of cell growth in fed-batch microbioreactors, 7TH International Conference on Miniaturized Chemical and Biochemical Analysis Systems, California, USA
- Zhang, Z., Perozziello, G., Szita, N., Boccazzi, P., Sinskey, A.J., Geschke, O., Jensen, K.F., (2005). Microbioreactor "Cassette" with integrated fluidic and optical plugs for high-throughput bioprocessing. Micro-TAS 2005
- Zhen Y., Matsumoto, S., Goto, H., Matsumoto, M., Maeda, R., (2001). Ultrasonic micromixer for microfluidic systems, Sensors and Actuators, A 93, 266-272

# Chapter 3

## Application of direct fluid flow oscillations to improve mixing in micro bioreactors

Part of this chapter has been accepted as X. Li, G. van der Steen, G.W.K. van Dedem, L.A.M. van der Wielen, M. van Leeuwen, W.M. van Gulik, J.J. Heijnen, E.E. Krommenhoek, J.G.E. Gardeniers, A. van den Berg, and M. Ottens, *Application of direct fluid flow osillations to improve mixing in micro bioreactors, AICHE J.* 

#### **Abstract**

This chapter describes an active mixing method for a micro bioreactor that was designed, simulated, tested and successfully implemented. By applying a varying pressure to a micro-channel looping tangentially into a cylindrical micro-reactor an oscillating fluid flow was shown to occur. Such an oscillating fluid flow improved mixing, both by diffusion and convection. The oscillating fluid flow has a large impact on the ratio between the diffusion domain and the convection domain. A good match was obtained between experimental mixing results, computational fluid dynamics (CFD) simulation results and the results of a simplified mixing model thus demonstrating the potential of simulation on improving the design of micro reactors. The possibility of parallizing this mixing method for multi-reactors application has been tested experimentally.

## 3.1 INTRODUCTION

In recent years, there has been a growing interest in developing minute "laboratories on a chip" and in micro-chemical reactors able to perform chemical and biological experiments and analysis. Many industrial companies and research institutes are involved in research into developing micro reaction technology. All the parties involved are convinced of the unique possibilities of micro reaction technology comprising relatively fast mixing, sufficient heat transfer, sensitive and efficient reaction control, and simple scaling up in principle allowing for environmentally friendly production methods (Ehrfeld et. al. 1999). Some of these micro devices have been produced on commercial production scales, and many more possible designs have been tested on a laboratory scale. For instance, Kostov et al. (2001) described a 24-well plate with unit working volume 2 ml micobioreactor, which can be used to study cultivate Escherichia coli. Zanzotto et al. (2004) developed a batch microbioreactor with volume 5 and 50 µl also for Escherichia coli fermentation. Zhang et al. (2003, 2005) utilized an array of four 80 µl fed-batch and continuous microbioreactor for E coli growth. Balagadde et al. (2005) demonstrated a 16 nl microchemostat on a chip to monitor a long-term bacteria growth. Doig et al. (2005) used three different microplates (24-, 96- and 384-wells) with working volume 65 μland 1,182 μl to grow Bacillus subtilis. To have those reactors work properly different mixing methods were applied.

Normally achieving a well-mixed situation in a micro system consumes less energy than in a macro system, and theoretically due to the smaller working volume, it is believed to be easier to control the mixing behavior in a micro system. However, due to the low Reynolds numbers achievable (<100) on a micro-scale, mixing in a micro fluidic system is typically dominated by diffusion rather than turbulence. Furthermore, mixing by diffusion only may be time-consuming and inefficient.

Improved mixing thus relies on two principles: first the need to create a more chaotic flow on a small scale; second the need to increase the interfacial area between the liquids to achieve fast mixing via diffusion. Most of the research has focused on the second principle, since an increase in the diffusion area can easily be achieved by simply changing the mixer geometry while chaotic flow would require the liquids to travel at high velocities and hence energy to be introduced into the flow from an external source.

Micro fluidic systems can also be broadly categorized into continuous-flow systems and batch systems. Continuous-flow systems may have either a PFR (plug flow reactor) or a CSTR (continuous stirrer tank reactor) configuration, and have a continuous input liquid flow and an equal output flow. Batch systems utilize isolated volumes of liquid. Within each system mixing can be carried out passively or actively. Passive mixing requires no energy input other than used to drive fluid flow at a constant rate. Active mixing, on the other hand, requires an external actuator, which inputs extra energy to induce chaotic mixing.

Most recent research focuses on continuous operations. With the passive continuous mixer, the basic design is a T-shaped or Y-shaped mixer (Zhao et. al., 2007). Based on this principle, people have developed other types of micromixers that only require structured microchannels. Examples are utilizing surface tension effects to create a time-dependent flow pattern inside a multi-sample liquid plug as this plug moves through a chamber (Melin et. al. 2004); repeated dividing and merging of fluids (Kim et. al., 2002; Kimer et. al., 2003); and varying the 3D structure to enhance the convection around bends (Nguyen, et. al., 2005; Hong et. al., 2004; Liu et. al., 2000; Schwesinger et. al., 1995; Ehrfeld et. al., 1999; Kolbl et. al., 2008). For active mixing, several actuators have been implemented, including, ultrasonic wave induction (Monnier et. al., 1999; Zhen et. al., 2001), order-changing microfluidic devices (Chung et. al., 2001), cross-channel micromixer with oscillatory flow (Tabeling, et. al., 2004) magnetic stirring (Zhang et. al., 2003) and piezoelectric leadzirconate-titanate actuators (PZT) (Zhen et. al., 2001), and recently recycle flow mixing (Li et al., 2008).

The most commonly used energy source to drive fluid flow through static mixers is pressure difference, which is very easy to implement and which can be very accurately controlled within a relatively large range. However, the complex structure of the static mixers limits the potential application. For active mixers, the commonly used energy sources are ultrasonic wave, magnetic energy and PZT. All these energies can be created by using small size devices, which is a big advantage for microscale applications. However, reducing the size of those devices to a smaller scale will certainly limit the energy that each individual device can produce. Therefore, most of those active mixers operate at a high frequency. Furthermore, because of the physical

limitation of actuators, present active mixing methods can only be scaled down for microreactors, whose working volume are around 100 or larger. By combining the advantages of both passive and active mixing strategies, i.e. a powerful driving force e.g. induced by pressure and a high frequency operating mode, we expect that an effective new mixing strategy, which is suitable for varies scales can be developed.

In this chapter we will demonstrate, both on the basis of computational fluid dynamics (CFD) simulations and their experimental validation, the possibility of applying a pump-based oscillating mixing in a micro reactor, which is developed as a fed-batch micro bioreactor for micro scale fermentations (e.g., Krommenhoek et.al, 2007). In what follows, we first briefly describe the model used in the simulation before presenting the simulation results. Subsequently, we describe the experimental system, the experimental results, and the comparison between experiments and simulations. Furthermore, it is validated that this novel mixing method is applicable in yeast cell fermentation, and it has no negative impact on cell viability, contrary to other traditional mixing methods, i.e. magnetic stirrer mixing.

#### 3.2 MATERIALS AND METHODS

## $3.2.1~\mu ext{-}Bioreactor/mixer design and simulation}$

In order to optimally design the mixing performance of the micro bioreactor, its mixing performance was simulated using the commercially available CFD software package FEMLAB 3.1 (COMSOL, Sweden). A choice needs to be made between active and passive mixing. We chose a passive mixing, as it doesn't require the installation of moving parts (which is difficult to realize at such small scales). Passive mixing strategies have the advantage of higher reliability because there are no moving parts that would require additional power and control. But, to achieve good mixing, most passive mixers have complex structures in order to increase the diffusion area or enhance convective radial diffusion (Taylor dispersion) in a micro-channel. Such unique passive structures may limit the use of the mixer, especially in a multi-phase system. Therefore, to avoid such a complex structure, a simple cylindrical microreactor was used, as shown in Figure 3-1. A pressure difference is induced

in the micro-channel, which is connected to the bottom port of the reactor (Boundary 5, Figure 3-2). A square wave pressure oscillation with a certain frequency and amplitude is imposed on the inlet (Figure 3-3 a). Under different pressures, a solution, which resides in the micro-channel and the reactor, is pushed out of the micro-reactor into the channel or vice-versa. The movement of the solution follows the square wave in phase with the pressure variation. This alternating fluid motion induces convection in the reactor, thus improving the mixing in the reactor. To investigate the mixing performance of the proposed mixing mode, FEMLAB 3.1 was used for a computational fluid dynamics (CFD) analysis. The physical properties of water were applied in the simulation. The diffusion coefficient of the dye in an aqueous solution was

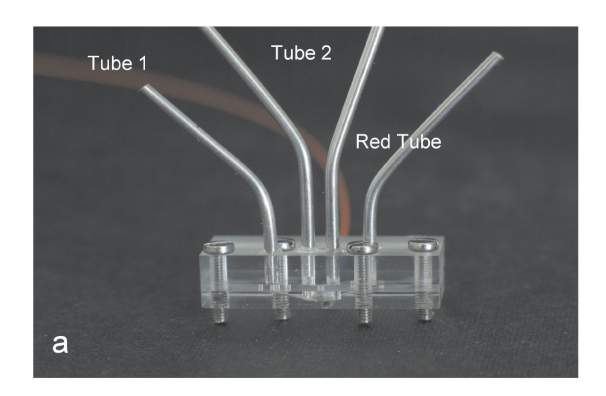






Figure 3-1 Micro reactor a) overall picture of the micro rector; b) bottom view of the micro reactor; c) side view of the micro reactor;

set to  $3.5 \times 10^{-10}$  m<sup>2</sup> s<sup>-1</sup>. (Suirani et al., 2004) To simplify the simulation, initially a 2D simulation was selected instead of a full 3D simulation. Because of the limited height of the reactor of only 1/3 to 1/4 of the reactor diameter, a bottom

view (Figure 3-1 b) shows the extent of mixing more clearly than the side view (Figure 3-1 c). Therefore, the bottom view geometry of the reactor was used in the simulation as shown in Figure 3-2.

Only tube 1 was open during the experiments, all the other three tubes were sealed, therefore, in the simulation, tube 1 was the only tube included.

The model uses the Incompressible Navier-Stokes equations and the Convection and Diffusion equation. The model equations are formulated below (Bird et al, 1960):

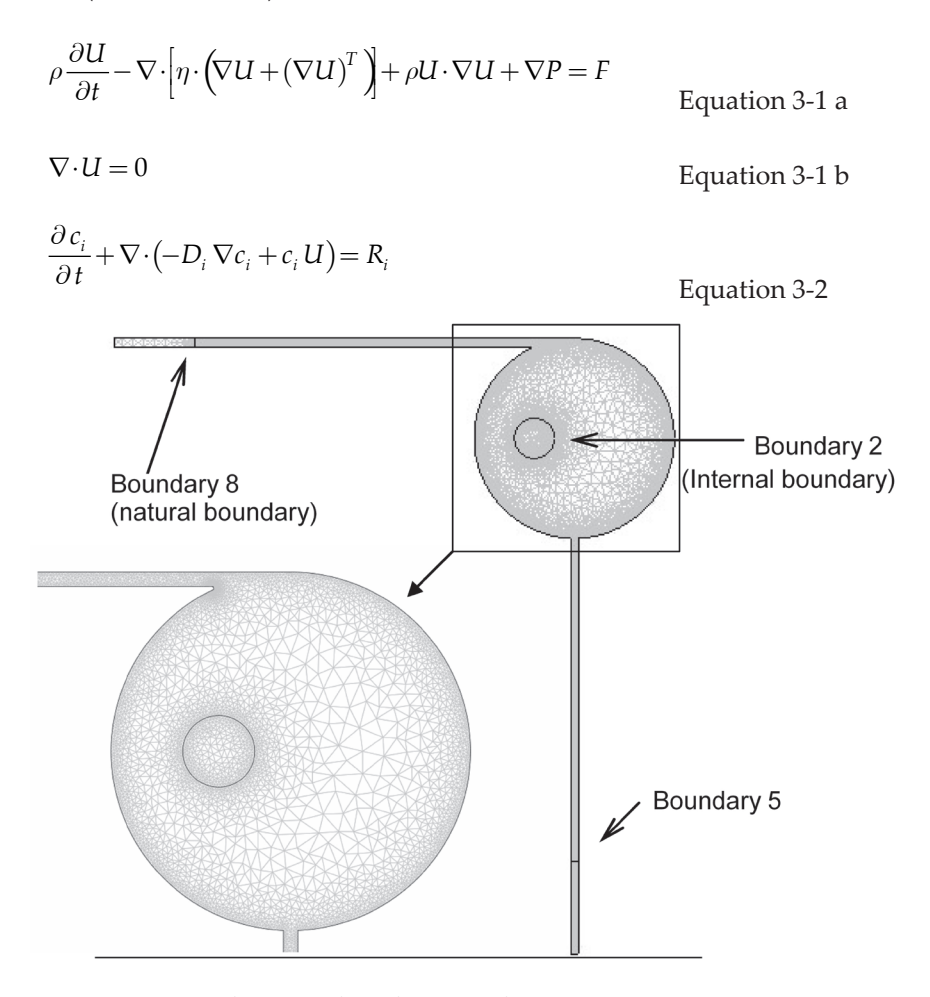


Figure 3-2 Simulation grids and 2D simulation geometry

In the above equations, U denotes the velocity vector (m s<sup>-1</sup>),  $\rho$  denotes the density (kg m<sup>-3</sup>), P is the pressure (Pa),  $c_i$  denotes the concentration of chemical i in solution (kg m<sup>-3</sup>),  $D_i$  denotes its diffusion coefficient, and  $R_i$  denotes the reaction term (kg s<sup>-1</sup> m<sup>-3</sup>). F denotes the select volume force field (i.e. gravity), which influences the velocity field (N m<sup>-3</sup>). The expression within brackets in Equation 3-2 represents the flux vector, where the first term describes the transport by diffusion and the second represents the convective flux.

The oscillation term in the simulation was set on boundary 5 (Figure 3-2), by using the following formula:

$$U = v_1 - 2 \cdot v_1 \cdot f_{HS,c1}(x, x_{max})$$
 Equation 3-3

$$x = \sin\left(\frac{a \cdot t}{\pi}\right)$$
 Equation 3-4

In the above equations, U denotes the linear flow rate on the set boundary in m s<sup>-1</sup>.  $v_1$  denotes the maximum linear flow rate of the pushing flow in m s<sup>-1</sup>. t denotes the time in seconds. a is a constant, which helps to convert time t into the frequency function to the certain time interval. The function  $f(x) = f_{HS,c1}(x, x_{max})$  is used to calculate the value of the smooth version of

the Heaviside function (e.g. Wolfram, 1999). The function is 0 at  $x < -x_{max}$ ,

and 1 at  $x > x_{\rm max}$ . In the interval of  $-x_{\rm max} < x < x_{\rm max}$ ,  $f_{HS,c1}(x,x_{\rm max})$  is a smooth Heaviside function with a continuous first derivative without overshoot, defined by a fifth-order polynomial.

Boundary 2 was set as the internal boundary, which had no influence on the main part of the simulation, but only helped the dye injection simulation. Boundary 8 was set as natural boundary, which is used to balance the velocities of the overall system.

Two different parameters were discussed in the simulation, as mentioned previously, one was the set velocity in m/s, and the other was the oscillation period in seconds.

As shown in Figure 3-2, for the designed geometry 14,471 nodes were

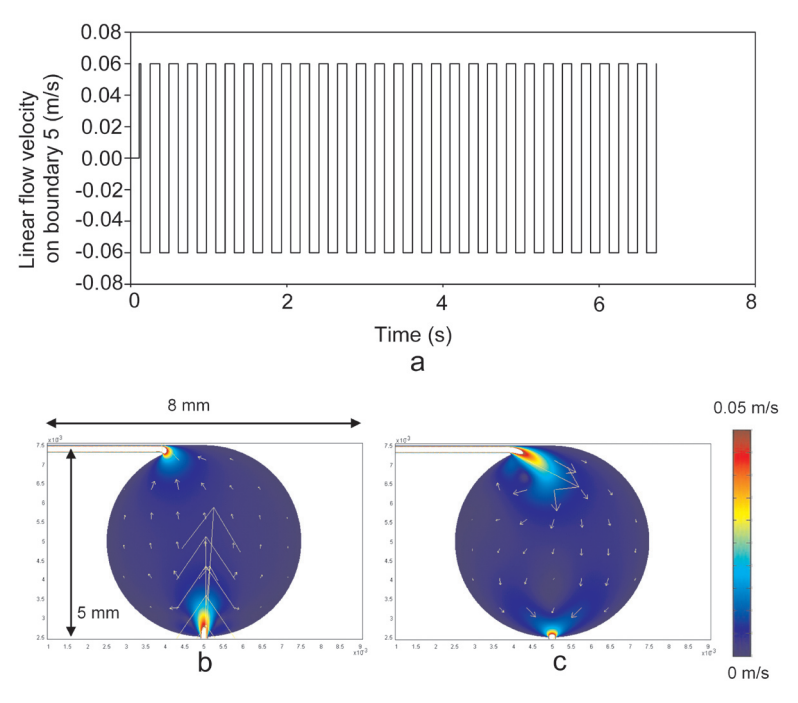


Figure 3-3 a) Linear flow rate on boundary 5 during the simulation; b) Velocity field in the reactor when boundary 5 has a positive value; c) Velocity field in the reactor when boundary 5 has a negative value

used in the simulation. The degree of freedom is 98,976. For a simulated operating time of 10 s, it took around 20,000 s CPU time in a 3GHz microprocessor.

Figure 3-4 shows the geometry of the full 3D simulation. In order to reduce the simulation complexity, only the reactor part was included in the simulation. The model also uses the Incompressible Navier-Stokes equations and the Convection and Diffusion equation. The oscillation term was set as same as the 2D model. Finer meshes (triangle) were set around two oscillation ports and dye injection spot. Coarser meshes were used for the major part of the reactor in order to reduce the amount of the nodes. In total, 23,662 nodes were used in the simulation. The degree of freedom is 148,547. For a simulated operating time of 1 s, it took more than 12,000 s CPU time in a 3GHz microprocessor.

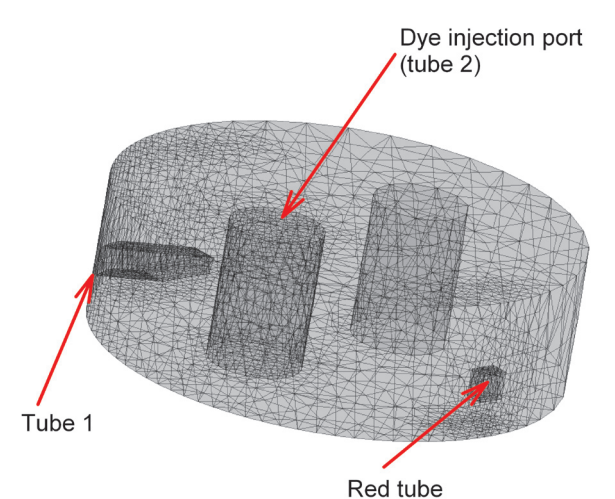


Figure 3-4 Simulation grids and 3D simulation geometry

#### 3.2.2 Experimental setup

#### Chemicals

All reagents were analytical grade. Rhodamine B powder was supplied by SIGMA company (Steinheim, Germany). ( $NH_4$ )<sub>2</sub>SO<sub>4</sub>,  $KH_2PO_4$  and  $MgSO_4$ - $7H_2O$  were purchased from Baker Analyzed reagent (Deventer, The Netherlands). All solutions were prepared with doubly distilled water and passed through a 0.22  $\mu$ m cellulose acetate filter (Molshelm, France). 2.5 g ( $NH_4$ )<sub>2</sub>SO<sub>4</sub>, 1.5 g  $KH_2PO_4$  and 0.51 g  $MgSO_4$ - $7H_2O$  were dissolved into 50 ml deionized water to prepare the pH 4 buffer solution. 1mM Rhodamine B solution was prepared by dissolving 1.2 g Rhodamine B power into 30 ml buffer solution. 2 ml fermentation broth was taken from a 4 L batch fermentation culture, which was started from overnight grown of a preculture (0.5 litres) of Saccharomyces cerevisae in a shake flask at 30 °C on pH 4 buffer and sufficient glucose feeding (Verduin et. al., 1992). Dry weight of cell culture was around 15 g/l.

#### Micro bioreactor

Photographs of the micro reactor are shown in Figure 3-1. The reactor consisted of two parts. i.e. the lid layer, and the reactor layer. Both layers were made of poly(dimethylsiloxane) PDMS. For the reactor layer, the main reactor

volume was drilled out by using a 5 mm diameter flat surface drilled on a PDMS plate. Using a 0.1mm driller, several side channels with a diameter of 100-120  $\mu m$  were drilled in the reactor plate. Ared PEEK (polyetheretherketone) polymer tubing was connected to the bottom port of the reactor. Four metal tubes were fixed to the lid layer. Tube 1 and tube 4 were connected to the side channels of the reactor. Tubes 2 and 3 were placed above the central reactor axis. The micro reactor had a diameter of 5 mm, a height of 1.5 mm and a volume of 27  $\mu l$ . The side channels had a diameter of approximately 300-500  $\mu m$ . The backside port diameter was 800-1200  $\mu m$ . The two layers were placed on top of each other and secured with four screws.

## Additional equipment

A Leica DFC 280 digital camera (Heerbrugg, Germany), a KD-scientific S-101 syringe pump (USA), a Single stirrer motor (RET B, IKA Werke, Germany) and a Leica Qwin image control and analysis program were used in this work.

## 3.2.3 Experimental Procedure

## Micro bioreactor mixing experiment

Experimental set-up is illustrated in Figure 3-5. To characterize the actual mixing in the micro-reactor, 1.5  $\mu$ l of a solution of Rodamine red B dye in demineralised water was injected into the reactor via tube 2. Subsequently, by continuously running the oscillating syringe pump, which was connected to the red PEEK tube, the dye was dispersed. The syringe pump displaced a fixed volume (2  $\mu$ l) at a fixed pumping rate. The digital camera was used to record on video the mixing performance by measuring the change in color distribution in the reactor. Thus, at the beginning of the experiment only the injected dye spot showed up as a red spot. During the oscillation, the dye was dispersed to the other parts of the reactor. One of the driving forces for dye dispersion is the dye concentration gradient (diffusion), but more importantly, the dye's dispersion was caused by the oscillation-induced convection flow. At the end of the experiment, the color in the reactor was the same everywhere, indicating that the dye was homogeneously distributed in the reactor. The

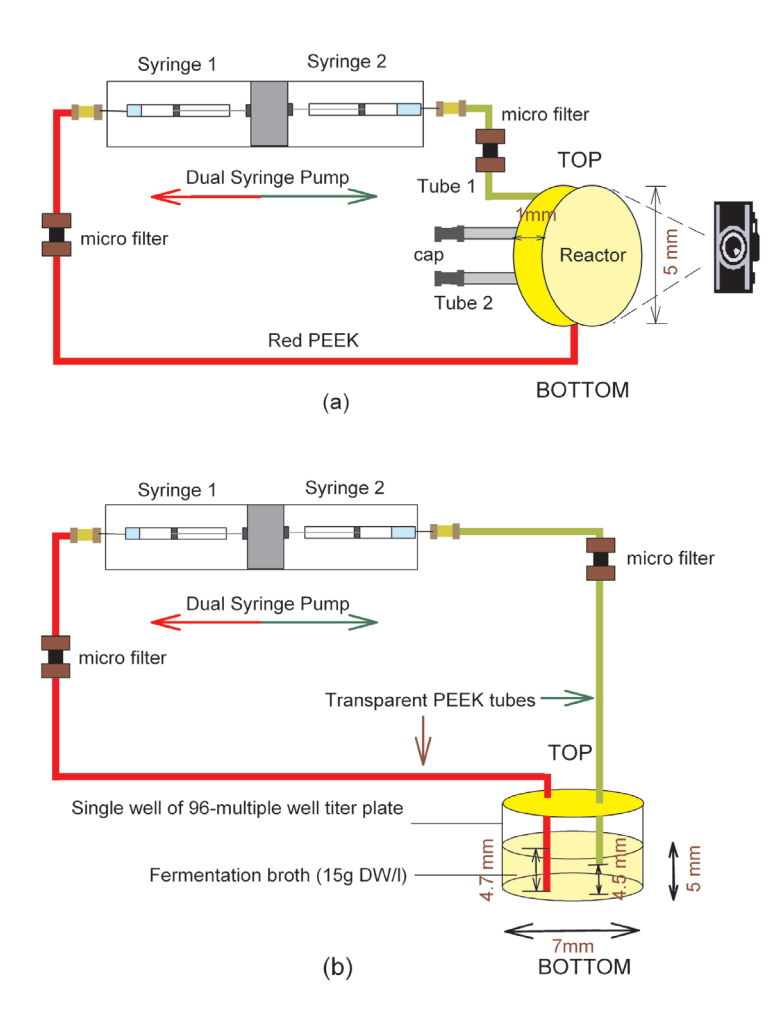


Figure 3-5 Schematic representation of experimental set-up, a) Cell settling experiment with  $27\mu l$  micro bioreactor; b) Cell settling experiments with single well from 96 multiple well titer plate

color density of the images was measured and it showed that mixing was achieved after a certain time.

#### Oscillation mixing on multi-reactors

To prove the principle, oscillation mixing was tested in a 96 multiple well titer plate. The experimental setup is shown in Figure 3-6. Three wells were closed by transparent PDMS caps. Three holes were drilled on each cap. Three transparent PEEK tubes (tube 1, tube 2 and tube3) were connected to 1 ml syringe (syringe 1) via a cross shape adaptor. Another three transparent PEEK tubes (tube 1', tube 2' and tube3') were connected to 1 ml syringe (syringe 2) via a cross shape adaptor. Tube 1 and tube 1', tube 2 and tube 2', tube 3 and tube 3' were coupled and then placed in three wells, respectively. The position

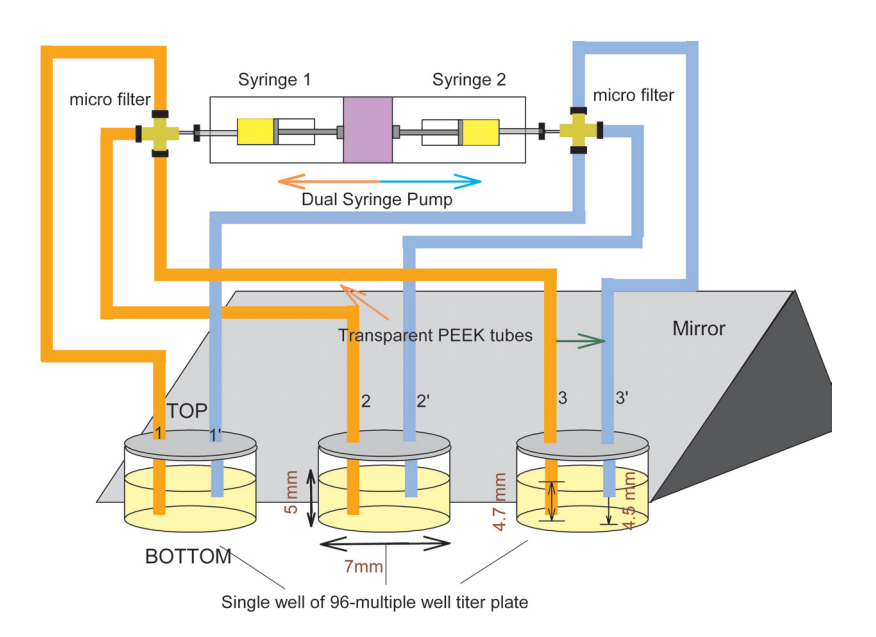


Figure 3-6 Schematic representation of experimental set-up for oscillation mixing of multi-reactors

of the coupled tubes was fixed via holes on the caps. Syringes were fixed on opposite sides of an oscillation pump. The oscillation syringe pump was set with fixed displacement volume (15  $\mu$ l) and fixed pumping rate (2000  $\mu$ l/min). A mirror was placed beside titer plate; the reflection of the mirror is the side view in the wells. 150  $\mu$ l clean water was filled into wells. 2  $\mu$ l of a solution of Rodamine red B dye in demineralised water was slowly injected into four wells as shown in Figure 3-9. Syringe pump was turned on. Pictures were

taken via digital camera. Top views, side views and transparent tubes were included in the pictures.

## Cell settling experiment & cell viability test

Fermentation broth was filled into microreactor , a micro filter was placed between the PEEK tube and the syringe pump to keep the cells inside the reactor and PEEK tubes. The reactor was placed vertically as illustrated in Figure 3-5 (a). The oscillation syringe pump displaced a fixed volume (2  $\mu$ l) at a fixed pumping rate (1000  $\mu$ l min $^{-1}$ ). The oscillation mixing was started and kept overnight.

The cell settling issue was additionally tested in a single well of a 96 multiple well titer plate as shown in Figure 3-5 (b). First, two transparent PEEK tubes were placed in the well and connected to two syringes, fixed on opposite sides of an oscillation pump. Second, the well was filled with 200  $\mu l$  fermentation broth, and the oscillation pump was set to a fixed displacement volume (10  $\mu l$ ) at a fixed pumping rate (1000  $\mu l$  min $^{-1}$ ). The oscillation mixing was started and kept overnight. At the end of the experiment, 2  $\mu l$  fermentation broth was taken from the well and was placed under a microscope equipped with the above mentioned CCD camera to take pictures of S. cerevisae.

For comparison, a micro magnetic stirrer bar experiment was performed. 200  $\mu$ l fermentation broth was filled into a single well of a 96 multiple well titer plate. The well was closed using a rubber cap. A hole was drilled in the magnetic stainless steel stirrer bar of 1.67mm × 2.01mm × 4.80mm dimensions (VP 711-1, V&P Scientific, Netherland) A needle was pinched through the center point of the rubber cap. The tip of the needle was bent as to fixate the stirrer bar at elevated height. The mixing started with a fixed speed 600 rpm. After four hours mixing, 2  $\mu$ l fermentation broth was taken from the well and was placed under a microscope equipped with the above mentioned CCD camera to take pictures of S. cerevisae.

#### 3.2.4 Data processing

#### Single reactor experiments

The mixing performance of the oscillating flow in the reactor can be quantitatively analyzed from the recorded pictures. However, unlike in the static mixer, which uses outlet concentration against inlet concentration to indicate the mixing performance, the quantitative analysis in this case uses a factor called colored area ratio. This colored area ratio is defined as A<sub>t</sub>/A<sub>t</sub>. A is the colored area size in m², subscript "t' is the time in s, and subscript "f" is indicates the equilibrium condition at the final state. The colored area is defined as the area where the dye has a more intense color than the final state color. Because the color intensity is directly related to the Rhodamin B concentration, the colored area is actually the area where the dye solution has a higher concentration than in the final state. One thing that needs to be noted is that for every single picture, the color intensity is influenced by the noise from the surrounding, which is mainly the slight change in light during the experiment. In order to eliminate the influence of that background, light change is monitored and it is excluded from the measured color intensity.

## Multi- reactors experiments

For the multi-reactors experiment, in order to simultaneously measure the mixing performance in all reactors, the quantitative analysis in this case uses the color density in several small areas in the reactor and in the transparent oscillation tubes. Because the color intensity is correlated with the Rhodamin B concentration, the constant color densities at the end of the experiments indicate a steady state dye concentration and full dispersion. Other factors, which were obtained from the images analysis, like, Standard deviation in the reactor area were used to describe the mixing in the reactor.

## 3.3 RESULT & DISCUSSION

#### 3.3.1 Simulation results

As mentioned in the simulation procedure, two parameters were set in the simulations, i.e. the maximum linear flow velocity on boundary 5 and the switching time. In Figure 3-7 the results are shown for a linear flow velocity of  $0.06 \text{ m s}^{-1}$ ,  $(v_1 = 0.06)$ , and a switching time of 0.12 s. (a = 83) The reactor very easily achieved complete mixing within 4 s. The mixing in the overall reactor system can be divided into two parts. The first part is the mixing inside the reactor unit where, due to the unevenly distributed flow velocity field, as shown in Figure 3-3 (b) and (c), a larger dye-influenced area was obtained (Figure 3-7). The main mixing mechanism in this part of the system is convection flow-based dispersion. The second part is the mixing in the microchannel, which follows a two-directional Taylor dispersion. Taylor dispersion arises from the velocity profile near the channel walls due to the no-slip flow condition at the solid-fluid interface. (Taylor et. al. 1953; Dutta et. al., 2006) Obviously, as discussed in many papers, the velocity profile will significantly contribute to the mixing behavior (i.e., Hong et. al., 2004; Beard et. al., 2001).

The Taylor-Aris dispersivity (K) is used to describe the impact of the Taylor dispersion compared to the molecular diffusion. The Taylor-Aris dispersivity

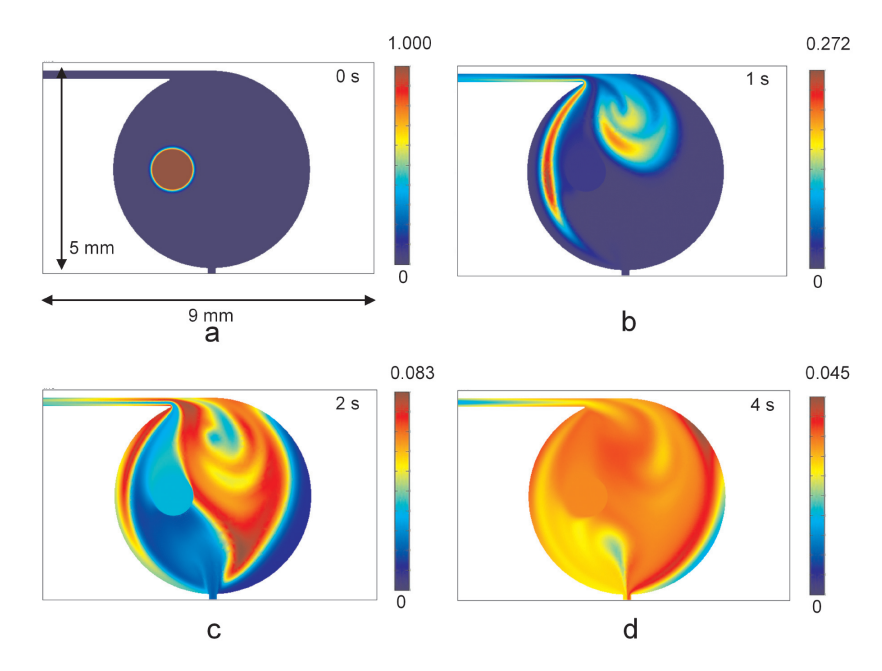


Figure 3-7 Simulation result of the concentration profile of oscillation mixing in the reactor at different times with the floe velocity set at 0.06m/s and the oscillation frequency 8.33Hz. a) t=0s; b) t=1s; c) t=2s; d) t=4s

(K) for pressure-driven flow between two parallel plates is given by (Wooding et. al., 1960):

$$\frac{K}{D} = 1 + \frac{1}{210} \left(\frac{Ud}{D}\right)^2$$
 Equation 3-5

where D is the molecular diffusion coefficient of the species (m² s⁻¹), U is the average fluid velocity (m s⁻¹) and d is the separation distance between the parallel plates (m). The above expression indicates that the overall mass transfer in the pressure-driven system arises from two additive contributions, diffusion transport in the flow direction (the first term of the equation) and the effective dispersivity due to the fluid shear (the second term of the equation). The latter term of the equation scales with the square of the Peclet number Ud/D, which estimates the relative magnitude of convection to diffusive transport rates in the system. The coefficient multiplying this dimensionless group in the above equation is a function of the channel cross section and has a value of 1/210 for two parallel plates. For a closed microchannel, it is

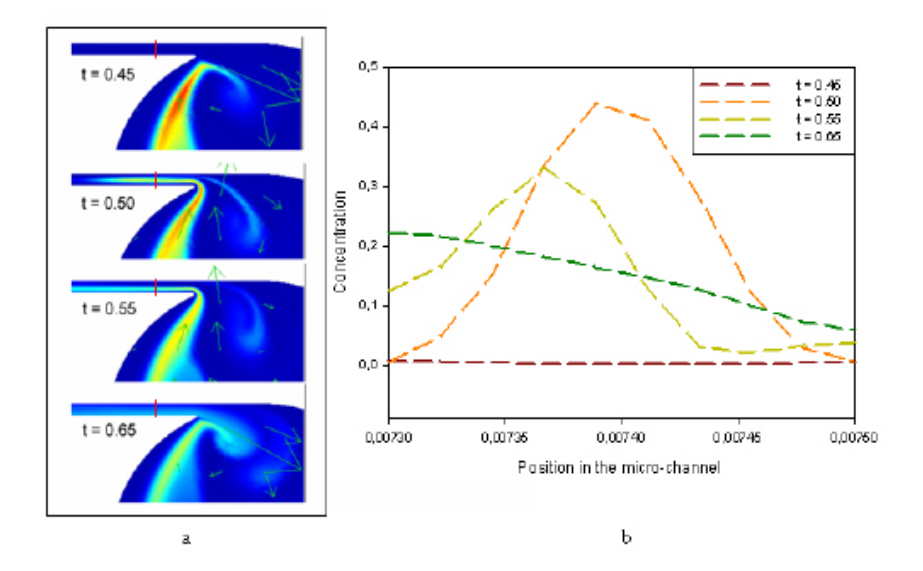


Figure 3-8 Simulation result of oscillation mixing in the micro reactor close to the micro channel inlet part for one pulling and pushing process, a) simulation results displaying the concentration field; b) time dependant concentration profile along the cross-sectional line in the micro reactor

important to note that the exact cross section of the channel can significantly affect the actual dispersion. Mathematically, that effect can be evaluated by introducing a function f in Equation 3-6 as (Dutta et. al., 2006):

$$\frac{K}{D} = 1 + f \left(\frac{Ud}{D}\right)^2$$
 Equation 3-6

The factor f relates to the shape of the channel cross section. The effect of the typical microchannel cross sections geometry on the hydrodynamic dispersion of the solution slugs has been well investigated in the past (Doshi et. al., 1978; Guell et. al., 1987; Dutta et. al., 2006). These studies have shown that the function f for this profile increases monotonically with an increase in the aspect ratio of the conduit. For a square cross section, which is close to our geometry, (Dutta et. al., 2006). On our microfluidic devices, since the diffusion coefficients for most analytes have values smaller than 10-5 cm<sup>2</sup> s<sup>-1</sup>, with channels having a diameter around 100 μm, linear flow rates larger than 1 cm s<sup>-1</sup>. K/D ratio has a value larger than 104, which indicates the

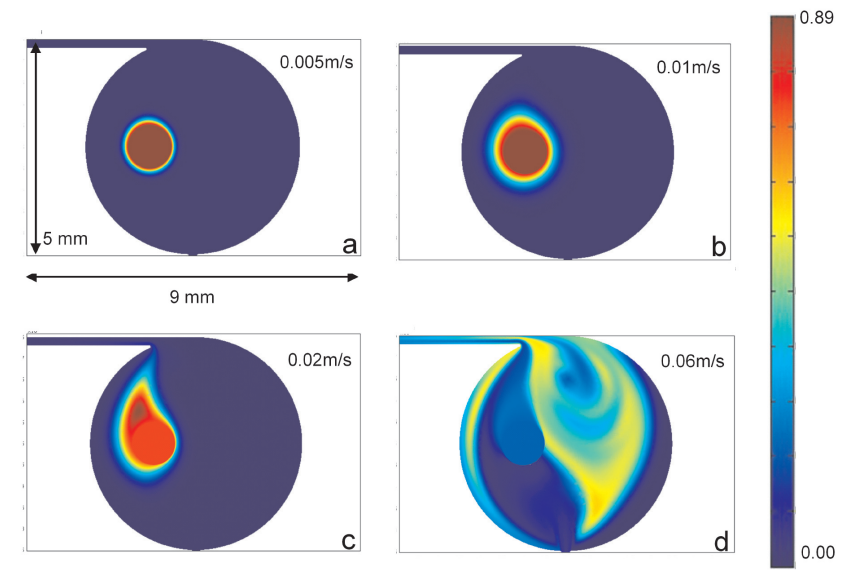


Figure 3-9 Simulation results of concentration profile of the oscillation mixing with different pulling and pushing linear flow rates; a) 0.005m/s; b) 0.01m/s; c) 0.02m/s; d) 0.06m/s with same oscillation frequency 8.33Hz at time 2s

dispersivity of the chemical significantly exceeds its diffusional limit (K/D = 1).

Two-directional Taylor dispersion gives very good mixing as shown in Figure 3-8 (a), which means that within one oscillating cycle, the dye concentration was already more homogeneously dispersed as shown in Figure 3-8 (b). Figure 3-9 clearly shows that the mixing time in the reactor decreases as the pulling and pushing flow velocity increases due to the impact of the increase in energy input. With a linear flow rate of 0.06 m s<sup>-1</sup> and an oscillation frequency 8.33 Hz, well mixing can be obtained within 10 s. However, the energy input is not the only factor that has an impact on this mixing method. The positions of the oscillation tubes also play an important role. During reactor design, it is necessary to make sure that the flow field evenly covers most area of the reactor, leaving minimal room for dead zones within the reactor.

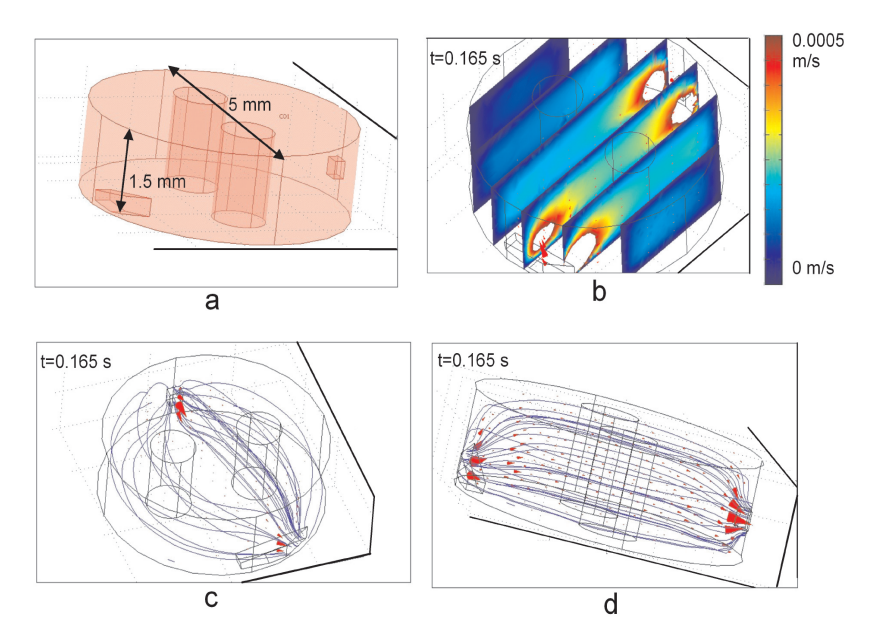


Figure 3-10 3D simulation results for oscillation linear flow rate 0.01m/s, frequency 8.33Hz, a) simulated geometry, b) linear flow velocity profile at time 0.165s, c) streamline profile on velocity field at time 0.165s (top view), d) streamline profile on velocity field at time 0.165s

The full 3D simulation results are shown in Figure 3-10, the streamline plots from the top view (Figure 3-10 c) and the side view (Figure 3-10 d) were compared. The parallel streamlines along the z-axis shown in Figure 3-10 (d) indicate that in the most part of the reactor the flow velocity is evenly distributed along the z-axis. That is also proved by the flow velocity profile shown in Figure 3-10 b. In the overall reactor only the spaces near the input port and output port are different, and it is caused by the size difference between the reactor and oscillation tube. In other words, the 3D simulation shows the validity of using 2D simulation to simplify this 3D geometry. Of course because of the size difference between the reactor and the oscillation tubes, 2D simulation may lose some details, and the simulated result deviates from the experimental one, however, the simulated result still represents sufficient fluid flow information in the reactor and in the oscillation tube.

#### 3.3.2 Experimental results

## Single reactor mixing experiment

Fig. 3-11 shows the comparison between the experimental results with an oscillating flow rate of 1000  $\mu$ l min<sup>-1</sup> (linear flow rate approximately 0.015 m s<sup>-1</sup>) and an oscillation frequency of 8.33 Hz and the simulation results with a fixed maximum linear flow rate of 0.02 m s<sup>-1</sup> and an oscillation frequency of 8.33 Hz. The correlation between A<sub>t</sub>/A<sub>t</sub> and time was used to characterize the micro mixing. The mixing time was defined as the time to reach an A<sub>t</sub>/A<sub>t</sub> value of > 95%. Figure 3-11 clearly shows that with a certain oscillation volume, the higher the pumping flow rate, the faster complete mixing will be achieved. The experimental mixing times are shown in Table 3-1.

It is also possible to use a simplified method to estimate the mixing time in the micro reactor by using a micro-mixing equation (e.g. Hofland et al., 2003):

$$t_{micro} = 0.1 \frac{\lambda_k^2}{D} = 0.1 \frac{v^{3/2}}{\varepsilon^{1/2}D}$$
 Equation 3-7

where  $t_{micro}$  denotes the mixing time in the microscale system in seconds;  $\lambda_K$ 

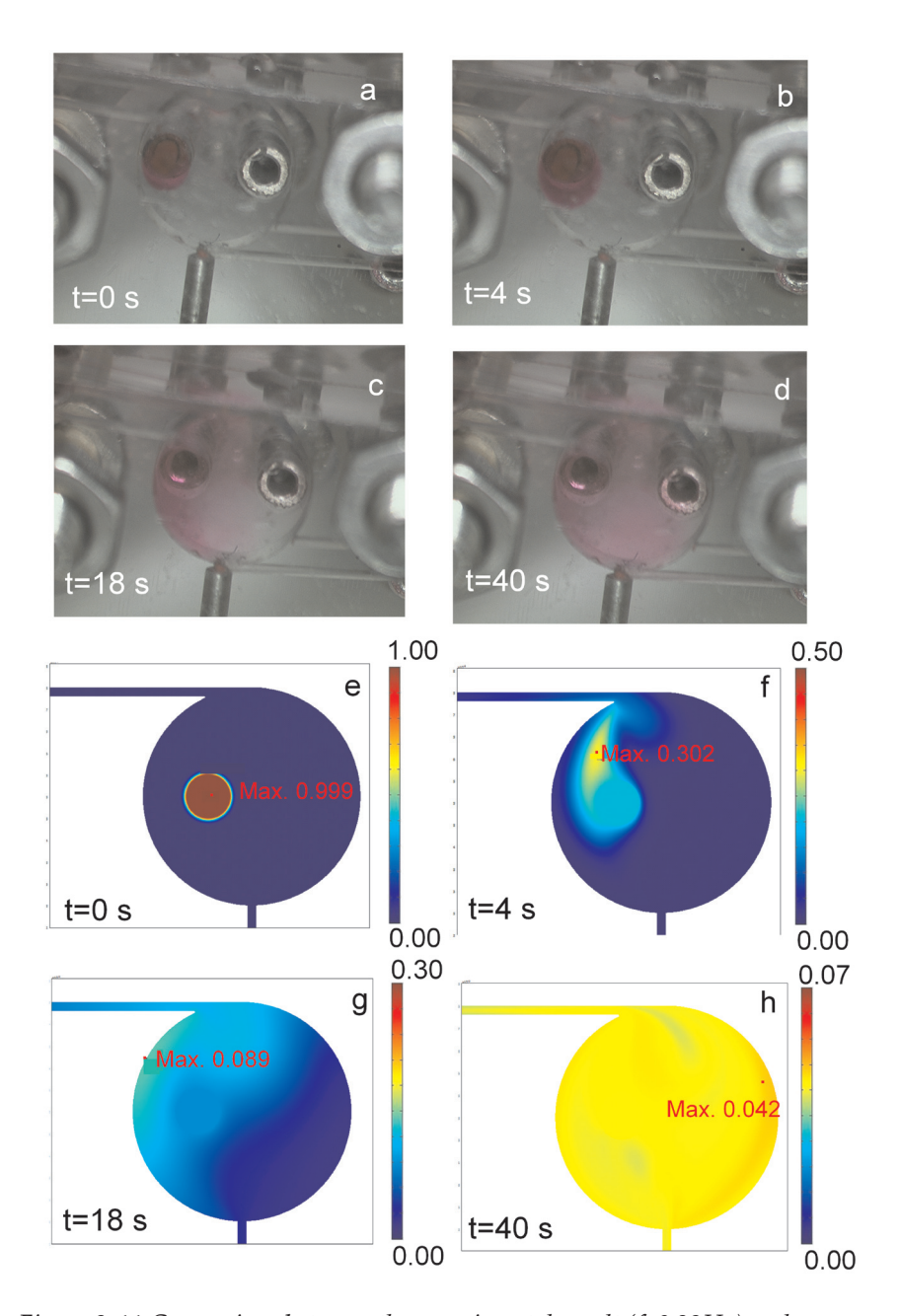


Figure 3-11 Comparison between the experimental result (f=8.33Hz) and simulation result (0.02m/s; 0.12s) a) t = 0s; b) t = 4s; c) t = 18s; d) t = 50s; e) t = 0s; f) t = 4s; g) t = 18s; h) t = 40s

denotes the Kolmogorov length scale in meters; D denotes the diffusivity in the liquid phase in  $m^2 \, s^{\text{-1}}$ ;  $\upsilon$  denotes the kinematic viscosity in  $m^2 \, s^{\text{-1}}$ ;  $\varepsilon$  denotes the energy dissipation rate in W kg<sup>-1</sup>.

The kinematic viscosity (v) can be calculated by:

$$v = \frac{\eta}{\rho}$$
 Equation 3-8

where  $\eta$  is the viscosity of the solution in kg m  $^{\text{-1}}$  s  $^{\text{-1}}$ ;  $\rho$  denotes the density of the solution in kg m  $^{\text{-3}}$  .

The energy dissipation rate  $(\epsilon)$  is defined as the energy input per kilogram solution, therefore, it can be estimated from:

$$\varepsilon = \frac{E_{Diss}}{V_R \cdot \rho} = \frac{E \cdot f}{V_R \cdot \rho} = \frac{\frac{1}{2} \cdot m \cdot v^2 \cdot f}{V_R \cdot \rho} = \frac{\frac{1}{2} \cdot V_{IN} \cdot \rho \cdot v^2 \cdot f}{V_R \cdot \rho} = \frac{V_{IN} \cdot v^2 \cdot f}{2 \cdot V_R}$$
Equation 3-9

where  $E_{\rm Diss}$  denotes the energy dissipation in Watt; E denotes the kinetic energy of the injected fluid in Joule; f denotes the frequency in Hz; m denotes the mass of injected liquid in kg;  $V_{\rm R}$  is the volume of the reactor in m³;  $V_{\rm IN}$  is the injected volume per cycle in m³; v is the linear flow rate around the port in m s¹. The mixing time can be estimated on the basis of the above equations. The results are given in Table 3-1.

Figure 3-12 compares the results from the 2D CFD simulation, the oscillation mixing experiments and the micro-mixing model correlation. A good match was obtained, especially within the high energy input range. However, a somewhat larger deviation was observed around the low energy input range. This can be partly explained by the fact that the influence of the dead-zone areas, which was obviously not taken into account in the micro-mixing correlation, has a larger impact in the low energy input range. Within the dead-zone areas, diffusion instead of convection takes a dominant role in the mass transfer mechanism.

Table 3-1 Comparison of results of mixing times from oscillation mixing measurement, a simplified micro-mixing correlation and CFD simulation results

Mixing time (s)	Flow rate (µl/min) (and corresponding Oscillation Frequency (HZ))			
	0 *	50	500	1000
	(0)	(0.42)	(4.17)	(8.33)
Experimental	>2500	412	132	45
Correlation	17860	698	70	35
FEMLAB simulation (2D)	16600	_		37

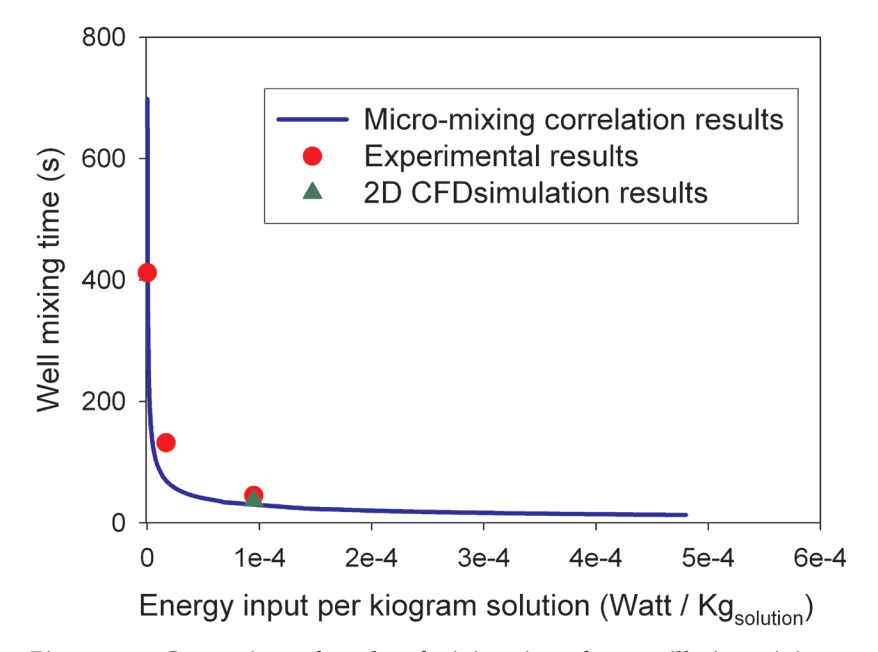


Figure 3-12 Comparison of results of mixing times from oscillation mixing experiments and a simplified micro-mixing correlation and 2D CFD simulations

The experimental curves (50  $\mu$ l min<sup>-1</sup>) given in Figure 3-13 indicate that the oscillation mixing process may have two different periods. In the first period rapid mixing takes place, and the  $A_t/A_f$  value (27% <  $A_t/A_f$  < 90%) shows a sharp increase (slope = 2.5×10<sup>-3</sup> per second). In the second period, the  $A_t/A_f$  value still increases (90% <  $A_t/A_f$  < 100%) but with a smaller slope (9×10<sup>-5</sup> per second). For the 1000  $\mu$ l/min curve, only the rapid increase period was observed. Furthermore, for the 500  $\mu$ l/min curve, a much shorter second period (95% <  $A_t/A_f$  < 100%) was observed. From the above illustration, it can be concluded that the fraction of the first period in the total mixing process increased as the oscillating flow rate increased. In other words, the slope of  $A_t/A_f$  vs. time curve increased with an increase in the convection flow rate, which proves that during the first period convection is the dominant factor that affects mixing. Furthermore, during the second period diffusion is the dominant factor, since the slope in the second period is close to the slope of the diffusion only curve (2×10<sup>-4</sup> per second).

For fermentation broths, it is possible to treat yeast cells as very small

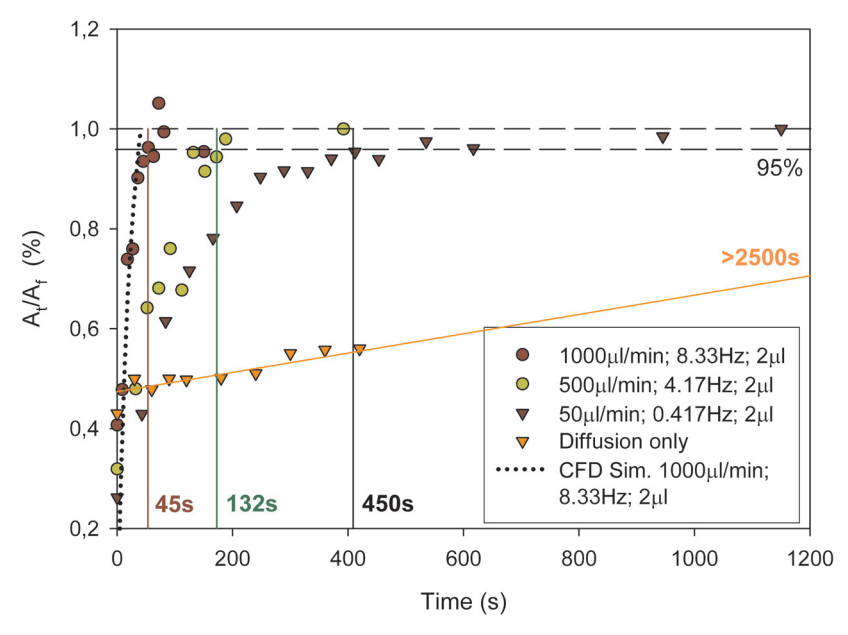


Figure 3-13 Experimental oscillatory micro reactor mixing, Different symbols indicate different frequencies and different flow rates

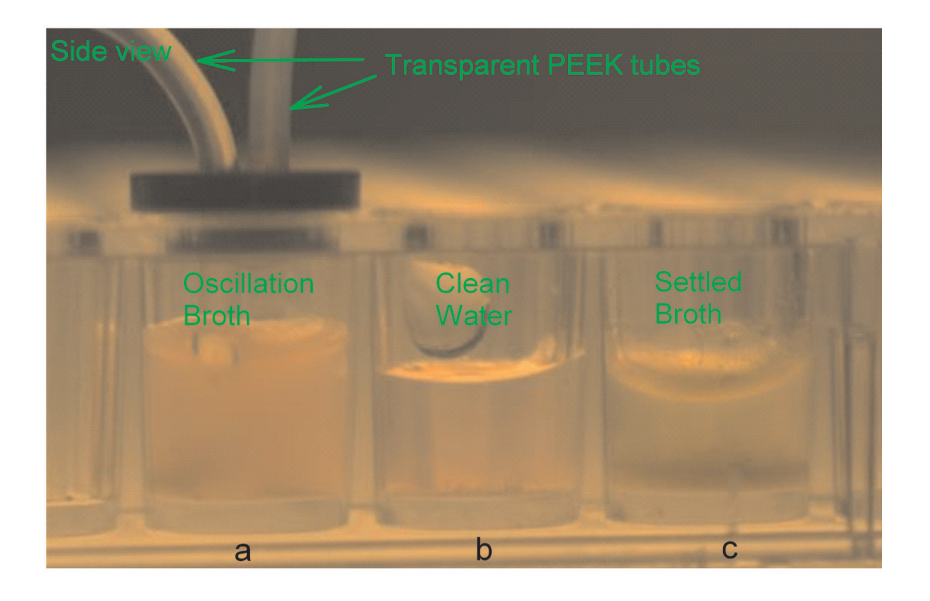
particles, which means the cells will follow the streamlines in the micro bioreactor. The dispersion of the cells within the reactor will mainly based on convection. Figure 3-13, clearly indicates that although in the micro reactor dye dispersion normally is due to both diffusion and convection, convection takes the dominant place especially under a high oscillation frequency. Therefore, both dye and the cells will follow the convective patterns (flow field) in the reactor. Thus, good convective dye mixing indicates good yeast cell mixing.

## Yeast cells settling issue

In the micro bioreactor, after overnight mixing, many cells kept suspended. This can be explained by the fact that there is less than 5% density difference between S. cerevisae and water. Therefore, with flow oscillation on the bottom of the reactor, which, in this case, is the oscillation around the PEEK port, cells gain sufficient drag to stay suspended. One thing needs to be noted is that because of the large distance between the top of the reactor and bottom of the reactor well (5 mm), and the relatively small oscillation area, the experiment with yeast concentrations of 15 g/l dry weight showed small areas with slightly higher cell concentrations than the rest of the reactor well. However, by switching the position of the oscillation tube as illustrated in Figure 3-5 b, during overnight mixing a more or less homogeneous cell suspension was maintained in the micro bioreactor as shown in Figure 3-14.

## Multi-reactors mixing experiment

Fig. 3-15 shows the experimental results of dye distribution conditions in four reactors. One is the diffusion based mixing reactor and other three are parallel reactors with same oscillation frequency 2.22 Hz (reactor 1 to reactor 3) as illustrated in Figure 3-16. The grey level in tube 1, tube 2 and tube 3 were monitored, the correlation between grey level and time was used to characterize the mixing in each reactor. The mixing time was defined as the time for the grey level to reach steady state. Because of the small dimensions of oscillation tubes, the measured grey level from the 2D pictures directly indicates the concentration of the dye solution in the tube, which is connected with a reactor.



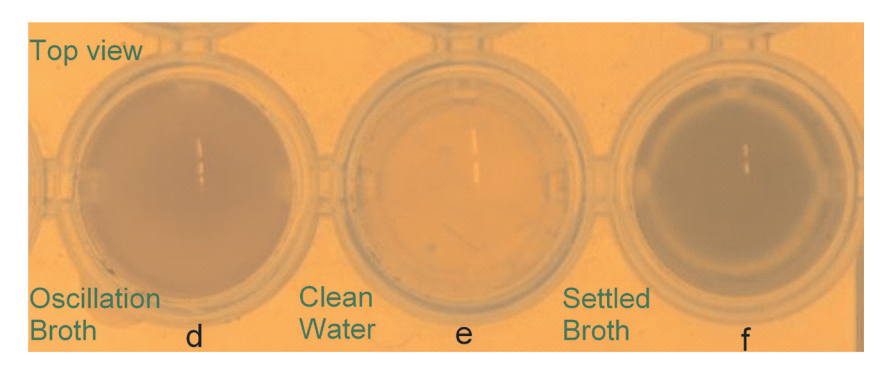


Figure 3-14 Experimental results of cell settling test for single well, a) side view of oscillated fermentation broth after overnight mixing with oscillation flow rate 1000µl/min, frequency, 1.66Hz; b) side view of clear water; c) side view of settled fermentation broth after overnight stand still; e) top view of oscillated fermentation broth after overnight mixing with oscillation flow rate 1000µl/min, frequency, 1.66Hz; f) top view of clear water; g) top view of settled fermentation broth after overnight stand still

Figure 3-16 indicates the correlation between the grey level and the time in the tubes. Mean grey level curves of three parallel reactors follow same trend, and reach to steady states at 120s, 122s and 128 s, respectively. The comparison of results between various tubes indicate a similar mixing behavior in different reactors. Hence, the result shows the possibility of using one central actuator to

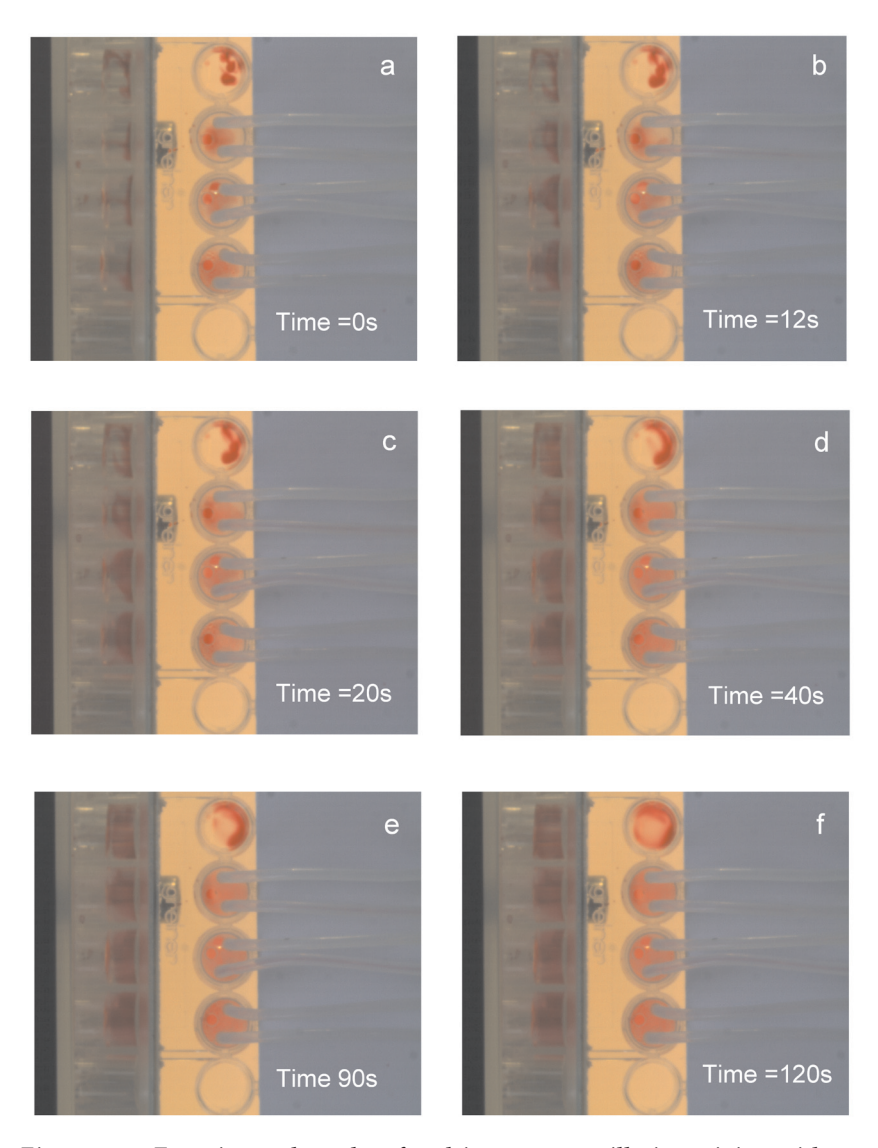


Figure 3-15 Experimental results of multi- reactors oscillation mixing with oscillation frequency 2.22 Hz, at time: (a) 0s, (b) 12s; (c) 20s; (d) 40s; (e) 90s; (f) 120s;

create oscillation fluids to achieve well mixing on multi- micro reactors. The small difference between the measured mixing times might caused by the slight deviation of initial dye injections. The calculated mixing time based on Equation 3-7 was 69 s, which is smaller than the experimental determined mixing time, but still in the same order of magnitude. The difference can be explained by the appearance of dead-zone area, in which mass transfer is

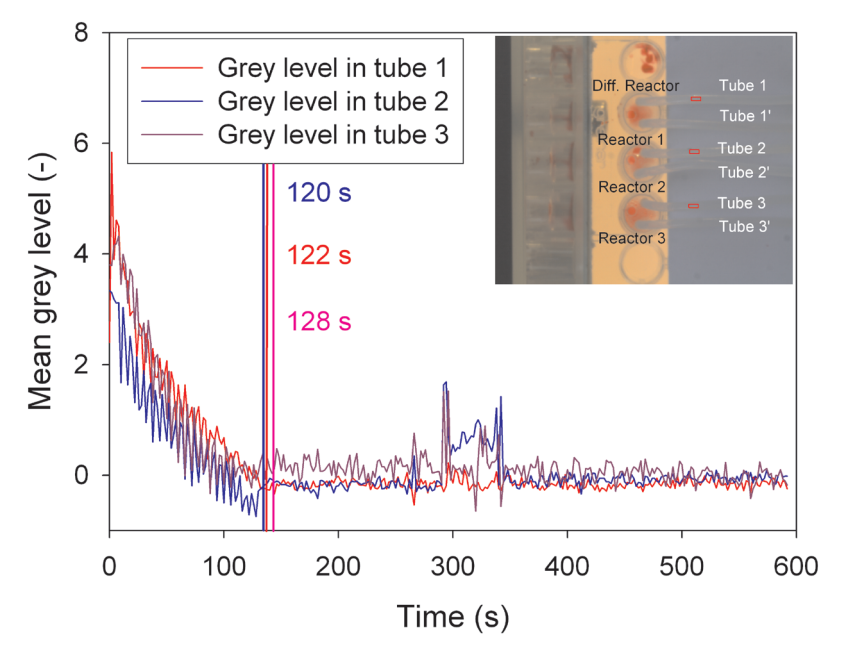


Figure 3-16 Experimental results for multi-reactors oscillation mixing experiment with oscillation frequency 2.22Hz

much slower than other parts of the reactor since diffusion is the dominant factor.

Figure 3-17 shows the standard deviation (SD) (curve) within four reactors from both side view and top view. The SD curve (side view) in Figure 3-17 (a) indicates the well mixing time (around 120 s), which is as same as the determined mixing time from Figure 3-14. However, the SD curve (top view) in Figure 3-17 (b) indicates a different well mixing time (around 60 s). As shown in Figure 3-15 (d), at time around 40 s, from top view, the dye already close to evenly distribution, however, from side view, clear color difference still exist. It indicates that the convection on the x-axis and the y-axis are much better than the convection on the z-axis. Because convection on z-axis is the bottleneck of the overall mass transfer, the mixing time indicated in Figure 3-17 (a) is the well mixing time of the reactor (around 120 s). For further improvement on this mixing method, increase convection on the z-axis will be the most efficient way.

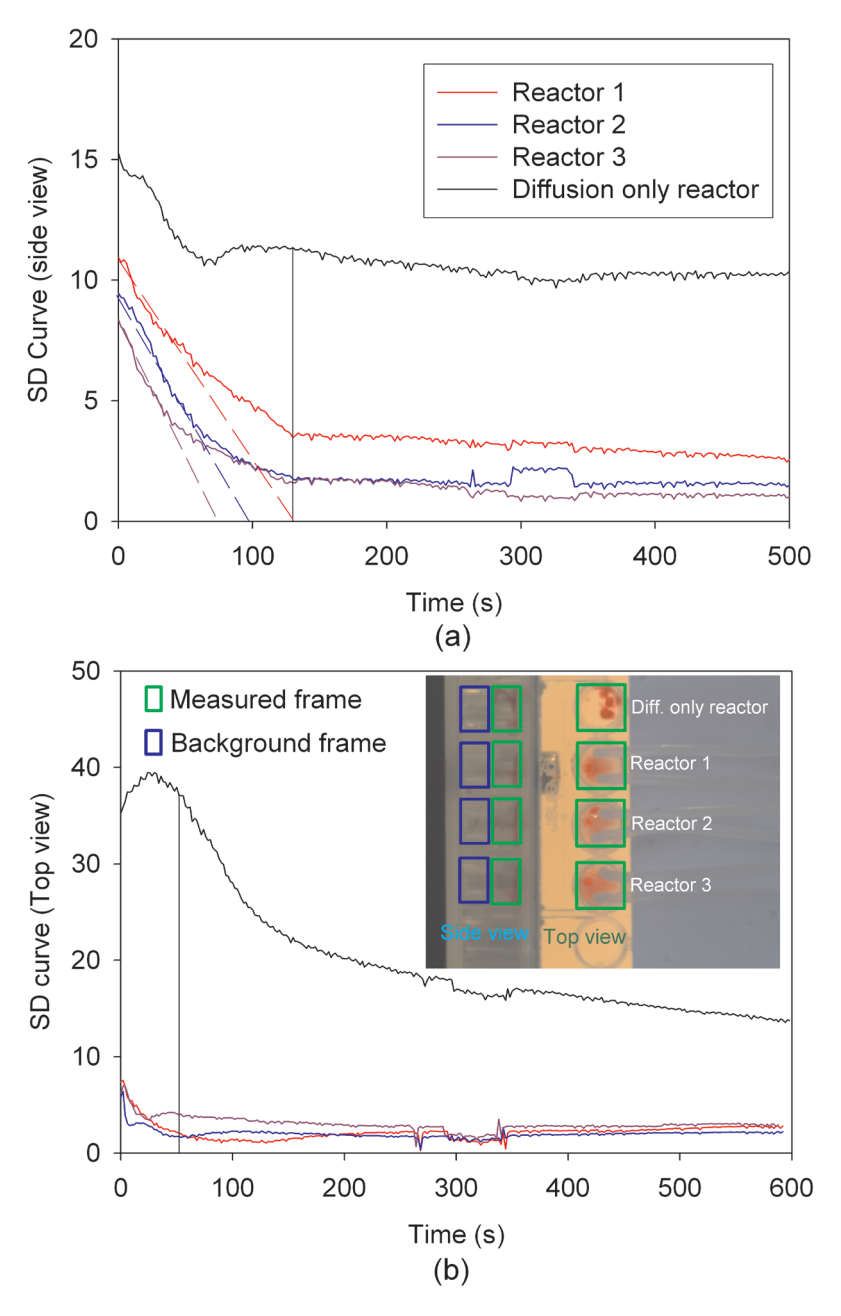


Figure 3-17 Experimental results of multi-reactor oscillation mixings with oscillation frequency 2.22 Hz (a) side view; (b) top view.

## Cell viability test

In Krommenhoek's work, serious cell damage, caused by the vigorous mixing (400–1200 rpm) of a magnetic stirrer in a single well of a 96 multiple well titer plate was reported. (Krommenhoek et. al., 2008). Figure 3-18 shows the comparison of cells condition between the overnight oscillation mixing and 4 hours magnetic stirrer mixing (600 rpm). It clearly indicates that more than 80% of the cells were broken after four hours magnetic stirrer mixing. In contrast, barely any cell breakage was observed after overnight mixing with the oscillation mixing method. Furthermore, a relatively long mixing time might not be a problem as long as the mixing prevents cell settling and the transport within the reactor of substrate and oxygen doesn't become limiting.

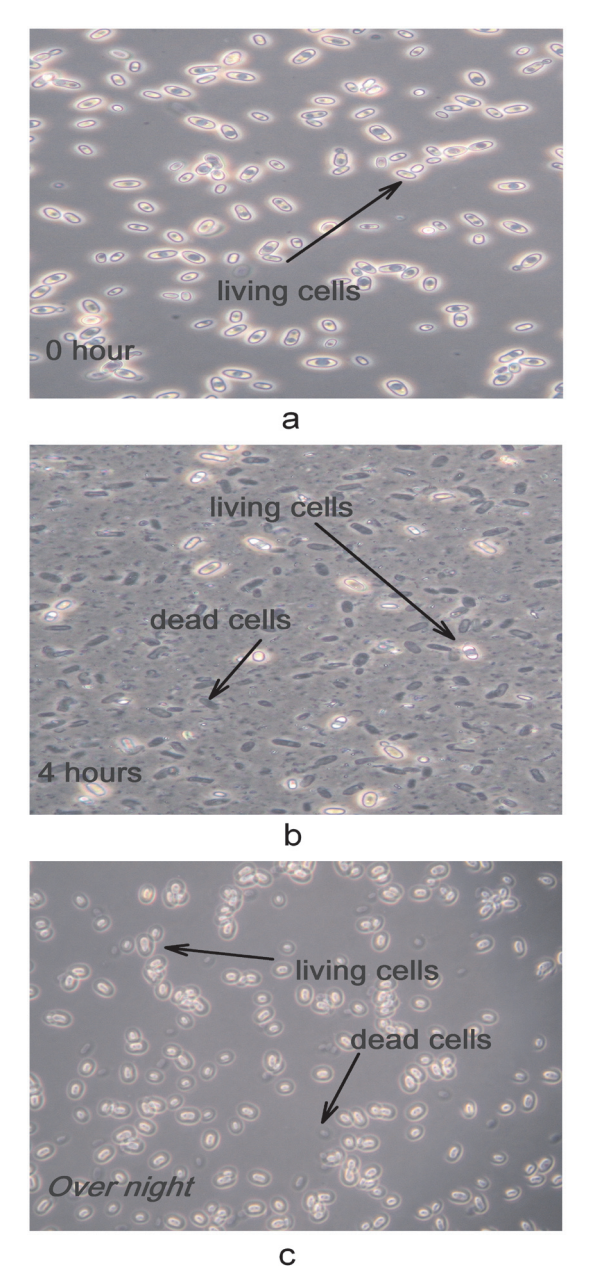


Figure 3-18 Experimental results of cell viability tests a) original fermentation broth, b) fermentation broth after 4 hours vigorous mixing with magnetic stirrer (600rpm), c) fermentation broth after overnight oscillation mixing in single well of 96 multiple well titter plate with oscillation flow rate 1000µl/min; frequency 1.66Hz; light cells indicate living cells, dark cells indicate dead cells

#### 3.4 CONCLUSION

In this chapter, a simple active mixing method for a micro bio-reactor using a pressure-based oscillating driving force was designed, simulated and tested. Good mixing performance was achieved under a high oscillate flow conditions. The experimental results show a reasonably good match with the simulated results and the model-based calculated results. The mixing performance shows that both diffusion and convection contribute to mixing, however, with a large oscillating flow rate the contribution from convection predominates. This method can be easily implemented on most simple micro-devices in the volume range several to hundreds microliter, without requiring any complex structures. No extra internal apparatus like stirrer bar or PZT crystal is needed. Preliminary experiments have been done to test the possibility of implementing this oscillation mixing method for multiple parallel reactors; it has been proved that a single central oscillation source is enough to create oscillation flow in different reactors. Furthermore, the position of the oscillation tubes definitely helps to prevent possible cell settling. Compared to the most commonly used microbioreactor mixing method, i.e. magnetic stirring, the effect of the oscillating flow on cellular viability and behaviour is considered to be not a problem, as the oscillation flow induced shear stress is not strong enough to damage the cells.

## Acknowledgements

This work is part of the ACTS-IBOS programme (IBOS 053.63.009), which is funded by the Dutch Science Foundation (NWO), DSM Anti-Infectives BV, Diosynth/Organon and Applikon BV

#### **Notation**

```
a = constant
A = the color area size, m^2
c<sub>i</sub> = concentration of chemical i in solution, kg/m<sup>3</sup>
d = separation distance, m
D<sub>1</sub> = diffusion coefficient, m<sup>2</sup> s<sup>-1</sup>
Diss = dissipation power, W
E = kinetic energy of the injected fluid, J
f = frequency, Hz
F = select volume force field, N
K = Taylor-Aris dispersivity, m<sup>2</sup> s<sup>-1</sup>
m = mass of injected liquid, kg
p = pressure,
                           Pa
R_i = reaction term for species i, kg s<sup>-1</sup> m<sup>-3</sup>
t = time, s
t_{micro} = the well mixing time, s
                          m s<sup>-1</sup>
u = velocity,
U = average fluid velocity in the channel, m s<sup>-1</sup>
v = linear flow rate around the port, m s<sup>-1</sup>
v_0 = the linear flow rate on the set boundary, m s<sup>-1</sup>
v_1 = the maximum linear flow rate of the pushing flow, m s^{-1}
V_{IN} = inject volume per cycle, m<sup>3</sup>
V_p = volume of the reactor, m^3
```

#### Greek letters

```
    ε energy dissipation rate, W kg<sup>-1</sup>
    η = dynamic viscosity, kg m<sup>-1</sup> s<sup>-1</sup>
    η = viscosity, kg m<sup>-1</sup> s<sup>-1</sup>
```

- $\lambda \kappa$  = Kolmogorov length scale, m
- $\rho$  = density, kg m<sup>-3</sup>
- $v = kinematic viscosity, m^2 s^{-1}$

#### References

- Balagaddé, Frederick K, Lingchong Y, Carl L, Hansen FH. Arnold, Stephen R. Quake, Long-Term Monitoring of Bacteria Undergoing Programmed Population Control in a Microchemostat, Science, 2005;309, 137-140
- Beard DA, Taylor Dispersion of a solute in a Microfluidic Channel, J. Appl. Phys., 2001; 89, 4667
- Bird RB, Stewart WE, Lightfoot EN, Transport Phenomena, NewYork, Wiley, 2001 book chapter;
- Chung YC, Order-changing microfluidic mixer, U.S.Patent, 2001; No. 6,331,073 B1
- Doig SD., Pickering SCR, Lye GJ, Baganz F, Modelling surface aeration rates in shaken microtitre plates using dimensionless groups, Chemical Engineering Science, 2005; 60, 2741-2750
- Doshi MR, Daiya PM, Gill WN, 3 dimensional laminar dispersion in open and closed rectangular conduits, Chemical Engineering Sci. 1978; Vol 33, 795-804
- Dutta D, Ramachandran A, Leighton Jr DT, Effect of channel geometry on solute dispersion in pressure-driven microfluidic systems, Microfluid Nanofluid 2006; 2 275-290
- Ehrfeld W, Golbig K, Hessel V, Lowe H and Richter T, Characterization of Mixing in Micro mixers by a Test Reaction: Single Mixing Units and Mixer Arrays, Ind. Eng. Chem. Res. 1999; 38, 1075-1082
- Guell DC, Cox GR, Brenner H, Taylor dispersion in conduits of large aspect ratio, Chem. Eng. Comm. 1987; Vol., 58, 231-244
- Hofland GW, Berkhoff MR, Witkamp GJ and van der Wielen LAM, Dynamics of Isoelectric Precipitation of Casein Using Sulfuric Acid, AIChE Journal, 2003; 49(8), 2211-2223

- Hong CC, Choi JW and Ahn CH, A novel in-plane passive microfluidic mixer with modified Tesla structures, Lab ON A CHIP, 2004; 4, 109 –113
- Melin J, Giménez G, Roxhed N, van der Wijngaart W and Stemme G, A fast passive and planar liquid sample micromixer, Lab on a chip, 2004; 4, 214-219
- Nguyen, NT and Wu Z, Micromixers--- a review, J. Micromech. & Microeng., 2005; 15, R1-16
- Kim DS, Lee SW, Kwon TH and Lee SS, Barrier embedded chaotic micromixer, IEEE, The Sixteenth Annual International Conference on Micro Electro Mechanical Systems, Kyoto, Japan, 2003; 19–23
- Kirner T, Albert J, Gunther M, Mayer G, Reinhackel K and Kohler JM, Static micro mixers for modular chip reactor arrangements in two-step reactions and photochemical activated processes, Book of Abstracts: IMRET7th International Conference on Micro reaction Technology, Lausanne, Switzerland 2003;101-105
- Kolbl A, Kraut M, and Schubert K. The lodide lodate method to characterize microstructured mixing devices, AICHE Journal, 2008; Vol. 54, No. 3, 639-645
- Kostov T, Harms P, Randers-Eichhorn L and Rao G. Low-Cost Microbioreactor for High-Throughput Bioprocessing, Biotechnology and Bioengineering, 2001; 72 (3) 346-352
- Krommenhoek, EE, van Leeuwen M, Gardeniers JGE, van Gulik WM, van den Berg A, Li X, Ottens M, van der Wielen LAM, Heijnen JJ, Lab-scale fermentation tests of micro chip with integrated electrochemical sensors for pH, temperature, dissolved oxygen and viable biomass concentration, Biotechnology and Bioengineering, 2008; 99(4) 884–892
- Li X, van der Steen G, van Dedem GWK, van der Wielen LAM, van Leeuwen M, van Gulik WM, Heijnen JJ, Krommenhoek EE, Gardeniers JGE, van den Berg A and Ottens M, Improving mixing in micro bioreactors, accepted for Chem Eng. Sci. 2008; 63, 3036-3046

- Liu R, Stremler HMA, Sharp KV, Olsen MG, Santiago JG, Adrian RJ, Aref H, and Beebe DJ. Passive Mixing in a Three-Dimensional Serpentine Micro-channel, Journal of Micro-electromechanical Systems, 2000; 9 (2) 190-197
- Monnier H, Willhelm AM, and Delmas H. Influence of ultrasound on micing on the molecular scale for water and viscous liquids, Ultrasonics Sonochemistry, 1999; Vol. 6, 67-74
- Monnier H, Willhelm AM, and Delmas H.The influence of ultrasound on micromixing in a semi-batch reactor, Chemical Engineering Science, 1999; Vol. 54, 2953-2961
- Schwesinger N, Frank T and Wurmus H. A modular microfluid system with an integrated micromixer. Jouranl of Micromech, Microeng. 1996; Vol (6), 99-102
- Suriani AR, Pitts B, Stewart PS, Rapid Diffusion of Fluorescent Tracers into Staphylococcus epidermidis Biofilms Visualized by Time Lapse Microscopy, Antimicrobial Agents and Chemotherapy, 2005; Vol. 49, 2, 728-732
- Tabeling P, Chabert M, Dodge A, Jullien C and Okkels F. Chaotic mixing in cross-channel micromixers, Phil. Trans. R. Soc. Lond. A, 2004; 362, 987-1000
- Taylor GI Dispersion of soluble matter insolvent flowing slowly through a tube Proc R Soctlond 1953; 219A: 186-203
- Verduyn C, Postma E, Scheffers WA, van Dijken, JP. Yeast, 1992; 8, 501-517
- Wolfram.1999; Mathworld wolfram, http://mathworld.wolfram.com/ HeavisideStepFunction.html
- Wooding RA Instability of a viscous liquid of variable density in a vertical Hele-Shaw cell, J Fluid Mech 1960; Vol. 7, 501-515
- Zanzotto A, Szita N, Boccazzi P, Lessard P, Sinskey AJ, Jensen KF. Membrane-Aerated microbioreactor for High-Throughput Bioprocessing, Biotechnology and Bioengineering, 2004; 87 (2), 243-254

- Zhao Y, Chen G and Quan Y. Liquid-liquid two-phase mass transfer in the T-Junction microchannels, AICHE Journal, 2007; Vol 53, No. 12, 3042-3053
- Zhang Z, Szita N, Boccazzi P, Sinskey AJ and Jensen KF. Monitoring and control of cell growth in fed-batch micro bio-reactors, 7TH International Conference on Miniaturized Chemical and Biochemical Analysis Systems< California, USA; 2003
- Zhang Z, Perozziello G, Szita N, Boccazzi P, Sinskey AJ, Geschke O, and Jensen KF. Microbioreactor "Cassette" with integrated fluidic and optical plugs for high-throuput bioprocessing. Micro-TAS 2005
- Zhen Y, Matsumoto S, Goto H, Matsumoto M, Maeda R. Ultrasonic micromixer for mixfofluidic systems, Sensors and Actuators A, 2001; Vol. 93, 266-272

# Chapter **4**

Quantitative determination of glucose transfer between cocurrent, laminar flowing water streams in H-shaped microchannel

Part of this chapter is submitted to *Biotechnology progress* as M. van Leeuwen, X. Li, E.E. Krommenhoek, W.M. van Gulik, J.G.E. Gardeniers, M. Ottens, L.A.M. van der Wielen, J.J. Heijnen for publication

#### **Abstract**

The transfer of glucose was investigated between cocurrent laminar flowing water streams in a rounded H-shaped microchannel. Two miscible water streams were joined in microchannel in which the mass transfer took place. This joined channel had a length of 4 mm, a depth of 50 µm, and a width of 100 and 200 µm at the bottom and the top of the channel, respectively. The microchannel was operated at residence times of less than 1 s ensuring high mass transfer rates. Fully developed laminar flow in the microchannel was confirmed by computational fluid dynamics (CFD) simulations as well as by microscope observations. Special attention was paid to flow splitting at the end of the channel, because CFD simulations indicated that the experimental results were very sensitive to unequal flow splitting. The measured difference in outflow volume of the two streams was measured to be very small (1.25%  $\pm$  0.6 %). The measured glucose concentration in the both exit ports at a fixed residence time was found to be stable in time and reproducible over multiple experiments. CFD simulation provided as a very powerful tool for estimating the mass transfer in an H-channel even at very short residence times. The experimental and computational results for glucose transfer compared well.

The results obtained in this work are a proof of principle for the controlled diffusive supply or removal of a solute to / from a water stream by making use of cocurrent laminar water - water flow micro devices. The microdevice could potentially be used in the simultaneous addition of substrate to and removal of product from a microbioreactor to be able to perform fed-batch cultivations with In-Situ product removal (ISPR).

#### 4.1 INTRODUCTION

Microfluidic devices consist of channels with dimensions of tens or hundreds of micrometres in which fluids are manipulated. They are becoming powerful tools in analytical and (bio)chemical research because they exhibit unique features and hold the promise to perform high-throughput experiments on small sample volumes at reduced labor costs.

Probably the most important characteristic of fluids moving through a micrometer-scale channel is the absence of turbulence in the fluid. Turbulence is characterised by the Reynolds number. The Reynolds numbers in a microchannel is typically less than 100 indicating a strictly laminar flow regime. Because of the lack of turbulence, diffusion is the predominant mixing mechanism in the microchannel. When two miscible streams come together in a microchannel, they flow in parallel to each other, forming a stable liquid-liquid interface over which components can be transferred via diffusion, therefore it is sometimes called a laminar fluid diffusion interface (LFDI) (Kamholz and Yager, 2001; Shui et al., 2007; Whitesides, 2006). This unique feature of microfluidics is applied for example in enzymatic (Maruyama et al., 2003) and chemical conversions (Kenis et al., 1999) that occurred at the interface of the two liquid streams, in the measurement of diffusion coefficients (Hotta et al., 2007) and most frequently in separation and extraction processes (Brody and Yager, 1997; Jandik et al., 2002; Oakey et al., 2002; Weigl et al., 2001).

For the practical application of a device that consists of two laminar flowing liquids in an H-shaped channel, three aspects are crucial: a) stable liquid-liquid interface b) well defined mass transfer in the microdevices, c) equal splitting of the two flows at the end of the device. In the current literature the focus is very much on the stability of the interface, while little attention is paid to the quantitative mass transfer in the device especially in combination with flow splitting. In most articles that discuss the quantitative transfer over LFDI, only the theoretical aspects are discussed (Kamholz and Yager, 2001), or the solute concentration is directly measured within the channel (Curran and Davies, 2005; Ismagilov et al., 2000) and little attention was paid to the splitting of the streams.

Furthermore, the main focus on applicability of the H-shaped microchannels is for extraction processes, i.e. the H-filter (Jandik et al., 2002), while the fast

and controlled addition of molecules to a stream, without diluting the stream, is also very interesting, but is hardly investigated. For extraction processes the design of the H-shaped channel is based on the maximization of the total amount of a desired compound in the receiving stream, and minimizing the mass transfer of undesired component; for this purpose relative long contact times are required. For the fast addition of solutes to a stream, the H-shaped channels should be designed for fast mass transfer rates, yielding short contact times.

The H-shaped device that is designed for short contact times has the potential to be integrated to a small scale cell cultivation system. Such a device allows for the simultaneous addition of substrate to or continuously removal of (by)-product from a small scale cell micro-organism cultivations system or microbioreactor, to perform fed-batch cultivations with in-situ product removal integrated. Fed-batch is important to reach high product concentrations during cultivations in which the substrate concentration affects the productivity and the yield of the desired product in a negative way, because fed-batch operation makes it possible to maintain the substrate concentration in the bioreactor at a low level during the cultivation. In practice, high cell density cultivation usually has limited performance, which is normally due to product inhibition causing a decrease in microorganism activity, or product degradation resulting in low yield. Keeping the dissolved product concentration low in the reactor can obviously circumvent these limitations. An approach that can accomplish this task is the implementation of an in situ product recovery/removal (ISPR) technique. Figure 4-1 shows a schematic representation of the possible application of the H-shaped microchannel in a microbioreactor set-up.

In this chapter two water streams in an H-shaped micro channel that is designed for large mass transfer rates was jointed, and then was split at the end. Equal outflow was checked and the transfer rate of glucose in the device was calculated for different residence times, by measuring the concentration in both outflows. The experimentally determined glucose transfer rates were compared to CFD calculations. The robustness of the setup was checked by measuring the glucose concentration at each of the two outflows for multiple hours after the start of the experiments.

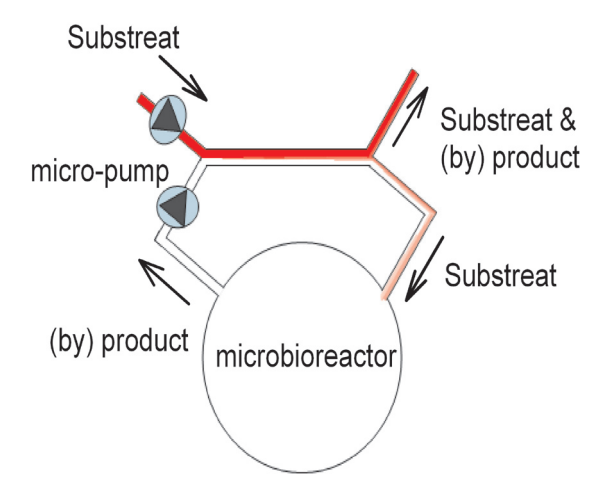


Figure 4-1 Schematic representation of possible application of H-shape microfluid device, i.e., for micro-bioreactor

#### 4.2 MATERIALS and METHODS

# 4.2.1 CFD design and Simulation

3D simulations were performed by using the commercially available computational fluid dynamics (CFD) software package COMSOL 3.3 (COMSOL, Sweden). The geometry of the model was shown in Figure 4-2 a. Channel 1 and Channel 2 were set as entrances of pure water and glucose solution respectively, channel 3 and channel 4 were exits of solutions; all four channels were designed as a quarter circle with a radius of 950  $\mu$ m to reduce the impact of flow direction conflict. Channel 5 was a straight joint channel with length 4mm. The depths of all channels were 50  $\mu$ m. The width of the channel was 50  $\mu$ m and 150  $\mu$ m at the top and the bottom of channel 1 to 4 respectively and was 100  $\mu$ m and 200  $\mu$ m for channel 5.

The model uses the Incompressible Navier-Stokes equations (Equation 4-1 a, b) and the Convection and Diffusion equation (Equation 4-2). The model equations are formulated below (Bird et al, 1960):

$$\rho \frac{\partial U}{\partial t} - \nabla \cdot \left[ \eta \cdot \left( \nabla U + (\nabla U)^T \right) \right] + \rho U \cdot \nabla U + \nabla P = F$$
Equation 4-1 (a,b)
$$\nabla \cdot U = 0$$

$$\frac{\partial c_i}{\partial t} + \nabla \cdot (-D_i \nabla c_i + c_i U) = R_i$$
 Equation 4-2

In the above equations,  $\eta$  denotes the dynamic viscosity of the solution (kg m<sup>-1</sup> s<sup>-1</sup>), U denotes the velocity vector (m s<sup>-1</sup>),  $\rho$  denotes the density (kg m<sup>-3</sup>), P is the pressure (Pa),  $c_i$  denotes the concentration of chemical i in solution (kg m<sup>-3</sup>), D<sub>i</sub> denotes its diffusion coefficient (m<sup>2</sup> s<sup>-1</sup>), and R<sub>i</sub> denotes the reaction term (kg s<sup>-1</sup> m<sup>-3</sup>). F denotes the selected volume force field (i.e. gravity), which influences the velocity field, (N m<sup>-3</sup>). The expression within the brackets in Equation 4-2 represents the flux vector, where the first term describes the transport by diffusion and the second represents the convective flux.

The dimensions of the simulation geometry were designed for laminar flow regimes. Therefore, mass transfer only happens in the joint channel, which is channel 5 as shown in Figure 2 (A). In order to control the calculation complexity and still gain detailed diffusion information from CFD simulation, only channel 5 was fully simulated as original dimensions, channel 1 to 4 were simplified from quarter circle channels to straight channel with channel length 0.5 mm and width 50  $\mu m$  and 100  $\mu m$  at the top and the bottom as shown in Figure 4-2 b.

For Incompressible Navier-Stokes equations, boundary 21 and boundary 43 was set as no slip boundaries to indicate two independent channels. The section at the entrance of the joined channel was found to be particularly important in order to create the appropriate velocity profile at the entrance of the joined channel. Combined point, split point and direct contact area were set as internal boundaries. Linear flow rates of water feeding stream and glucose feeding stream were set on boundary 3 and boundary 22 respectively. Steady state situations were simulated. Velocity field result was stored and used in Convection and Diffusion equation afterwards.

For Convection and Diffusion equation, unique diffusion coefficient

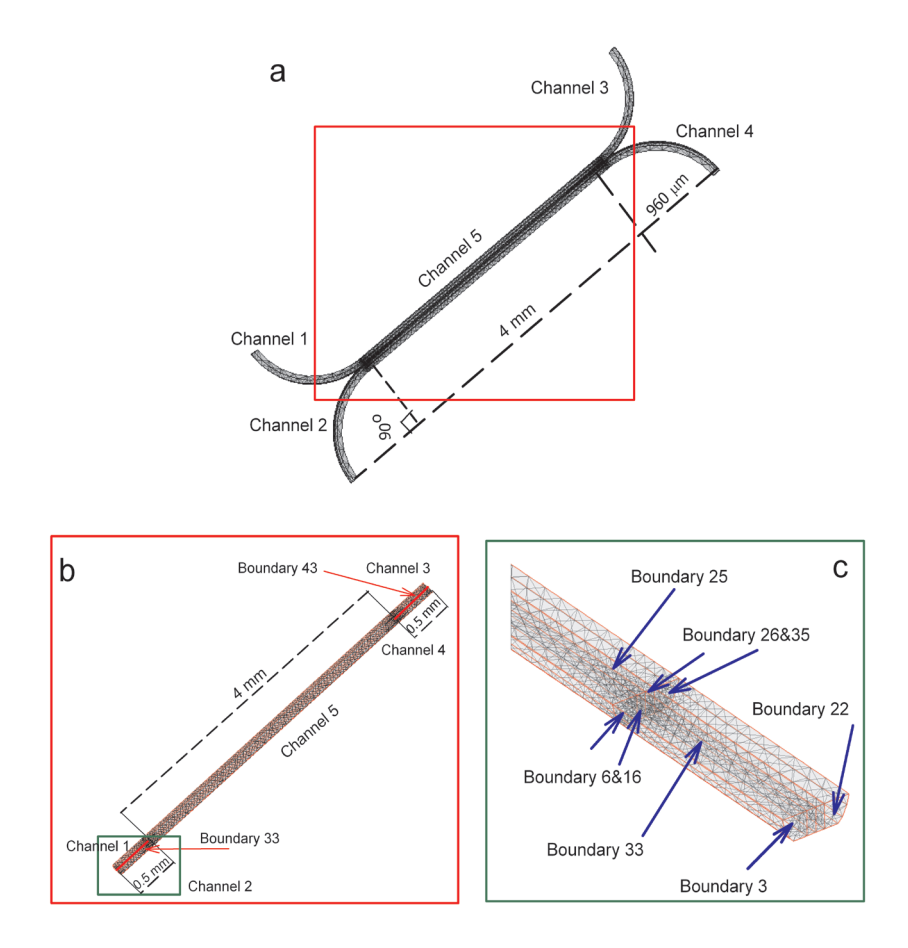


Figure 4-2 Simulation grids and simulation geometry, A, Original geometry and mesh of the experimental device; B, Modified geometry and mesh used for CFD simulation; C, Zoom in geometry and mesh at green position

6.7e-10 m² s⁻¹ was set for all boundaries. Concentration on boundary 3, 6 and 16 was set to 1, which indicates glucose solution stream (channel 1). Concentration on boundary 22, 26 and 35 was set to 0, which indicates pure water stream (channel 2). Boundary 33, 25, 9, 19, 29 and 38 were set as internal boundaries. Boundary 43 was set as discontinuous boundary to indicate channel 3 and channel 4. Linear flow rate in channel 1 and 2 were set to zero, which indicates only diffusion happens in the channel. After simulated the steady state condition, glucose concentration at combined point

was determined. By comparing the total glucose concentration between the combined point (boundary 6, 16 and 26, 35) and the split point (boundary 9, 19 and 29, 38), the amount of transferred glucose was calculated. Varying linear flow rates, which were preset in the simulation for boundary 3 and 22, the correlation between the residence times on the glucose mass transfer was studied. Set a constant value to linear flow rate at one of the two outlet boundaries (boundary 10 and boundary 42) and keep the other one neutral, the impact of unequal flow on glucose mass transfer was studied.

The simulation contained 13988 nodes in total. A finer mesh was used around the point where the two streams combined (boundary 6, 16, 26 and 35) and split (boundary 9, 19, 29 and 38) as well as at the contact plane (boundary 25) between both streams over which the mass transfer took place.

Pure water and a dilute glucose ( $D_i = 6.7 \times 10$ -10 m2/s) solution were used as model fluids ( $\eta = 10^{-3}$  kg m<sup>-1</sup> s<sup>-1</sup>,  $\rho = 998$  kg m<sup>-3</sup>) for the two entering streams. The linear flow rates ranged from of 3.7 - 88.8 mm s<sup>-1</sup>, which correspond to residence times in the joined channel of 1.08 - 0.045 s. The correlation of volumetric flow rate and residence time is given in Figure 4-3. At steady state conditions, the glucose concentration at both exits was determined at the point of flow splitting by integration of the two separate 3D glucose profiles.

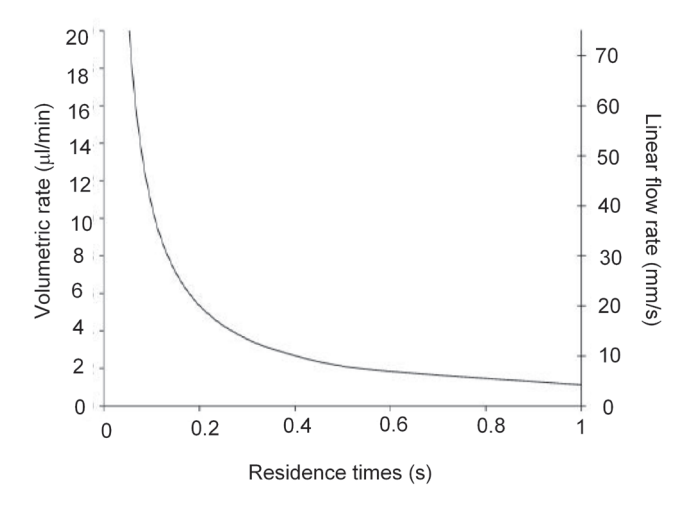


Figure 4-3 Correlation between volumetric rate (per stream), linear flow rate and residence time in microchannel

The effect of unequal flow splitting on the glucose concentrations in both exit streams was studied by setting the linear flow rate at one of the two outlet boundaries while keeping the other one neutral.

# 4.2.2 Microchannel fabrication

The Borofloat glass chips with a size of 8×12 mm were obtained from Micronit Microfluics B.V. (Enschede, The Netherlands). In the chip two channels were etched with a depth of 50 µm that joined together forming one joined channel for a length of 4 mm, in which exchange of molecules between the two streams could take place, and than split again into two separate channels. In order to reduce mixing at the point the two streams joined and to enhance splitting of the two streams, the entrance and exit channels were designed as quarters of a circle with a radius of 950 µm. Because of the isotropic etching process, the width was 50 and 150 µm at the bottom and the top of the individual channels respectively. Whereas the joined section of the channel had a width of 100 and 200 µm at the bottom and the top, respectively. The fabrication sequence for the chips in brief consists of the following steps: a chromium mask was made in order to define the channel structures; one side of the glass wafer was covered with a photoresist foil and treated with photolithograpy using the chromium mask; the structure was etched out of the glass by HF etching; after removal of the resist foil and thorough cleaning of the glass wafer, it was aligned and bonded to a second glass wafer, using a thermal process. This second glass wafer contained the through-holes micromachined by powder blasting. Finally the bonded pair of glass wafers was diced into individual chips. A photo of the chip is shown in Figure 4-4 b.

A chip holder was fabricated to connect the chip to the syringe pump was fabricated in house (Figure 4-4 b). The chip holder consisted of a PMMA block (width: 3.7 cm, length 1.8 cm, thick: 1.0 cm) out of which the dimension of the chip was milled. The chip was inserted in the cut away and enclosed by a 1 mm thick PMMA cover slip which was held in position by 4 screws. Four holes (1 mm diameter) in total were drilled from the left or right side of the chip holder to the powder blasted entrance and exit points on the chip. At the end of the four holes a 6-32 coned ports were micromachined in the PMMA to be able to connect steel capillaries (outer diameter: 1/32 inch, inner diameter:

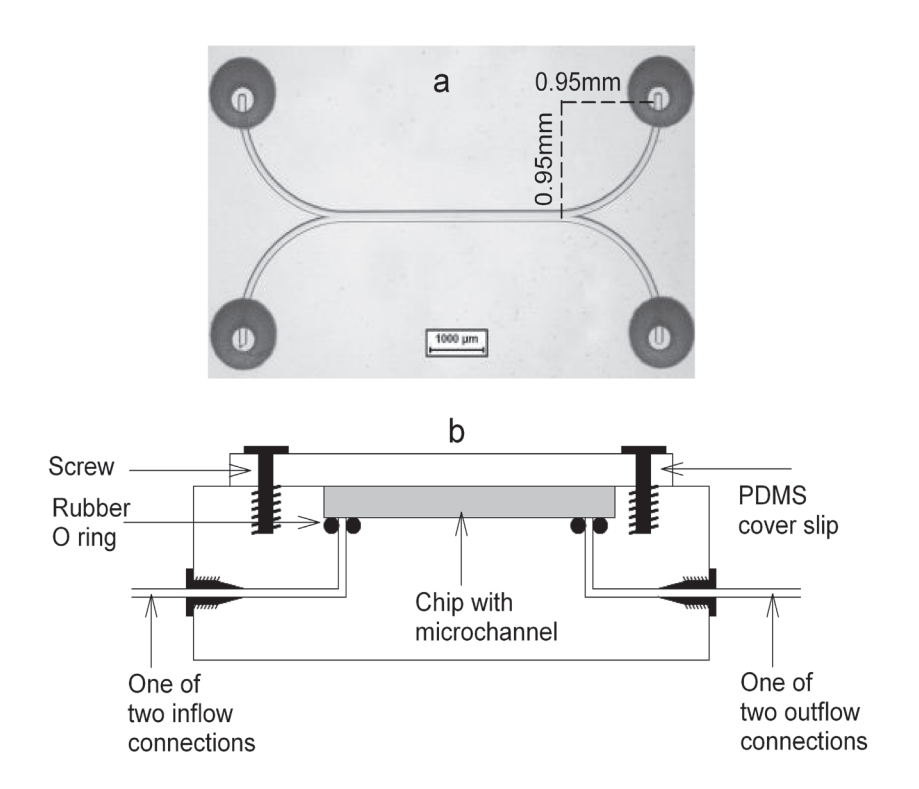


Figure 4-4 a) Micrograph of chip (top view) with the closed microchannel that was etched in a glass substrate, b) schematic cross section of the chip holder

 $600~\mu m$ ) using standard headless 6-32 coned fitting (Upchurch Scientific, Inc. Oak Harbor WA, USA). The two steel capillaries that were connected to the entrance channels of the chip, were connected two 2.5 ml glass syringes (SGE Analytical Science Pty. Ltd., Victoria, Australia) which were placed in a syringe pump (KD Scientific 210, Antec Leyden B.V., Zoeterwoude, The Netherlands). The liquid was collected at the other 2 capillaries.

# 4.2.3 Visual verification of the laminar flow regime

The chip holder that was connected to the syringw pump was placed under a microscope and pictures were taken of two concurrent water flows (residence time of 4 ms) in the microchannel of which one of the flows was colored with Rhodamine B (2.8 mM)

#### 4.2.4 Mass transfer experiments

For the glucose mass transfer experiments the supply liquid was aqueous glucose solution (10.4 mM) and the receiving liquid was demineralized water. Both solutions were pushed through the microchannel by syringe pump with a constant flow rate. During a glucose mass transfer experiment, half a dozen samples (75-150  $\mu L$ ) were taken in time from both outlet streams. The glucose concentration in those samples was determined with Enzytec TM enzymatic kits (kit 1002781). The enzymatic kit was scaled down for use with 96-well titer plates. Absorption was read on a Tecan plate reader (Tecan, Salzburg, Austria). All solutions prepared freshly and were filtered (Millex®HV, 0.45  $\mu m$  pore size, Millipore, Ireland) before use.

Similar mass transfer experiments were carried out at varies volumetric flow rates, namely 20, 10, 5, 2.5, 1.25  $\mu$ l/min per inflow stream, corresponding with residence times in the diffusion channel of 54, 107, 214, 428, 857 ms.

#### 4.3 RESULT AND DISCUSSION

The specific interfacial area for mass transfer in a diffusion channel of our microstructure was calculated to be 11.2×10³ m²/m³, which is three orders of magnitude higher than the specific interfacial area in conventional higherficiency equipment for liquid/liquid extraction, which was reported to be in the order of 1-20 m²/m³ (Lee et.al., 1997; Venkatanarasaiah and Varma, 1998). The high specific interfacial area in the microchannel under development as compared to conventional equipment clearly shows the advantage of laminar fluid diffusion interface (LFDI) devices for processes in which high mass-transfer rates are important.

In order to investigate and predict the mass transfer characteristics of the device, the mass transfer of glucose between two concurrently flowing water streams was used as a model system. For the practical applicability of such devices, three aspects are crucial: a) laminar flow regime, ensuring a stable liquid-liquid interface; b) proper separation of the two liquid streams at the

end of the diffusion channel; c) well defined mass transfer in the microdevices. These aspects are discussed subsequently.

# 4.3.1 The flow field

The Reynolds numbers that were calculated for the range of liquid flow rates that were applied in the experiments varied between 1 and 15. These low Reynolds numbers clearly indicate that the flow regime in the microchannel was laminar.

Computational fluid dynamic (CFD) simulations provided detailed information on the flow and velocity patterns in the micro channel as shown in Figure 4-5. The two entrance channels with a length of 0.5 mm were necessary

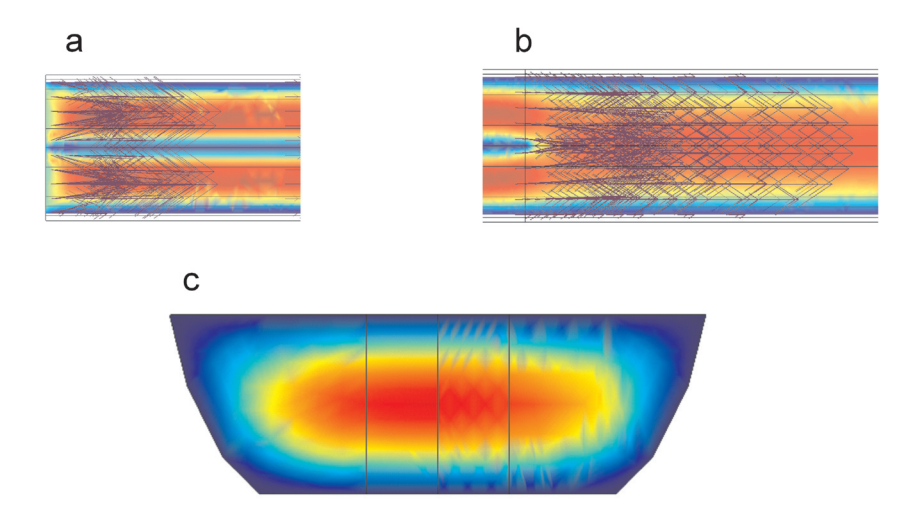


Figure 4-5 CFD simulation results of linear flow velocity fields in micro channel at different positions in the channel. (a) The velocity field (bottom view) in the two inlet channels; (b) In the diffusion channel at the position where the two channels join; (c) Flow velocity field (cross area) at 1mm after the two channels joined; The full simplified microchannel that was used for the CFD calculation including the grid is depicted by Figure 4-2 b. The flow rates are expressed as relative to the average velocity, which was 22.2 mm/s

for developing the parabolic, Hagen-Poiseuille flow profiles before reaching the diffusive channel. The steady state flow, as was simulated by the COMSOL 3.3 software package, showed that the flows are fully developed well before the pointed where the two separate channels were joining (Figure 4-5 a).

These simulations also indicated that at the joining point the mass transfer as a result of the convective mixing was small, but significant, for residence times below approximately 0.5 seconds (Figure 4-10) and was therefore taken into account in the calculations of the mass transfer rate. Furthermore, 0.1 mm after the joining point fully developed parabolic flow was achieved with a stable interface between both water streams as illustrated in Figure 4-5 b. Because of the dimensions and shape of the channel the flow was parabolic both across the channel height and width as can as can clearly be seen when taken a cross section of the channel as shown in Figure 4-5 c.



Figure 4-6 Micrograph of two aqueous streams at the joining point of the streams, halfway the channel and at the separation point (from left to right); the upper stream is coloured with Rhodamine B. The total residence time of the fluid in the diffusive channel was 54 ms

A stable liquid-liquid interface was confirmed in experimental observations. The liquid-liquid interface of the cocurrent flow of two water streams was visualised by colouring one of the streams with Rhodamine B and micrographs were taken at different positions of the joined channel (see Figure 4-6). At the position where the two streams combined, a stable liquid-liquid interface was formed and no turbulent mixing was observed between the two colliding streams. Along the length of the channel liquid-liquid interface remained sharp, indicating laminar flow.

#### 4.3.2 The concentration profiles

Because of the difference in glucose concentration between both streams, mass transfer takes place over the contact plane. Provided laminar flow and short residence times, the concentration profile around the contact plane is steep, resulting in a high mass transfer rate of glucose between both streams. A short residence time was defined as a Fourier number of less than 0.2. This design criterion was met at average residence times in the joined channel of less then 1 second.

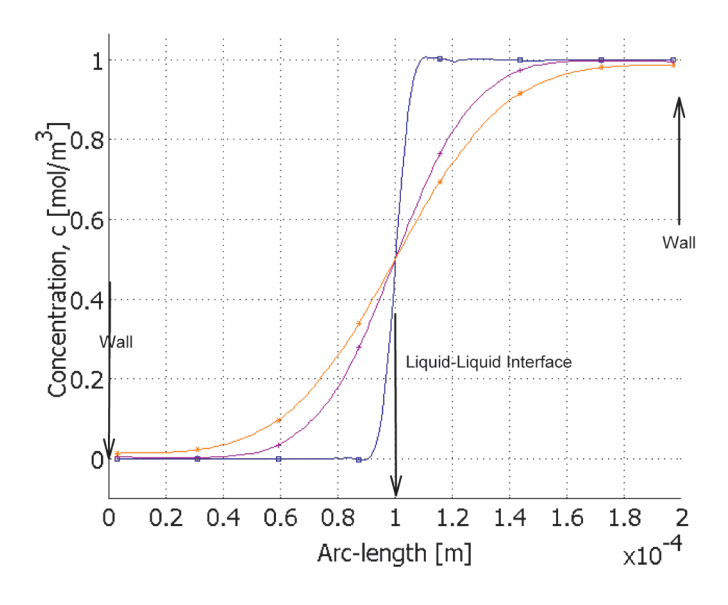


Figure 4-7 Concentration profiles perpendicular on the flow direction at residence times of 0, 0.36 and 0.72  $\rm s$ 

The glucose concentration profile around the contact plane was calculated with CFD simulations. Figure 4-7 depicts the simulation results for glucose profile perpendicular to the channel at different positions in the channel when a linear flow rate of 5.56 mm s<sup>-1</sup> (residence time at the split point is 0.72 s) was applied. The simulation results confirm the expected steep concentration profile around the liquid-liquid interface and at the joining point. As expected, at loner residence times the concentration profile becomes flatter while the inter-diffusive zone broadens. These simulation results were used for the quantification of the glucose transfer at different residence times.

The parabolic flow velocity profile in the micro channel induces widening of the inter-diffusion zone at the sides where contact plane between both streams comes near the wall of the channel. This curving of the diffusion front near the wall is sometimes called the butterfly effect (Kamholz and Yager, 2001). In the 3D CFD simulations this effect was clearly observed as shown in Figure 4-8, and taken into account for the quantification of the glucose transfer.

Because the experiments were performed at residence times smaller than 1 second, the glucose concentration in both the supply stream and the receiving stream were still far from equilibrium when they were split again, ensuring high mass transfer rates. However when this inter-diffusive zone is not split in the middle of the liquid-liquid interface, because of inequalities in the outflow volume, it causes differences between the measured and predicted glucose transfer. For instance, when the outflow volume of receiving stream is larger than the outflow volume in the feed stream, then, a proportion of the glucose that is found in the receiving outflow port was not transferred via diffusion

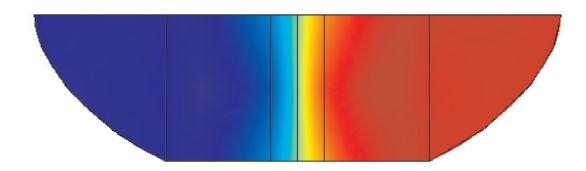


Figure 4-8 Glucose concentration profile in micrchannel, cross area at 2mm after joining the streams. The results are obtained from CFD simulation at a residence time 0.72 s at the end of the channel. The colour scale has the units of mM

to this stream but ended up in the receiving stream because of the unequal outflow. Besides, unequal flow splitting should be prevented also because it will, in the case of a recycle stream from / to a micro-bioreactor, result in draining or flooding the micro-bioreactor.

The effect of unequal outflow on the glucose concentration in the outflow ports was quantified with CFD simulations and is summarized in Table 4-1. It can be inferred from this table that the amount of glucose in the receiving stream is very sensitive to unequal flow splitting, especially at short residence times. When there is unequal flow appears in either inflow streams or outflow

streams, the contact area will switch from the middle of the channel. Because there is a large concentration gradient around contact area (Figure 4-7), a little change on splitting flows will cause a huge difference on the glucose concentration in the outflow stream as shown in Table 4-1. With 5% change on outflow stream in channel 3, which causes 10% unequal flow splitting (outflow in feed stream / outflow in receiving stream = 90% or 110%), the amount of transferred glucose in channel 4 varies from 6% to 48% based on different residence time. As it is indicated in Table 4-1 that the slower flow velocity case has a better stability to handle the flow disturbance, which can be explained by the fact that with a slower flow velocity the concentration gradient around the contract area at the split point is more modified than the concentration gradient at same position with a higher flow velocity. In one word, this result shows the importance of having a stable liquid-liquid interface and flow splitting in the system, furthermore, to reduce the impact of potential small flow disturbance on the outlets, the system prefer to be operated under low flow velocity.

Equal flow splitting was checked experimentally by subsequently collecting and weighing the liquid from both outlet channels during a certain time interval. It must be noted that for equal flow splitting serious attention should be paid to remove air bubbles or particles that could restrict one of the flows as well as to the precise fabrication of the H-shaped channel.

Triplicate measurements resulted in a difference in volumetric outflow between both exits of 1.25 %  $\pm$  0.6 % (average  $\pm$  standard deviation), which is much better compared to earlier findings of flow splitting (Hotta et al., 2007). This result significantly increases the practical applicability of these devices.

Table 4-1 The deviation on glucose concentration in the outflow stream (channel 4) as a result of unequal flow splitting

Residence	Deviation of linear flow rate	Glucose transfer rate	Deviation of glucose transfer
time (ms)	at channel 3	(g/l/s)	rate at channel 4
,	(%)	,,	(%)
	0.00%	2.224	
45	-5.00%	3.282	47.54%
	5.00%	1.230	-44.71%
	0.00%	0.958	
180	-5.00%	1.148	19.80%
	5.00%	0.783	-18.29%
	0.00%	0.434	
720	-5.00%	0.472	8.57%
	5.00%	0.410	-5.62%

# 4.3.3 Quantification of the glucose transfer

Integration of the simulated glucose concentration profiles after flow splitting, yielded the glucose concentration in both outlet streams. The experimentally determined glucose concentrations in both outflow streams were determined for five different residence times (54, 107, 214, 428 and 857 ms). Half a dozen samples were taken successively over a time period of multiple hours for each residence time. The concentrations at both outflow streams were found to be very constant for multiple hours (data not shown). The glucose concentrations in both outflow streams at different residence times as were determined by CFD simulations. The simulated and experimentally determined glucose concentrations in both streams are plotted as a function of the residence time in Figure 4-9. It indicated from this figure that the relation between the glucose concentration sin both streams and the residence time in the diffusion channel, obtained from the CFD calculations, compared very well with the experimental results. Furthermore, the obtained results confirm that partitioning of the glucose over both streams is still far from equilibrium.

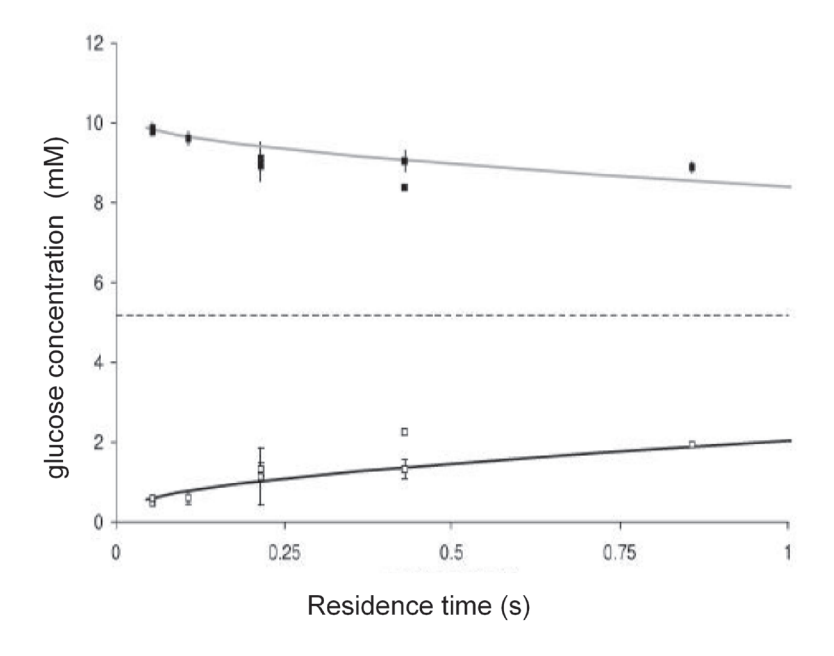


Figure 5-9 Comparison of the glucose concentration at the outflow streams (channel 3 (black) and channel 4 (white)) at different residence times in the joined sction of the microchannel obtained by measurements and CFD simulation (solid line). The dashed line (---) indicates the equilibrium concentration. The error bars of the measurement points show the standard deviation of the measurement

The glucose transfer in the microdevice different residence times were calculated from the concentration differences in the inlet and outlet streams. Complementary mass transfer rates were calculated based on the concentration data obtained from the feed or the receiving stream. The glucose transfer result that original the measurements correspond well to the data obtained by the CFD simulations as is shown in Figure 4-10. Glucose transfer rates of 2.4 – 11.9 nmol/min were obtained for average residence times of 54 – 847 ms, respectively between cocurrent flowing water streams with a glucose concentration of 10.4 mM. It is indicated from Figure 4-10 that the average glucose transfer rate decreased at increasing residence times. The reason for this is that the glucose concentration gradient at the contact plane decreases at increasing residence times, resulting in a decreasing mass transfer rate.

Because of the high volume to surface area in the channel, i.e. 11.2×10<sup>3</sup>

 $m^2/m^3$ , the average transfer rates are high (0.73 – 3.58 mol  $m^2$   $h^{-1}$ ) even at small concentration gradient between the two streams as is the case in our experiments.

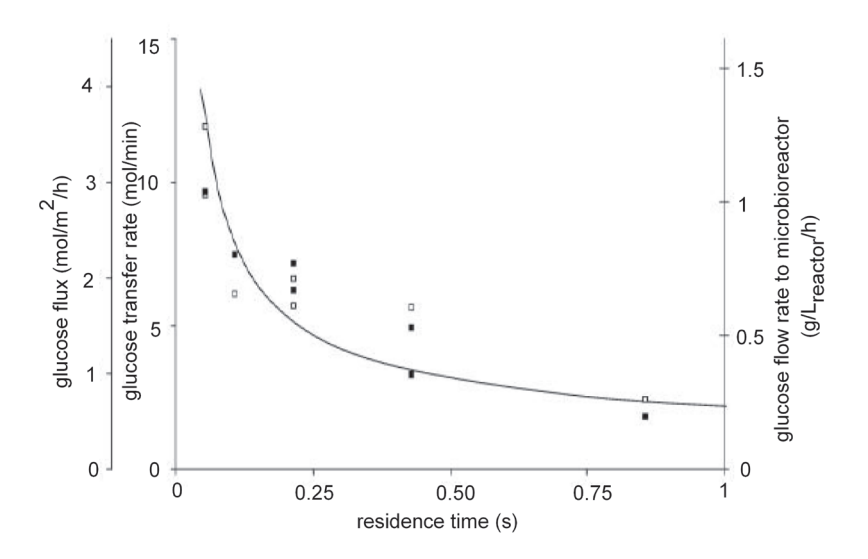


Figure 5-10 Comparison of the experimental (based on feed (black) and receiving (white) streams) to CFD (solid line) results for glucose transport at different residence. The glucose transfer is expressed as rate, as flux and as flow rate

If the microchannel would be applied for a fed-batch cultivations in a 100  $\,\mu l$  microbioreactor, glucose feed rates ranging from 0.26 to 1.3 g  $L_{\rm reactor}^{-1} \, h^{\text{-}1}$ , could be achieved, which is sufficient to perform fed-batch cultivations at high biomass concentrations.

It can be concluded from the above results that CFD simulation was found to be a very powerful tool for estimating the mass transfer in an H-shaped microchannel, even at very short residence times. Furthermore, the experiments results proved to be reproducible.

For an even closer match between simulation and experiment, in the CFD simulations the flow velocity profile at the upstream position of the diffusion

channel should be improved. Furthermore, the isotropic etching of the channel resulted in a non-perfect link up to the two separate channels into the diffusion channel. This was not taken into account in the CFD simulation.

#### 4.4 CONCLUSIONS

The mass transfer of glucose between cocurrent flowing water streams in an H-shaped microchannel was used as a model system to investigate and predict the mass transfer over the liquid-liquid interface. The joined section of the microchannel that was fabricated in a glass substrate had a specific interfacial area for mass transfer of 11.2×10<sup>3</sup> m<sup>2</sup>/m<sup>3</sup>. Residence times in the joined channel of less than 1 second were applied, ensuring high mass transfer rates.

CFD simulations provided detailed information on the flow patterns as well as the glucose concentration profiles and resulting mass transfers in the diffusion channel of the device. The measured glucose concentration in the both exit ports at a fixed residence time was found to be very stable in time and reproducible over multiple experiments. From the measured concentration differences, glucose transfer rates of 2.4 -11.9 nmol/min and glucose fluxes of 0.73 – 3.58 mol m<sup>-2</sup> h<sup>-1</sup> were calculated for average residence times of 54 -857 ms and at a glucose concentration in the feed of 10.4 mM. From the good match between the CFD simulation and experimental results for glucose transfer it can be concluded that CFD simulations are a powerful and reliable tool for estimating the mass transfer in the H-shaped laminar fluid diffusion interface (LFDI device, even at relatively short residence times.

The results presented in this work contribute to the increased understanding of the mass transfer in LFDI devices and thus improving their applicability for the fast and controlled transfer of compounds between two liquid streams.

One such an application of LFDI devices could be the feeding and in-situ product removary in microbioreactors. If the microchannel would be applied for fed-batch cultivations in a 100ml microbioreactor, glucose feed rates ranging from 0.26 to 1.3 g  $\rm L_{reactor}^{-1}\,h^{-1}$ , could be achieved, which is sufficient to perform fed-batch cultivations at high biomass concentrations.

# Acknowledgements

This work is part of the ACTS-IBOS programme (IBOS 053.63.009), which is funded by the Dutch Science Foundation (NWO), DSM Anti-Infectives BV, Diosynth/Organon and Applikon BV

#### **Notation**

c<sub>i</sub> = concentration of chemical i in solution, kg/m<sup>3</sup>

D<sub>i</sub> = diffusion coefficient, m<sup>2</sup> s<sup>-1</sup>

F = volume force field,  $N m^{-3}$ 

g = gravitational acceleration, m s<sup>-2</sup>

P = pressure, Pa

Re = Reynolds number, -

R<sub>i</sub> = reaction term for species i, kg s<sup>-1</sup> m<sup>-3</sup>

t = time, s

U = velocity vector, m s<sup>-1</sup>

#### Greek letters

 $\eta$  = viscosity, kg m<sup>-1</sup> s<sup>-1</sup>

 $\rho$  = density, kg m<sup>-3</sup>

# References

Bird R.B. (1960), Transport Phenomena, Stuart WE and Lightfoot EN.

Brody J.P. and Yager P., (1997) Diffusion-based extraction. Sens. Actuators B Phys, 58, 13-18

Curran, K. and Davies M., (2005) Spectral intensity mapping and analysis of dyed microflows, Microfluidcs and Nanofluidics, 1, 146-154

Hotta, T., Nii, S., Tajima T. and Kawaizaumi F., (2007) Mass transfer characteristics of a microchannel device of split-flow type, Chem. Eng. Technol., 30, 208-213

Ismagilov, R.F., Stroock, A.D., Kenis, P.J.A., Whitesides, G. and Stone, H.A., (2000) Experimental and theoretical scaling laws for transverse diffusive broadening

- in two-phase laminar flows in microchannels, Applied Physics. Letter, 76, 2376-2378
- Jandik, P., Weigl, B.H., Kessler, N., Cheng, J., Morris, C.J., Schulte, T. and Avdalovic, N., (2002) Initial study of using a laminar fluid diffusion interface for sample preparation in high-performance liquid chromatography, J. Chroma. A, 954, 33-40
- Kamholz, A.E. and Yager, P., (2001) Theoretical analysis of molecular diffusion in pressure-driven laminar flow in microfluidic channels, Biophys. J., 80, 155-160
- Kenis, P.J.A., Ismagilov, R.F. and Whitesides, G., (1999) Microfabrication inside capillaries using multiphase laminar flow patterning, Science, 284, 83-85
- Lee, S.C., Lee, K.H., Hyun, G.H. and Lee, W.K., (1997) Continuous extraction of penicillin G by an emulsion liquid membrane in a countercurrent extraction column. J. Memb. Sci. 124, 43-51
- Maruyama, T., Uchida, J.I., Ohkawa, T., Futami, T., Katayama, K., Nishizawa, K.I., Sotowa, K.I., Kubota, F., Kamiya, N. and Goto, M., (2003) Enzymatic degradation of p-chlorophenol in a two-phase flow microchannel system, Lab on a Chip, 3, 308-312
- Oakey, J., Allely, J. and Marr, D.W.M., (2002) Laminar-flow-based separations at the microscale, Biotechnology Progress, 18, 1439-1442
- Shui, L.L., Eijkel, J.C.T. and Van den Berg, A., (2007) Multiphase flow in micro and nanochannels, Sensor and Actuators, B-Chemical, 121, 263-276
- Venkatanarasaiah, D. and Varma, Y.B.G., (1998) Dispersed phase holdup and mass transfer in liquid pulsed column, Bioprocess Engineering, 18, 119-126
- Weigl, B.H., Bardell, R.L., Kesler, N. and Morris, C.J., (2001) Lab-on-a-chip sample preparation using laminar fluid diffusion interfaces-computational fluid dynamics model results and fluidic verification experiments, Fresenius J. Ana. Chem., 371, 97-105

Whitesides, G.M., (2006) The origins and the furture of microfluidics, Nature, 442, 367-418

# Chapter 5

# In Situ Product Removal in Micro Bioreactors

This chapter is submitted as X. Li, L.A.M. van der Wielen, E.E. Krommenhoek, M. van Leeuwen, W.M. van Gulik, J.J. Heijnen, J.G.E. Gardeniers, M. Ottens *to Biotechnology progress* 

#### **Abstract**

In this paper, a micro membrane solvent extraction based micro bioreactor ISPR method was designed, simulated and tested. The removal of lactic acid from an aqueous phase was selected as a good example to mimic lactic acid removal during mammalian cell culture. The optimum organic solvent was 30% TOA as extractant, 20% decanol as modifier and 50% dodecane as diluent. A hollow fiber was used with a 100  $\mu$ l micro bioreactor from a 96 multiple well titer plate. Experiments as well as mathematical simulations showed that sufficient lactic acid could be removed at a rate that would classify this method as a good candidate for real ISPR for inhibitor removal in mammalian cell culture in a micro bioreactor platform.

#### 5.1 INTRODUCTION

In the last decades, there has been a growing interest in developing minute "laboratories-on-a-chip" and micro-(bio)chemical reactors for chemical and biological experiments and analysis at a small scale (Yi et al., 2003). Miniaturization of a device provides several advantages, for instance, the possibility to operate within a shorter time, which especially for gene identification and the related protein production, normally requiring enormous numbers of experiments, is highly advantageous. Several mini- and microbioreactors have been described in the literature. Kostov et al., (2001) described a 24-well plate with 2 ml micobioreactors, to study cultivating Escherichia coli. Zanzotto et al. (2004) developed a batch micro bioreactor with volumes between 5-50 µl, also for Escherichia coli fermentation. Zhang et al. (2003, 2005) utilized an array of four 80 µl fed-batch and continuous micro bioreactors for E coli growth. Balagadde et al. (2005) demonstrated a 16 nl micro chemostat on a chip to monitor long-term bacterial growth. Doig et al. (2005) used three different microplates (24-, 96- and 384-wells) with working volumes of 65 µl and 1,182 µl to grow Bacillus subtilis. All above works have been successful in studying low cell density fermentations in micro bioreactors.

However, in many industrial fermentation processes, high cell densities have to be retained in the reactor and long-term stability has to be ensured in order to achieve high productivities (Schepers et. al., 2006). In practice, high cell density fermentations usually have limited performance, which is normally due to product inhibition causing a decrease in microorganism activity, or product degradation resulting in low yield. Keeping the dissolved product concentration low in the reactor can obviously circumvent these limitations. An approach that can accomplish this task is the implementation of an in situ product recovery/removal (ISPR) technique. Many lab-scale ISPR studies have been reported, using various separation methods, like, crystallization, (Baque-Taboada, et. al., 2004) extraction (Van Halsema et. al. 1998) adsorption (Freeman, et. al., 1993) or chromatography (Makart, et. al., 2006). ISPR on a micro scale for cell growth has hardly been explored.

In this paper we will demonstrate, on the basis of simulations as well as by experimental validation, a possible micro scale ISPR system. This ISPR system is based on hollow fiber liquid/liquid micro solvent extraction. Lactic acid was taken as a model inhibitor in mammalian cell culture. Extraction experiments by using a hydrophilic micro hollow fiber were carried out to remove lactic acid. The hollow fiber has the sole task of ensuring that the interaction between the microorganism and organic solution is minimized. The organic phase was transported through the hollow fiber and samples were collected of the exiting organic phase and subsequently analyzed using enzymatic kits. In what follows, we first briefly describe the selection of the chemicals and solvents and the experimental system. Subsequently, the model used in the simulation is described before presenting the simulation results. The experimental results are compared with the simulations, and the paper ends with a discussion of the results and with some conclusions.

#### 5.2 MATERIAL and METHOD

#### 5.2.1 Selection of the target product

Many microorganisms and mammalian cells produce carboxylic acids, under anaerobic growth conditions. Although carboxylic acids are useful raw materials for chemical industry, in mammalian cell culture elevated carboxylic acids concentrations beyond a certain level have a negative effect on the cell activity (Pattison et. al., 2001; Driehuis et. al., 1999). Various carboxylic acids have different critical concentrations; typical maximal nontoxic concentrations of chemicals during fermentations are for ethanol, 30mM; acetic acid, 50mM; lactic acid, 10mM; butyric acid, 10mM; and succinic acid, 10mM. The toxicity increases with the concentrations of individual items (Playne et. al., 1983). Based on the reasoning above, lactic acid qualifies as a model toxic or activity inhibiting product in cell culture and serves therefore as a suitable candidate for ISPR. In order to keep sufficient cell activity, it is necessary to control the acid concentration below dangerously toxic levels by using a suitable ISPR method.

# 5.2.2 Selection of a suitable ISPR method

Many separation methods can be integrated with ISPR technologies. Like, chromatography (Makart, et. al. 2006), crystallization (Buque-Taboada et. al., 2005), adsorption, extraction, evaporation etc. (Stark et. al., 2003; Lye et. al., 1999; Freeman et. al., 1993). The advantages of a miniaturized ISPR

device are the short molecular diffusion distance, the large specific interfacial area relative to its volume, the possibility to handle multiphase flows. The properties of carboxylic acids point out that liquid/liquid extraction have good potential to be used as a separation method to be integrated in a micro scale ISPR device. Few micro extraction studies have been carried out, e.g., for metal ions and an organic compound using a two phase flow in a micro channel (Hou et. al., 2003; Maruyama et. al., 2004; Chen et. al., 2005; Aota et. al., 2007). Kiani and Prasad have studied the extraction of acetic acid from aqueous solution into methyl isobutylketone or xylene through several flat and thin microporous film having different pore sizes and porosity, and being composed of different materials at a larger scale (Kiani et. al., 1984; Prasad et. al., 1986). Shen and coworkers reported a sample pretreatment method using hollow fiber-protected liquid phase microextraction to prepare GC-MS samples (Shen et. al., 2002). In order to reduce the possible interaction between the fermentation broth and organic extractant, which may influence the behavior of microorganism, micro membrane solvent extraction (MMSE) is chosen to be the most suitable micro ISPR method to be integrated with the micro bioreactor.

# 5.2.3 Selection of organic solvent

The recoveries of carboxylic acids from fermentation broth have been investigated by several groups (e.g., Van Halsema et. al., 1998; Schepers et. al., 2006). Amine containing solvents are frequently used as reactive extractants for organic acid removal, especially for lactic acid, which is the most interesting target. Different amines and diluents have been used for extraction of lactic acid. Tertiary amines and quaternary ammonium salts have been found to be a better choice than primary and secondary amines. The primary alkyl ammonium lactates are either water soluble or exhibit surfaceactive properties, or both. Secondary aliphatic amines are sensitive to thermal degradation and gel formation on the interface between the phases (Kertes et. al., 1986). Several tertiary amines have been tested with trioctylamine (TOA) being reported as the most effective one (Han et. al., 2000). Morales and coworkers investigated the influence of the extractant (tributyl phosphate (TBP) and TOA) on different carboxylic acids. TOA showed at least ten times better extraction ability than TBP for most monocarboxylic acids (Morales et. al., 2003). Due to their extreme physical properties (viscosity, specific gravity and surface tension), TOA and most of other possible extractants are not suitable to be directly used in extraction experiment. In order to modify their physical properties, normally a so called modifier is blended with the extractant. It is found that an additional diluent was also needed to modify the solubility of the formed complex in the organic solvent (Yankov et. al., 2004; Yang et. al., 1991; Chen et. al., 1997; Morales et. al., 2003).

The properties of diluents and modifiers in the extractant have a significant impact on the extraction ability of amines. Yankov used various diluents (dodecane, kerosene, mineral oil) with decanol as modifier and various modifiers (hexanol, octanol, decanol and ethyl acetate) with dodecane as a diluent for the preparation of the organic phase to extract lactic acid. The increased percentages of TOA and modifiers improved the extraction ability. It was found that hexanol has the most effective extraction ability, whereas decanol and octanol are a little bit weaker but still can contribute to significantly high distribution coefficient during extraction.

The toxicities of diluents and modifiers also have been studied e.g., by Playne's group and Martak's group. The toxicity of the solvent depends on whether yeast or bacteria are used and even on the particular environment; therefore, there is huge uncertainty to precisely predict the toxicity impact of a certain solvent on a target microorganism. From Playne's work it is known that the toxicity of alcohols to the bacteria decreases with increasing the length of alkyl chain; n-alkanes are normally non-toxic and primary amines are more toxic than rest of the amines (Playne et. al., 1983; Martak et. al., 1997).

To minimize the toxicities of diluents and modifiers, but meanwhile still trying to get the best extraction ability, the organic phase used in our work was prepared by using TOA as extractant, dodecane as diluent and decanol as modifier with a composition of 30%, 50% and 20% TOA, dodecane and decanol respectively.

#### 5.3 EXPERIMENTAL SETUP

#### 5.3.1 Chemicals

85% pure DL-lactic acid was supplied by Acros (Steinheim, Germany).

All reagents were analytical grade. (NH<sub>4</sub>)<sub>2</sub>SO<sub>4</sub>, KH2PO4 and MgSO<sub>4</sub>-7H<sub>2</sub>O were purchased from Baker Analyzed reagent (Deventer, The Netherlands). n-Dodecane and 1-Decanol were supplied by Aldrich (Steinheim, Germany). Trioctylamine was supplied by Fluka (Japan). All aqueous solutions were prepared using double distilled water and passed through a 0.22 μm cellulose acetate filter (Molshelm, France). 2.5 g (NH<sub>4</sub>)<sub>2</sub>SO<sub>4</sub>, 1.5 g KH<sub>2</sub>PO<sub>4</sub> and 0.51 g MgSO<sub>4</sub>-7H<sub>2</sub>O were dissolved into 50 ml deionized water to prepare the pH 4 buffer solution. 70mM lactic acid solution was prepared by diluting 85% pure DL-lactic acid into pH 4 buffer solution. Organic extractant solution was prepared with the composition as 30% TOA (extractant), 20% decanol (modifier) and 50% dodecane (diluent).

#### 5.3.2 Micro bioreactor

As shown in Figure 5-1, a single well was taken from a 96-well micro titer plate. The well was closed using a rubber cap. Three holes were drilled in the cap with a diameter of 350  $\mu m$ . As shown in Figure 5-1, two holes were located on the side of the rubber cap to fixate the position of hollow micro fiber. The hollow fiber is a hydrophilic membrane, which is made of polyethersulfone, with a pore size 0.5  $\mu m$ . The fiber has an internal diameter 300  $\mu m$ , external diameter 400  $\mu m$  (MicroPES TF10, Polypore, Germany). The other hole was around the center of the cap. Red PEEK (polyetheretherketone) polymer tubing was fixed in this hole and placed above the magnetic stirrer bar in order to take samples. A hole was drilled in the magnetic stainless steel stirrer bar of 1.67mm×2.01mm×4.80mm dimensions (VP 711-1, V&P Scientific). A needle was pinched through the center point of the rubber cap. The tip of the needle was bent as to fixate the stirrer bar at elevated height.

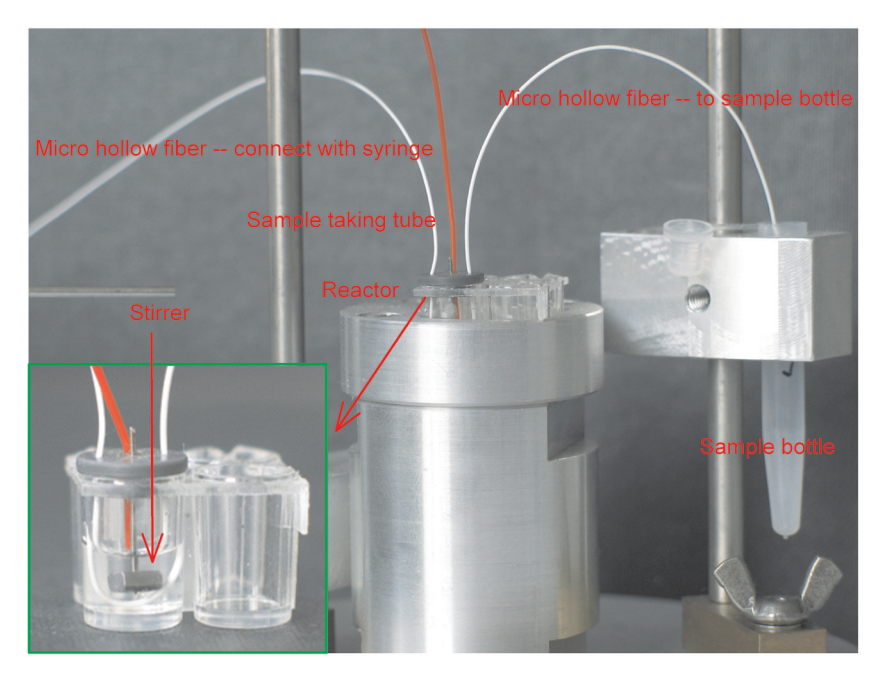


Figure 5-1 Picture of the experimental set-up used for ISPR (micro extraction) experiments. Inlay left lower corner picture shows an enlarged view of the actual micro bioreactors used

# 5.3.3 Equipment

A KD-scientific S-101 syringe pump (Holliston, USA), several different sized Hamilton syringes (Reno, USA), Single stirrer motor (RET B, IKA Werke, Staufen, Germany), Tecan plate reader (Salzburg, Austria), Eppendorf thermomixer Confort (Hamburg, Germany) were used.

# 5.3.4 Extraction experiments

Extraction experiments were carried out with a 2.5 ml sample tube. The aqueous phase was 0.5 ml lactic acid solution (pH 4, 70 mM). The organic phase was 1.0 ml organic extractant solution of compositions described before. The organic and the aqueous phases were shaken for 2 hours at room temperature on shaking machine with frequency 800 rpm. Then, a 50  $\mu$ l aqueous sample was taken from this sample tube and was diluted 5 times. 500  $\mu$ l organic phase solution was moved into another 2.5 ml sample tube, and then mixed with

1ml pH 10 buffer solution. After another 2 hours shaking, a 100  $\mu$ l aqueous sample was taken from the second sample tube.

#### 5.3.5 Micro-scale ISPR experiments

The lactic acid micro extraction set-up is illustrated in Figure 5-2. A syringe pump was used to create a continuous organic flow with a constant flow rate. The organic phase was pushed through a micro hollow fiber, which was placed in the micro reactor. The position of the fiber was fixed through two holes in the cap, and fixing the U-shape bend close to reactor bottom. One side of the fiber was connected with a needle adaptor, which was linked with a 5ml syringe. Another side of the fiber was placed into a 400 μl sample bottle to collect organic phase sample (extractant). All sample bottles were numbered and weighted before an experiment. 100 µl lactic acid solution (70mM) was injected into the micro reactor as the aqueous phase. The liquid (organic solution) from the fiber exit was collected into a sample bottle. Every 5 minutes a clean sample bottle was used to replace the old one. The switched sample bottle was weighted and then mixed with 100 µl pH 10 buffer solution to back-extract lactic acid from the organic phase to the aqueous phase. The sample bottles were shaken for two hours on a shaking machine with frequency 800 rpm. This mixing time was sufficient to reach the liquid-liquid equilibrium. After that, 10 µl aqueous solution was pipetted out from each sample bottle and then diluted 5 times. Every hour, a 5 µl aqueous sample was taken from the reactor via the sample taking tube and then diluted with 55 μl pH 10 buffer solution, until the end of experiment. The organic phase flow rate was 5 µl/min. In total 870 µl organic solution was pushed through the micro hollow fiber.

The lactate concentrations in all treated aqueous samples were determined with Enzytec D Lactat /L lactat enzymatic kits (kit 11 112 821 035, Darmstadt, Germany). The enzymatic kit was scaled down for use with 96-well titer plates. Absorption was read on a Tecan plate reader.

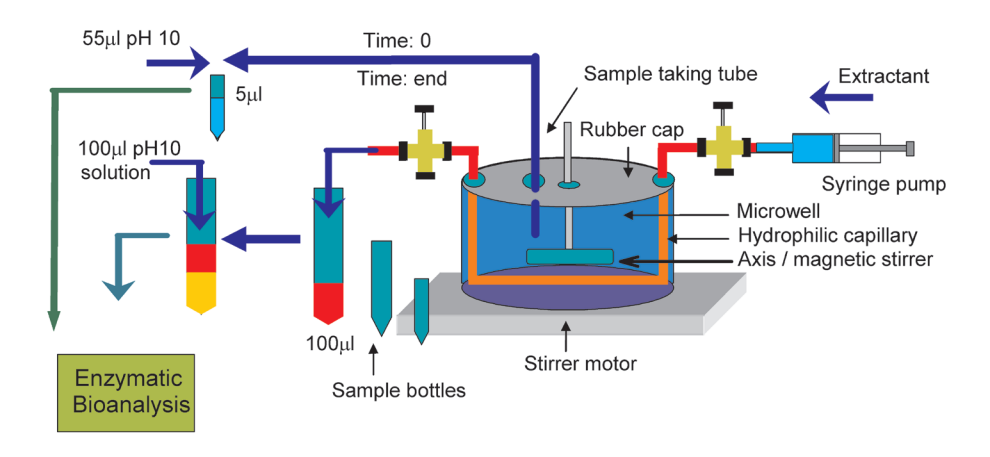


Figure 5-2 Schematic of overall lactic acid micro extraction set-up

#### 5.4 MICRO ISPR SIMULATION

The extraction equilibrium of a weak monocarbocylic acid (HA) with extractant trioctylamine (TOA) can be presented as follows:

$$HA + nE^{\circ} \rightleftharpoons E_n \cdot HA^{\circ}$$
 Equation 5-1

Where n is the number of reacting molecules of extractant. n normally equals 1 for monoacids when the organic phase only contains extractant. For an amine being used as extractant in a mixture with diluent and modifier in a reactive extraction as this case, the solubility of the extracted species increases in the organic phase, consequently, n >1.

The distribution coefficient  $(K_E)$  of the organic acid (HA) is:

$$K_{E(HA)} = \frac{C_{HA}^{\ o}}{C_{HA}^{\ aq}}$$
 Equation 5-2

Where the concentration of the species is denoted by C and expressed in molar concentration, superscript ° indicates the species in the organic phase, superscript <sup>aq</sup> indicates the species in the aqueous phase. HA is the organic

acid,  $E^o$  is the extractant,  $E_n \cdot HA^o$  is the reaction product in the organic phase, and  $K_{E(HA)}$  is the overall distribution coefficient, which represents the ratio of the total acid concentration in the organic phase to the total acid concentration in the aqueous phase in all possible forms. The value of  $K_E$  can be determined experimentally in steady state condition.

ISPR is a dynamic process; this simulation focuses on the micro extraction as illustrated in Figure 5-2. A continuous organic flow passes through a micro hollow fiber, which is made of a hydrophilic membrane. The interface between aqueous and organic phases can be supposed to be located in the inner surface of the membrane, i.e., on the organic side. The mass transfer between two phases can be presented as follows:

$$M^{T} = \beta \left( KC^{q} - C^{o} \right)$$
 Equation 5-3

Where  $\beta$  denotes the overall mass transfer coefficient in m s<sup>-1</sup>; K denotes the distribution coefficient; C<sup>aq</sup> denotes the concentration of organic acid in aqueous phase in mol m<sup>-3</sup>, C<sup>o</sup> denotes the concentration of organic acid in organic phase in mol m<sup>-3</sup>, M<sup>T</sup> denotes mass transfer rate in mol m<sup>-2</sup> s<sup>-1</sup>. A differential mass balance assuming no significant dispersion will yield for the organic phase:

$$\frac{dC^{o}}{dt} = -\frac{\phi^{o}}{A} \frac{dC^{o}}{dz} + \frac{S\beta}{A} \left( KC^{aq} - C^{o} \right)$$
 Equation 5-4

A mass balance over the aqueous phase assuming perfect mixing, yields:

$$\frac{dC^{aq}}{dt} = -\frac{S}{V_r} \frac{1}{L} \int_0^L \beta \left( KC^{aq} - C^o \right) dz$$
 Equation 5-5

Where A denotes the cross sectional area in  $m^2$ , S the perimeter in m, z denotes the position along the fiber, L the length of the fiber,  $\phi^o$  denotes the volumetric flow rate of organic flow in  $m^3$  s<sup>-1</sup> and  $V_r$  denotes the micro reactor volume in  $m^3$ . After expressing the differential plug flow by a series of N well

mixed compartments, we eventually yield:

$$\frac{dC_i^o}{dt} = -\frac{\phi^o}{V_i} \left(C_{i-1}^o - C_i^o\right) + \frac{S\beta}{AN} \left(KC^{aq} - C_i^o\right), \text{ for i = 1..N},$$

Equation 5-6

$$\frac{dC^{aq}}{dt} = -\frac{S}{V_r} \frac{1}{N} \sum_{i=1}^{N} \beta \left( KC^{aq} - C_i^o \right)$$
 Equation 5-7

Knowing the initial conditions ( $C_{t=0}$ ), these N+1 ordinary differential equations (ODE's) can be solved using a standard ODE solver e.g. as those supplied by Matlab (ODE23).

The effect of organic flow rate and the membrane area was studied by varying the volume flow rate of the organic phase and the diameter of the micro hollow fiber respectively.

## 5.5 RESULT and DISCUSSION

The distribution coefficient  $K_{E(HA)}$  was determined experimentally. For a lactic acid solution (70mM) with initial pH at 4, the measured distribution coefficient is  $0.55 \pm 0.05$ . This value is smaller than the normal distribution coefficient for organic acid extraction (Yankov, et. al., 2004). It can be explained by the fact that at pH 4, only part of lactic acid (pKa 3.86) remains in undissociated form, which can be extracted by tertiary amines, such as TOA (Yang, et. al., 1991). For lactic acid solutions with initial pH at 10, the measured distribution coefficient is close to 0. It indicated that after mixing the extracted solution with pH 10 buffer, nearly all lactic acid can be back-extracted from the organic phase.

The optimal extraction condition for lactic acid in the TOA mixture is in low pH range (pH<4). However, since the purpose of this ISPR is to continuously remove target chemical(s) from the fermentation broth in order to maintain the fermentation activity, the integrated separation method should not influence optimized fermentation conditions, like, pH. The extraction has to be applied

under the fermentation conditions, which is pH 4-7. Therefore, the TOA mixture is a suitable extractant only within a small pH range. It is necessary to find other extractants, which can be used for high pH extraction.

Quaternary ammonium salts can function as an anion-exchange reagent under both acidic and basic conditions, and can extract both undissociated and dissociated forms of organic acids. Quaternary ammonium salts have been proven to be a suitable extractants for a wide pH range from 2-10 (Yang, et. al. 1991). However, because this extractant is not sensitive for the pH, it is difficult to back-extract all lactic acid. Yang reported that by using quaternary ammonium salts (Aliquat 336) as extractant at pH 7 solution, the distribution coefficient of lactic acid is around 0.4-0.6. This value is close to our measured KE(HA) value. Since under the same experimental set-up, the extraction ability of this micro extraction system is mainly dependent on this  $K_{\rm E(HA)}$  value, as shown in Equation 5-2. In our study, the TOA mixture can still be used as the organic extractant in the experiment, and the measured extraction result should be comparable to the extraction result of using Aliquat 336 as extractant at pH 7, which is normally considered as the desired pH for mammalian cell culture fermentation.

With an organic flow rate 5  $\mu$ l/min, the residence time of the organic phase in the micro reactor was only 11.8s. Within a short time (5min), by assuming that there is a constant mass transfer rate between the aqueous phase and organic phase, the overall mass transfer coefficient ( $\beta$ ) was determined to be  $1.6 \pm 0.3 \times 10^{-6}$  m s<sup>-1</sup>, which value is in the same order of magnitude as the reported value from Tong's work (Tong et. al., 1998).

Stable organic flow was checked experimentally by weighing sample bottles before and after collecting the organic outflows. It must be noted that for stable flow serious attention should be paid to remove air bubbles or particles that could restrict the fiber as well as to prevent any possible shoving or squeezing on the micro hollow fiber by the cell wall or the stirrer. The measurement resulted in a difference between the pushed in organic (syringe) and measured outlet of less than ±5%. The total flow for both aqueous phase (reactor) and organic phase were weighted before and after experiment, the difference was less than 1%. It indicates that good membrane isolation between the phases was secured and barely any organic solvent leaked into aqueous phase (so, no negative influence on the micro organisms).

The pore size of the membrane was  $0.5~\mu m$ , which is small enough to keep the microorganisms at the outside of the fiber and further reduce the possible contact of the microorganisms and organic solvent.

In the simulation ten well mixed components in series were used to represent the micro hollow fiber (N=10), which is close to a plug flow. Additionally, the organic flow rate was set as  $5 \mu$ /min; distribution coefficient was set as 0.6; membrane area was set as  $7.07 \times 10^{-6} \,\mathrm{m}^2$ .

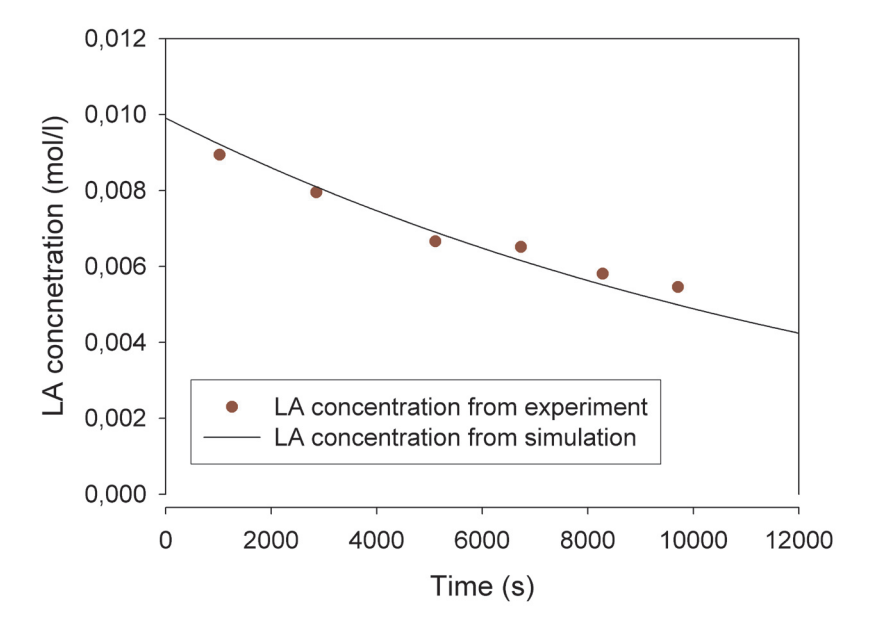


Figure 5-3 Comparison of model prediction ( - ) with measured results (● ) at organic phase (outlet) with organic phase flow rate 5 µl/min, distribution coefficient 0.6

Figure 5-3 and Figure 5-4 show a good agreement between the simulated result and the experimental result at the aqueous phase and organic phase, respectively. LA° indicates lactic acid concentration in the organic phase at the hollow fiber exit in mol l¹¹, and LAaq indicates the lactic acid concentration in the aqueous phase in mol l¹¹.

As it can be seen from Figure 5-4 that there is about 7% difference between experimental results from aqueous samples and back calculated results from organic samples. It can be explained by the lactic acid loss during organic samples' treatment (extraction/back-extraction). Model based simulation was found to be a good tool for estimating the ISPR behavior in the micro system. Only a few parameters need to be determined from simple experiments before the model can be used.

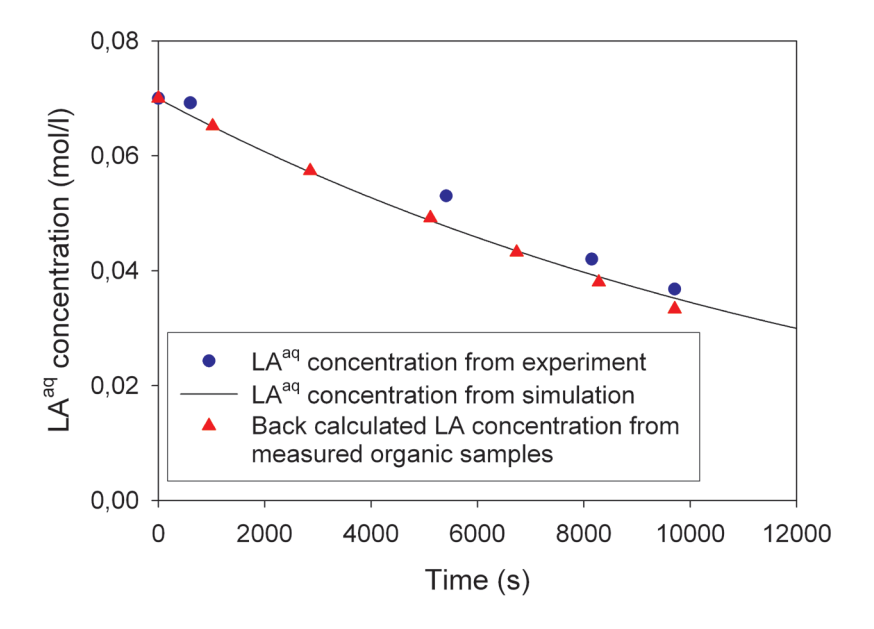


Figure 5-4 Comparison of model prediction (-) and measured results from aqueous phase samples ( $\bullet$ ) and back calculated results from organic phase samples ( $\triangle$ ) at organic phase.

The specific interfacial area for mass transfer in the hollow micro fiber was calculated to be 13.3×10<sup>3</sup> m<sup>2</sup>/m<sup>3</sup>. The specific interfacial area in conventional high-efficiency equipment for liquid/liquid extraction was reported to be in the order of 1-20 m<sup>2</sup>/m<sup>3</sup> (Lee et al., 1997; Venkatanarasaiah and Varma, 1998). The high specific interfacial area in the micro ISPR system under development as compared to conventional equipment shows the advantage of the microextraction for ISPR processes in which high mass-transfer rates are important.

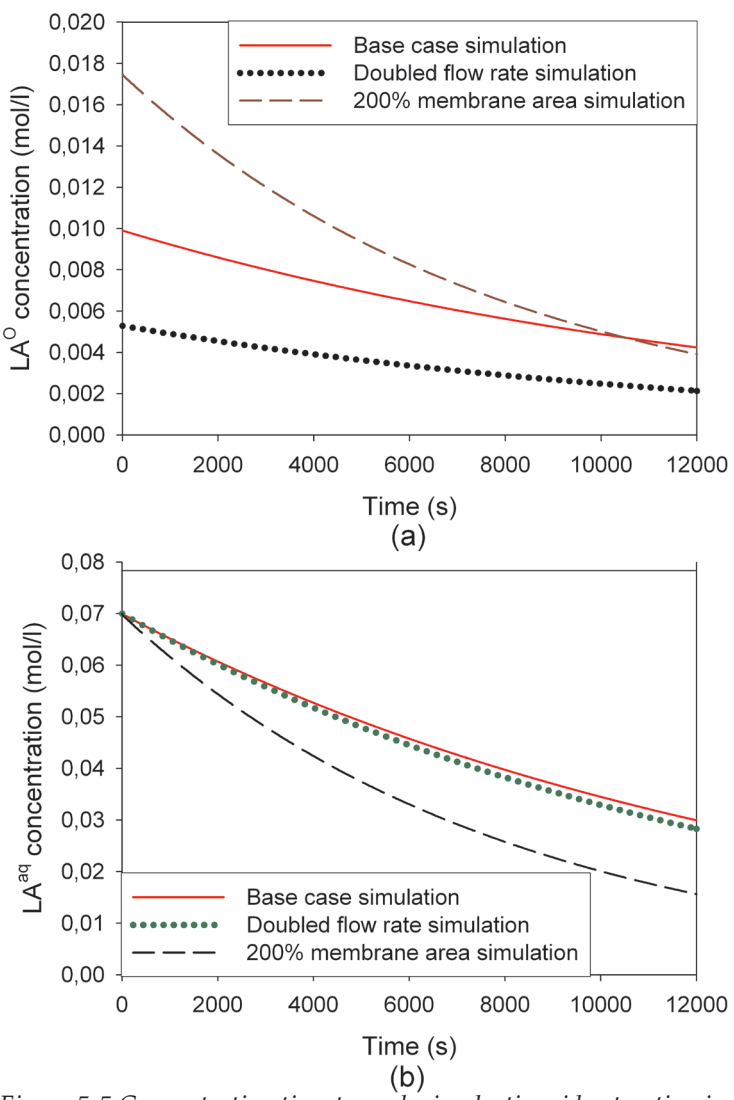


Figure 5-5 Concentration time trace during lactic acid extraction in (a) organic phase and (b) aqueous outlet in different simulations. Red curve is the base case with flow rate 5 µl/min, membrane area  $7.07\times10^6$  m²; Green curve is the case with flow rate 10 µl/min, membrane area  $7.07\times10^6$  m²; Brown curve is the case with flow rate 5 µl/min, membrane area  $1.414\times10^6$  m²

Figure 5-5 shows the simulation results for lactic acid concentration traces with various membrane areas and various organic flow rates, respectively.

Both increased membrane area and the organic flow rate show positive effect on the micro extraction. Furthermore, membrane area shows much larger impact on the extraction ability than the impact of organic flow rate. It can be explained by the fact that the residence time of organic phase is relatively short and still far away from the equilibrium time, but the membrane area has a proportional correlation to the extraction ability as it is indicated in Equation 5-3 to Equation 5-7.

The microreactor used in the experiment was a cell from a 96-well titer plate, which was also used as a fed-batch microreactor for yeast cell growth in our previous work (Krommenhoek, et. al., 2007). A single micro hollow fiber was used in the ISPR experiment. For this set-up it is easy to implement multiple micro hollow fibers within the micro reactor to increase interfacial area. Even for this single fiber setup, at critical lactic acid concentration of 10mM, the extraction rate was estimated to be 1.92×10<sup>-10</sup> mol s<sup>-1</sup>, which is a quite good value, especially after considering the large improvement possible for the KE(HA) value and membrane area.

Typical production rates of lactic acid in mammalian cell cultures are in the order of 7.09e-7 to 3.7e-5 mol l<sup>-1</sup> s<sup>-1</sup> (Hofvendahl and Hahn, 2000). This value is in the same order of magnitude as the achieved ISPR removal rate (1.92e-6 mol l<sup>-1</sup> s<sup>-1</sup>), with only one single micro fiber in a single well of a 96 well title plate. Therefore, this approach is a promising ISPR technique to be incorporated in a micro bio reactor platform currently under development (Krommenhoek et al, 2006, 2007, Li et al, 2007, 2008).

#### 3.6 CONCLUSIONS

In this chapter, a micro membrane solvent extraction based ISPR method was designed, simulated and tested. The removal of lactic acid from an aqueous phase was selected as a good example to mimic lactic acid during mammalian cell culture. The optimum organic solvent was 30% TOA as extractant, 20% decanol as modifier and 50% dodecane as diluent. A hollow fiber was used with a 200  $\mu$ l micro bioreactor from a 96 multiple well titer plate. Experiments as well as mathematical simulations showed that sufficient lactic acids could be removed at a rate that would classify this method as a good candidate for real ISPR for inhibitor removal in mammalian cell culture

in a micro bioreactor platform.

# Acknowledgements

This work is part of the ACTS-IBOS programme (IBOS 053.63.009), which is funded by the Dutch Science Foundation (NWO), DSM Anti-Infectives BV, Diosynth/Organon and Applikon BV

## **Notation**

```
A = interfacial area, m<sup>2</sup>
```

C<sup>aq</sup> = concentration of chemical in aqueous phase, mol l<sup>-1</sup> C<sup>o</sup> = concentration of chemical in organic phase, mol l<sup>-1</sup>

d = diameter, m

K<sub>E</sub> = distribution coefficient, 1 = microhollow fiber length, m

M = Mass transfer, mol S = cross area of fiber, m<sup>2</sup>

t = time, s

u = linear flow rate, m s<sup>-1</sup>

V = volume, m<sup>3</sup>

Vr = reactor volume, m<sup>3</sup>

#### Greek letters

```
\beta = overall mass transfer coefficient, m s<sup>-1</sup>,
\phi = volume flow rate, m<sup>3</sup> s<sup>-1</sup>
```

#### References

- Aota, Arata, Masaki Nonaka, Akihide Hibara and Takehiko Kitamori, 2007, Countercurrent Laminar Microflow for Highly Efficient Solvent Extraction, Angew. Chem. 119,896-898
- Balagaddé, Frederick K., Lingchong You, Carl L. Hansen Frances H. Arnold, Stephen R. Quake, Long-Term Monitoring of Bacteria Undergoing Programmed Population Control in a Microchemostat, Science, 309, 137-140
- Buque-Taboada, E. M., A. J. J. Straathof, J. J. Heijnen and L. A. M. van der Wielen, 2004, In situ product removal using a crystallization loop in the asymmetric reduction of 4-oxoisophorone by Saccharomyces cerevisiae, Biotechnology and Bioengineering, 86, 795-800
- Buque-Taboada, E. M., A. J. J. Straathof, J. J. Heijnen and L. A. M. van der Wielen, 2005, Microbial reduction and in situ product crystallization coupled with biocatalyst cultivation during the synthesis of 6R-dihydro-oxoisophorone, Adv. Syn. And catalysis, 347, 1147-1154
- Chen, Hong, Qun Fang, Xue-Feng Yin and Zhao-Lun Fang, 2005, Microfluidic chipbased liquid-liquid extraction and preconcentration using a subnanoliterdroplet trapping technique, Lab on a chip, 5, 719-725
- Chen, Rongfu and Y. Y. Lee, 1997, Membrane-mediated extractive fermentation for lactic acid production from cellulosic biomass, Appled Biochemistry and Biotechnology, Vol. 63-65, 435-448
- Doig, Steven D., Samuel C. R. Pickering, Gary J. Lye, Frank Baganz, (2005), Modelling surface aeration rates in shaken microtitre plates using dimensionless groups, Chemical Engineering Science, 60, 2741-2750
- Driehuis, F., S. J. W. H. Oude Elferink and S. F. Spoelstra, 1999, Anaerobic lactic acid degradation during ensilage of whole crop maize inoculated with Lactobacillus buchneri inhibits yeast growth and improces aerobic stability, Journal of Applied Microbiology, 87, 583-594
- Freeman, A., J. M. Woodley and M. D. Lilly, 1993, In situ product removal as a tool for bioprocessing, Biotechnology, Vol. 11, 1007-1012

- Han, D. H., Y. K. Hong, W. H. Hong, 2000, Separation characteristics of lactic acid in reactive extraction and tripping, Korean J. Chem. Eng., 17, 528-533
- Hofvendahl, K., B. Hahn-Hagerdal, 2000, Factors affecting the fermentative lactic acid production from renewable resources, Enzyme and Microbial Technology, 26, 87-107
- Hou, Li and Hian Kee Lee, 2003, Dynamic Three-Phase Microextraction as a sample preparation Technique Prior to Capillary Electrophoresis, Anal. Chem. Vol. 75, 2784-2789
- Kertes, A. S., C. J. King, 1986, Extraction chemistry of fermentation product carboxylic acids, Biotechnol. And Bioeng. Vol. 28, 269-282
- Kiani, A., R. R. Bhave, K. K. Sirkar, 1984, Solvent extraction with immobilized interfaces in a microporous hydrophobic membrane, J. Membrane Sci. 20, 125
- Kostov, T., Peter Harms, Lisa Randers-Eichhorn and Govind Rao, (2001) Low-Cost Microbioreactor for High-Throughput Bioprocessing, Biotechnology and Bioengineering, 72 (3) 346-352
- Krommenhoek, Erik E., Michiel van Leeuwen, Han Gardeniers, Walter M. van Gulik, Albert van den Berg, Xiaonan Li, Marcel Ottens, Luuk A.M. van der Wielen, Joseph J. Heijnen, (2008), Lab-scale fermentation tests of micro chip with integrated electrochemical sensors for pH, temperature, dissolved oxygen and viable biomass concentration, Biotechnology and Bioengineering, 99(4) 884–892
- Krommenhoek, Erik, 2007, Integrated electrochemical sensor array for on-line monitoring micro bioreactors, PhD thesis
- Lee S. C., Lee K. H., Hyun G. H. and Lee W. K. 1997. Continuous extraction of penicillin G by an emulsion liquid membrane in a countercurrent extraction column. J Memb Sci 124:43-51
- Li, X, G. van der Steen, G.W.K. van Dedem, L.A.M. van der Wielen, M. van Leeuwen, W.M. van Gulik, J.J. Heijnen, E.E. Krommenhoek, J.G.E. Gardeniers, A. van

- den Berg and M. Ottens, (2008), Improving mixing in micro bioreactors, accepted for Chem Eng. Sci. doi:10.1016/j.ces.2008.02.036
- Li, X., L.A.M. van der Wielen, G. van der Steen, G.W.K. van Dedem, M. van Leeuwen, W.M. van Gulik, J.J. Heijnen, J.G.E. Gardeniers, E.E. Krommenhoek, A. van den Berg, M. Ottens (2007) "The application of direct oscillations to improve mixing in micro bioreactors", submitted for publication
- Lye, G. J., and J. M. Woodley, 1999, Application of in situ product removal techniques to biocatalytic processes, Trends Biotechnol. , 17, 395-402
- Martak, Jan, Erika Sabolova, Stefan Schlosser, Michal Rosenberg and L'udmila Kristofikova, 1997, Toxicity of organic solvents used in situ in fermentation of lactic acid by Rhizopus arrhizus, Biotechnology Techniques, Vol. 11, No. 2, 71-75
- Makart, S., M. Bechtold, M. Heinemann and S. Pank, 2006, Integrated operation of continuous chromatography and biotransformations for the generic high yield production of fine chemicals, J. Biotechnol. 124, 146-162
- Maruyama, Tatsuo, Tomoaki Kaji, Tomohiro Ohkawa, Ken-ichiro Sotowa, Hironari Matsushita, Fukiko Kubota, Noriho Kamiya, Katsuki Kusakabe and Masahiro Goto, 2004, Intermittent partition walls promote solvent extraction of metal ions in a microfluidic device, ANALYST, Vol. 129, 1008-1013
- Morales, Areli Flores, Joel Albet, George Kyuchoukov Guy Malmary and Jacques Molinier, 2003, Influence of Extractant (TBP and TOA), Diluent, and Modifier on Extraction Equilibrium of Monocarboxylic Acids, J. Chem. Eng. Data, Vol. 48, 874-886
- Pattison T.-L., and A. von Holy, 2001, Effect of selected natural antimicrobials on Baker's yeast activity, Letters in Applied Microbiology, 33, 211-215
- Playne, M. J., B. R. Smith, 1983, Toxicity of Organic Extraction Reagents to Anaerobic Bacteria, Biotechnology and Bioengineering, Vol. XXV, 1251-1265
- Prasad R., A. Kiani, R. R. Bhave, K.K. Sirkar, 1986, Further studies on solvent extraction with immobilized interfaces in a microporous hydrophobic membrane, J.

Mem. Sci. 26, 79

- Schepers, Adolf Willem, Jules Thibault, Christophe Lacroix, 2006, Continuous lactic acid production in whey permeate/yeast extract medium with immobilized Lactobacillus helveticus in a two-stage process: Model and experiments, Enzyme and Microbial Technology, Vol. 38, 324-337
- Shen Gang and Hian Kee Lee, 2002, Hollow Fiber-Protected Liquid-Phase Microextraction of Triazine Herbicides, Anal. Chem. 74, 648-654
- Stark, D., A. Jaquet, U. von Stockar, 2003, In situ product removal (ISPR) in whole cell biotechnology during the last 20 years, Ads. Biochem. Eng. Biotech., 80, 149-175
- Tong, YanPing, Makoto Hirata, Hirokazu Takanashi, Tadashi Hano, Fukiko Kubota, Masahiro Goto, Fumiyuki Nakashio and Michiaki Matsumoto, 1998, Extraction of lactic acid from fermented broth with microporous hollow fiber membranes, Journal of Membrane Science, Vol. 143, 81-91
- Van Halsema, F. Emo D., Luuk A. M. van der Wielen, and Karel Ch. A. M. Luyben, 1998, The modeling of Carbon Dioxide-Aided Extraction of Carboxylic Acids from Aqueous Solutions, Ind. Eng. Chem. Res., Vol. 37, 748-758
- Venkatanarasaiah D and Varma YBG. 1998. Dispersed phase holdup and mass transfer in liquid pulsed column. Bioprocess Engineering 18:119-126
- Yang, ShangTian, Scott A. White, and Sheng-Tsiung Hsu, 1991, Extraction of Carboxylic Acids with Tertiary and Quaternary Amines: Effect of pH, Ind. Eng. Chem. Res., Vol. 30, 1335-1342
- YanKov, D., J. Molinier, J. Albet, G. Malmary and G. Kyuchoukov, 2004, Lactic acid extraction from aqueous solutions with tri-n-octylamine dissolved in decanol and dodecane, Biochemical Engineering Journal, 21, 63-71
- Yi, Mingqiang and Haim H. Bau, (2003), The kinematics of bend-induced mixing in micro-conduits, International Journal of Heat and Fluid Flow, Vol. 24 645-656

- Zanzotto, Andrea, Nicolas Szita, Paolo Boccazzi, Philip Lessard, Anthony J. Sinskey, Klavs F. Jensen, (2004), Membrane-Aerated microbioreactor for High-Throughput Bioprocessing, Biotechnology and Bioengineering, 87 (2), 243-254
- Zhang, Z., N. Szita, P. Boccazzi, A. J. Sinskey and K.F. Jensen, (2003) Monitoring and control of cell growth in fed-batch microbioreactors, 7TH International Conference on Miniaturized Chemical and Biochemical Analysis Systems, California, USA
- Zhang, Zhiyu, Gerardo Perozziello, Nicolas.Szita, Paolo Boccazzi, Anthony J.Sinskey, Oliver Geschke, and Klavs F.Jensen. (2005), Microbioreactor "Cassette" with integrated fluidic and optical plugs for high-throuput bioprocessing. Micro-TAS 2005

# Chapter 6

Outlook

The objective of this work was to develop a platform consisting of parallel fed-batch bioreactors with working volume around 100 µl for cultivation micro-organism(s) under an industrially relevant condition. The development of the platform starts with the design of a single micro-reactor; the single micro-reactor is the integration of well developed sensing system, control system, mixing system and other accessories, like, pumps, valves, adaptors, vessels etc.; all involved components play important roles. Some components are commercial available, but many components are not available or not suitable for our application. To complete the development of the microreactor, investigation on the particular parts of technologies is necessary. The work described in this thesis represents an advance forwards suitable mixing methods and possible ISPR methods for a platform for high-throughput screening and testing of micro-organism under industrially relevant fed-batch conditions. However, a number of issues, both in conceptual and experimental aspects, emerge from the described research and will need to be addressed in future research. These are briefly discussed below.

## Integration and parallelization

Since the development of the microbioreactor aims to be used within a high-throughput screening system, integration and parallelization should be the key theme in the future of the development of a platform of microbioreactors. Most of present research only show the possibility of integration and parallelization of their recent development. Further integration requires an even stronger emphasis on a multidisciplinary approach, where as industrial collaborations are essential to develop a robust and reliable integrated platform.

The design of the particular components, such as the sensor, mixing methods, ISPR parts, should also follow this principle, be easily integrated and parallelized with the microbioreactor. The highly integrated and parallelized system requires constant maintainance and adjustment. To reduce the complexity and the cost of the maintainance work, the micro components need to provide stable performance and be preferably to have a simple structures instead of the complex ones.

#### Mixing in microbioreactor

Mixing, as been considered as an important bottleneck, limits the micro organism cultivation application, especially under a high cell concentration condition. The present research on micro-mixing technology mainly focuses on the use of microfluidic-based-structure within microchannels in nanolitresscale; also the research of the mixing methods, which are suitable for the scale larger than mililitres were studied and reported; however, much less work was published on the novel mixing methods around the scale of hundreds microlitres, which was considered in our project as the most suitable volume range (30 - 200 µl) of the the development for microbioreactor. (Chapter 1) For the present miniaturized bioreactors, scaled downed magnetic stirrer and shake flask are the commonly used mixing methods. (Kostov, et al. 2001; Zhang et al., 2003; Klein et al., 2005; Micheletti et al., 2006; van Leeuwen, 2008) Although k, a values up to 156 h<sup>-1</sup> were achieved in stirred hundreds microlitres cultivations (van Leeuwen, 2008), a negative effect of stirring (cell damage), which was hypothesized caused by the mechanical stress, on the batch growth of Candida utilis was reported in van Leeuwen's work. Shaking was considered as an alternative mixing method for hundreds microliter-scale cultivation, however, for cell cultivation, under the required extreme violent condition, (shaking frequency >1000 rpm) shaking method may have the same risk as the stirrer method. (Hermann et al., 2003) The output of the research presented in this thesis shows several nove mlixing principles, which provide good mixing within a microbioreactor.

In chapter 2 the recycle flow method was presented. (Li et al., 2008a) Based on the experimental results and the further numerical analysis (MatLab) the mixing behavior in a 30  $\mu$ l microreactor was proved to be comparable with an ideal CSTR. Moreover, since the oxygen supply for microbial cultivations at high biomass concentration is the remaining challenge in miniaturized bioreactor system, the oxygen transfer ability of the recycle mixing method was studies via CFD simulations. The impact of various oxygen transfer abilities on high cell density fermentation was estimated by CFD simulations. With linear flow rate 0.001m/s, volume flow rate around 30  $\mu$ l/min in a recycle channel, the  $k_1$  a value is around 0.023 s<sup>-1</sup>, which is in the same order of magnitude as the  $k_1$  a value of a regular stirred tank (van 't Riet and Tramper, 1991). With recycle flow rate 30  $\mu$ l/min, the oxygen supply is enough for maintaining cells concentration up to 20 g/l. The oxygen transfer ability and the mixing performance can be further improved by increasing the recycle

flow rate or reducing the length of recycle tubes. In order to do so, it requires a stronger and smaller recycle micro pump. The recent development on the micro-pumping technology was briefly reviewed in Chapter 2, the current micro-pump technology is not suitable to be integrated with the recycle channel or it is difficult to be parallelized to multi- reactors. The usage of PZT pumping technology remains the best option for parallelization and the small scale integration, but the strength and stability of the small PZT pump is doubtful, and further investigation is necessary.

It is shown in chapter 3 that by applying a varying pressure to a microchannel looping tangentially into a cylindrical microreactor an oscillating fluid flow was shown to occur. Such an oscillating fluid flow improved mixing, both by diffusion and convection. (Li et al., 2008b) From CFD simulation as well as experimental results, rapid mixing was observed. With an oscillation frequency of 8.33Hz, mixing time in a 30 µl cylindrical microreactor was less than 45 second. Based on CFD simulations that under same frequency but stronger oscillation (linear flow rate 0.06 m/s), the well mixing time can be further reduced to less than 10 s. This mixing method can be applied for larger reactor volume up to hundreds microliter, experiments were carried out within a cell of a 96-well titer plate. Compare with the use of the stirrer, the mechanical stress of this method is much less, and hardly any cell damage (S. cerevisae) was observed after over night mixing. Instead of using multiple micropumps, parallelization of the micro-mixing method was successfully realized by using one central actuator to create oscillation flows for three independent wells with liquid volume 150 µl. The bottleneck of this mixing method is the existence of dead-zone area(s). CFD simulations can indicate the exact position of the dead-zone area(s), Based on such information, the problem can be solved by optimizing the shape of the microreactor or increasing the complexity of the fluid flows in the reactor.

# In-situ product removal

In practice, high cell density fermentations usually have limited performance, which is normally due to product inhibition causing a decrease in microorganism activity, or product degradation resulting in low yield. Keeping the dissolved product concentration low in the reactor can obviously circumvent these limitations. An approach that can accomplish this task is

the implementation of an in situ product recovery/removal (ISPR) technique. (Baque-Taboada, et. al., 2004; Woodley, et. al., 2008)

In chapter 4 the mass transfer of glucose in a microchannel was investigated. This idea is interesting because it can simultaneously add the substrate to and extract the product from the microbioreactor. The mass transfer in the microchannel is by diffusion. Because of the large diffusivity difference between the micro-organism and small molecules like glucose, cells can easily be retained in the microbioreactor but smaller molecules can diffuse out (in). With a pumping flow rate of several microliters per minutes, the glucose can be quantitatively induced into a microbioreactor of working volume 100  $\mu$ l, the transfer rate ranging from 0.26 to 1.3 g glucose L  $_{\rm reactor}^{-1}h^{-1}$  could be achieved. A recycle micropump was needed to accurately recycle the fermentation broth from the reactor through the microchannel and back into reactor again. Once such a micropump is available, it can be used to test the glucose feeding strategy for cell cultivation in microbioreactor.

A study of ISPR in microbioreactor is described in chapter 5. The ISPR system is based on hollow fiber liquid/liquid micro solvent extraction. Lactic acid was taken as a model inhibitor in mammalian cell culture. Extraction experiments by using a hydrophilic micro hollow fiber were carried out to remove lactic acid. The selected organic phase (minimum toxicity) was transported through the hollow fiber and lactic acid was extracted into the organic phase and was taken away from the reaction system. The high specific interfacial area (13.3 \*10<sup>3</sup> m<sup>2</sup>/m<sup>3</sup>) in the micro ISPR system ensure the high mass-transfer rates (1.92e-6 mol l<sup>-1</sup> s<sup>-1</sup>) of the lactic acid at the critical lactic acid concentration of 10 mM. The lactic acid removal rate is in the same order of magnitude as the reported lactic acid production rate. The work presented in chapter 5 shows great possibility of implementing ISPR method with a microbioreactor. The validity of this idea needs yet to be experimentally demonstrated by including microorganism growth system into reactor. Since the hollow fiber has the sole task of ensuring that the interaction between the microorganism and organic solution is minimized. To further improve the extraction ability, a different organic mixture with a larger toxicity can be tested within a relevant system. Besides that, it will thus be interesting to test different types of hydrophilic membranes with stronger structure and better flux transfer ability, like zeolite membrane, for the work presented in chapter 5.

The results from chapter 4 and chapter 5 show the potential of integrating ISPR method with a microbioreactor. Extraction methods including liquid-liquid extraction and liquid-liquid membrane solvent extraction were tested experimentally. The advantages of a miniaturized ISPR device, such as the short molecular diffusion distance, the large specific interfacial area relative to its volume, the possibility to handle multiphase flows, have been clearly shown from the presented results. Besides the extraction method, other separation methods, like, chromatography, crystallization and adsorption may also be beneficial from those advantages, thus, further development on ISPR for micro-scale applications will be interesting in the research field.

#### Reference

- Buque-Taboada, E. M., A. J. J. Straathof, J. J. Heijnen and L. A. M. van der Wielen, 2004, In situ product removal using a crystallization loop in the asymmetric reduction of 4-oxoisophorone by Saccharomyces cerevisiae, Biotechnology and Bioengineering, 86, 795-800
- Hermann, R., M. Lehmann and J. Büchs, (2003) Characterization of gas-liquid mass transfer phenomena in microtiter plates, Biotechnology and bioengineering, 81 (2) 178-186
- Kostov, Y., Peter Harms, Lisa Randers-Eichhorn and Govind Rao, (2001) Low-Cost Microbioreactor for High-Throughput Bioprocessing, Biotechnology and Bioengineering, 72 (3) 346-352
- Krommenhoek, Erik, (2007), Integrated electrochemical sensor array for on-line monitoring micro bioreactors, PhD thesis University Twente
- Li, X, G. van der Steen, G.W.K. van Dedem, L.A.M. van der Wielen, M. van Leeuwen, W.M. van Gulik, J.J. Heijnen, E.E. Krommenhoek, J.G.E. Gardeniers, A. van den Berg and M. Ottens, (2008a), Improving mixing in micro bioreactors, accepted for Chem Eng. Sci. doi:10.1016/j.ces.2008.02.036
- Li, X., L.A.M. van der Wielen, G. van der Steen, G.W.K. van Dedem, van M. Leeuwen, W.M. van Gulik, J.J. Heijnen, J.G.E. Gardeniers, E.E. Krommenhoek, A. van den Berg,, M. Ottens, (2008b). The application of direct oscillations to improve mixing in micro bioreactors, AICHE, submitted for publication
- Micheletti, M. and G.J. Lye, (2006) Microscale bioprocess optimization Curr. Opin. Biotech. 17 (6) 611-618
- Van't Riet, K, Tramper, J., (1991), Basic Bioreactor Design, 254
- Van Leeuwen, M. (2008) Development of a bioreactor with integrated on-line sensing for batch and fed-batch cultivation on a  $100\mu l$ -scale, Ph.D. Thesis, Technical University Delft
- Woodley, John M; Bisschops, Marc; Straathof, Adrie J J; Ottens, Marcel, (2008) Future directions for in-situ product removal (ISPR), J. of chemical technology and

biotechnology, 83 (2) 121-123

Zhang, Z., N. Szita, P. Boccazzi, A. J. Sinskey and K.F. Jensen, (2003) Monitoring and control of cell growth in fed-batch microbioreactors, 7TH International Conference on Miniaturized Chemical and Biochemical Analysis Systems, California, USA

## **Summary**

Of the thesis: 'Mixing and In-situ product removal in micro bioreactors' by Xiaonan Li

The work presented in this thesis is a part of a large cluster project, which was formed between DSM, Organon, Applikon and two university groups (TU Delft and University of Twente), under the ACTS and IBOS program. The aim of this cluster project was to develop a system consisting of parallel bioreactors of 30 to 200  $\mu l$  working volume for the cultivation of micro-organisms under well controlled industrially relevant condition (T, pH, DO etc.), and operated as fed-batch reactor in long term (>200h). This platform has the potential to be used for high throughput screening applications for gene identification or the related small scale protein fermentation to increase the protein production process development rate and to reduce the research cost.

The development of the platform starts with the design of a single micro-reactor; the single micro-reactor is the integration of well developed sensing system, control system, mixing system and other accessories, like, pumps, valves, adaptors, vessels etc. However many components are not available or not suitable for our application. In this thesis several novel mixing methods, which can provide sufficient mixing in a micro-reactor to satisfy the need of micro-organism fermentation, are developed. Furthermore, microfluidic components are important to facilitate substrate feeding as well as by product removing. An ISPR concept was experimentally demonstrated in this thesis to distinguish a wider scope of micro-reactor applications.

One of the main reasons to apply micro systems technology is that compared with traditional reaction (fermentation) technologies, a superior, rapid and sufficient mixing can easily be achieved using micro technologies, especially for those microfluidic devices, which integrated with passive micro structures, with working volume tens of nanoliters. However, the mixing in the microreactor, which with working volme around hundreds microliter, is still be considered as a bottleneck for the high biomass concentration fermentation. In chapter 2, recycle flow mixing (RFM) method was presented. By continuously moving liquid solution from high oxygen concentration area to low oxygen concentration area via multiple fluxes, the system obtains maximum oxygen transfer, which is considered as the bottleneck for high cell density fermentation. Meanwhile, the recycled flows create vigorous convection

in the micro-reactor and obtain good mixing. The mixing performance was experimentally verified with a prototype reactor (with working volume 30  $\mu$ l). Under a small recycle flow rate (20 $\mu$ l min<sup>-1</sup>), the measured well mixing time was around 800s. However, after taken into account the influence of the recycle tubes (50 $\mu$ l), the mixing in the microreactor was considered as comparable as an ideal mixed reactor. The impact of various oxygen transfer abilities on high cell density fermentation was estimated by 2D / 3D CFD simulations. With recycle flow rate 0.001m s<sup>-1</sup>, the k<sub>1</sub>a value of the microreactor was around 0.023 s<sup>-1</sup>, which was in the same order of magnitude as a regular stirred tank. This oxygen transfer was sufficient for a high biomass concentration fermentation (Max. biomass concentration > 20g l<sup>-1</sup>). The mixing performance of RFM method is dependent on the value of the recycle fluxes, therefore, a strong internal micro-pump plays an essential role in the system.

To avoid the dependence on the micro-pump development, an alternative micro-mixing method was presented in chapter 3. Oscillation flows, which are created by a central actuator, induce vigorous convection in the micro-reactor(s) to obtain good mixing. The mixing performance within a single reactor was estimated by CFD calculations, a simplified micro-mixing correlation and validated experimentally. With an oscillation frequency (f) of 8.33 Hz, oscillation flow rate ( $\phi_v$ ) 1000  $\mu$ l min<sup>-1</sup>, the experimental well mixing time was 45s; the CFD simulated well mixing time was 37 s; the model calculated well mixing time was 35s. With a stronger oscillation (f=8.33Hz,  $\phi_v$ =3000  $\mu$ l min<sup>-1</sup>) the well mixing time dropped to 4s.(CFD simulated result & model correlative result)

The oscillation mixing method has the potential to be easily integrated with parallel reactors rrelative This concept has been proven experimentally using a 96-wells micro titer plate and one oscillation pump (f=2.22 Hz,  $\phi_v$ =2000 $\mu$ l min<sup>-1</sup>). Three parallel reactors followed the same trend and reached to well mixing time at 120s, 122s and 128s, respectively. The comparison of dye distribution results between various tubes indicated a similar mixing behavior in different reactors. Hence, the result show the possibility of using one central actuator to create oscillation fluids to achieve mixing on multi-reactors.

Additional experiments have been done with oscillation mixing method to test the influence of the mixing methods on cells viability and influence of the oscillation mixing method on cells suspension. The experiment clearly indicated that compared to the magnetic stirrer mixing method, oscillation mixing method showed less damage on the cells during cell viability test. Homogeneous cell suspension was maintained in the micro bioreactor during overnight oscillation mixing.

The characteristics of microfluidic channels for mass transfer were explored in chapter 4. When two liquid streams join into one microchannel with diameter around 150 µm, both streams will behave as laminar flows and run parallel to each other with a stable interface in between. If for certain components there are concentration differences between two streams, over the interface, components can transfer from one stream to another via diffusion. In this chapter the quantitative transfer of glucose between two cocurrent streams was estimated by CFD and experimentally verified. A microchannel has a large surface to volume ratio; therefore, within a short time significant amount of glucose can be transferred from one stream to another. The transfer rate of glucose was measured to be 2.4 - 11.9 nmol min<sup>-1</sup> at a residence time of 54 - 857ms and glucose concentration in the feed stream of a modest 10.4mM. If this transfer would be applied for a fed-batch cultivations in a 100µl microbioreactor, glucose feed rates ranging from 0.26 to 1.3 g L<sub>reactor</sub>-¹h-¹ could be achieved, which is sufficient to perform industrial fermentation processes of fed-batch cultivations at high biomass concentrations. This microfluidic channel also could be used for by-product removal application.

The reason by-product needs to be removed is because of the potential risk of the product inhibition, which may cause a decrease in microorganism activity. An implementaed In Situ Product Removal (ISPR) method can circumvent this risk by keeping the dissolved product concentration low in the reactor. Chapter 5 focuses on demonstrating the feasibility of applying a suitable ISPR method on micro-scale bioreactor. Lactic acid was selected as the target chemical. Extraction was selected as the separation method. By pushing a selected extractant (trioctylamine / decanol / dodecane) through a hydrophobic micro hollow fiber, lactic acid is extracted from the aqueous phase into organic phase, and then removed from the microreactor. The micro hollow fiber has the sole task to be the barrier to isolate microorganism from organic phase. The extraction ability was estimated by a model and then validated experimentally. The high specific interfacial area in the micro ISPR system (13.3×10³ m² m³) shows the advantage of the microextraction for ISPR processes. High ISPR removal rate (1.92e-6 mol l⁻¹ s⁻¹) was obtained

experimentally. This removal rate was in the same order of magnitude as the reported lactic acid production rates in mammalian cell cultures (7.09e-7 to  $3.7 \text{ e-5 mol } 1^{-1} \text{ s}^{-1}$ ).

In conclusion, this thesis presents the development of novel micro-mixing methods and the preliminary application of possible In Situ Production Removal (ISPR) methods, leading to the increased applicability of (fed-) batch micro bioreactor for long-term high-biomass concentration fermentation. However, a combined microbioreactor (including sensor, ISPR design and novel mixing design) has yet not been tested experimentally. A number of present challenges is discussed in Chapter 6.

## Samenvatting

Proefschrift Xiaonan Li 'Mengen en In-situ productverwijdering in microbioreactoren'

Het onderzoek van dit proefschrift is een onderdeel van een groot cluster project onder het ACTS en IBOS programma in samenwerking van de volgende bedrijven en universiteiten: DSM, Organon, Applikon, Technische Universiteit Delft en Universiteit Twente. Het doel van dit cluster project is het ontwikkelen van een High Throughput Screening (HTS) systeem bestaande uit parallelle 30 tot 200 µl fed-batch bioreactoren ter cultivering van micro-organismen onder goed controleerbare industrieel relevante condities (T, pH, DO etc.), onder langdurige fermentaties (>200h). Dit platform biedt daarmee de mogelijkheid voor snelle en gecontroleerde screening van zowel operatiecondities als type micro-organismen met het oog op het versnellen van de ontwikkeling van een industrieel fermentatieproces en daarmee het reduceren van de onderzoekskosten. Eveneens kan het platform worden gebruikt voor gen identificatie of voor gerelateerde kleinschalig fermentatieve eiwit productie.

Het startpunt van de ontwikkeling van dit platform begint met het ontwerp van een enkelvoudige microbioreactor; deze enkelvoudige microbioreactor is een integratie van een sensor systeem, controle systeem, meng systeem en andere onderdelen zoals, pompen, kleppen, aansluitingen, vaten etc. De meeste van deze componenten zijn echter niet beschikbaar of geschikt voor de hierboven beschreven toepassing. In dit proefschrift worden er een aantal nieuwe mengmethoden beschreven welke wél voldoende menging in een micro-bioreactor genereert. Daarnaast zijn microfluïde kanalen nodig voor substraat toevoeging, pH regulatie en tevens verwijdering van bijproduct. Een In-Situ Product Removal (ISPR) concept is experimenteel getest en beschreven in dit proefschrift en is inzetbaar in een breder toepassingsgebied van microbioreactor applicaties.

Eén van de voornaamste redenen voor toepassing van Micro Systeem Technologie (MST) is dat, in vergelijking met traditionele reactie (fermentatie) technologie, MST gemakkelijk en snel voldoende menging genereert , met name in de microfluïde apparaten die gebruik maken van passieve micro meng structuren, met een volume van tientallen nanoliters. Echter, de menging in microreactoren met een volume van enkele honderden microliters, blijft

tot op de dag van vandaag problematisch voor hoge biomassa concentratie fermentaties. In hoofdstuk 2 wordt de Recycle Flow Mixing (RFM) methode geïntroduceerd. Door de continue beweging van vloeistof vanuit het hoge zuurstof concentratie gebied naar lage zuurstof concentratie gebied via meervoudige microfluïde stromingskanalen, wordt een maximale zuurstofoverdracht bereikt, wat normaal gesproken het grote probleem is bij hoge biomassa concentratie fermentaties. De gerecirculeerde stromingen veroorzaken een sterke convectie in de microreactor en daarmee een goede menging. De menging is experimenteel getoetst met een 30 µl prototype microreactor. Met een kleine recirculatiestroom (20 µl min-1) is een mengtijd gerealiseerd van circa 800 s. Echter, na verdiscontering van de invloed van de recirculeerleidingen (50 µl), blijkt de menging in de microreactor als een ideaal gemengd beschouwd te kunnen worden. De invloed van de zuurstofoverdrachtsnelheid op hoge cel concentratie fermentatie is onderzocht via 2D / 3D CFD simulaties. Met een recirculeerstroomsnelheid van 1 mm s<sup>-1</sup>, was de kla waarde in de microreactor rond de 0.023 s<sup>-1</sup>, wat in dezelfde orde van grootte is als in een regulier gemengde reactor. Deze zuurstofoverdracht is voldoende voor een hoge biomassa concentratie fermentatie (max. biomassa concentratie > 20g/l). De menging die met behulp van de RFM methode kan worden gerealiseerd is afhankelijk van de snelheid en het moment van de gecirculeerde stroming. Een sterke interne micropomp is essentieel in dit type menging.

Om de afhankelijkheid van de micropompontwikkeling te vermijden, is een alternatieve micromengmethode gepresenteerd in hoofdstuk 3. Oscillatie stromingen, gecreëerd door een centrale aandrijving, induceren sterke convectie in de microreactor(en) en daarmee een goede menging. De menging in een enkele microreactor is berekend met CFD simulaties, een vereenvoudigde micromeng correlatie en experimenteel gevalideerd. Met een oscillatiefrequentie (f) van 8.33Hz, en een oscillatiedebiet ( $\phi_v$ ) van 1000  $\mu$ l min<sup>-1</sup>, wordt een experimentele mengtijd verkregen van 45 s; een CFD mengtijd van 37 s; 35 s via een vereenvoudigde correlatie. Met een sterkere oscillatie (f=8.33Hz,  $\phi_v$ =3000  $\mu$ l min<sup>-1</sup>) daalt de mengtijd naar 4s (CFD en correlatie).

De oscillatiemengmethode bezit de mogelijkheid om vrij eenvoudig geïntegreerd te worden in parallelle microreactoren. Dit concept is experimenteel bewezen in een micro titer 96-well plate en één oscillatiepomp (f = 2.22 Hz,  $\phi_v$  = 2000  $\mu$ l min<sup>-1</sup>). Drie parallelle microreactoren geven dezelfde

trend en hebben een mengtijd van respectievelijk 120s, 122s en 128s. De vergelijking van de kleurstofdistributie resultaten tussen de verschillende leidingen duidt op een gelijk menggedrag in de verschillende reactoren. De resultaten tonen hiermee de mogelijkheid aan van het gebruik van één centrale aandrijving om oscillatie stromen te genereren voor het mengen in reeks van meerdere microreactoren.

Additionele experimenten zijn uitgevoerd met de oscillatiemengmethode om de invloeden van de mengmethoden te testen op de levensvatbaarheid van de cellen en de invloed van de oscillatiemengmethode op de suspendeerbaarheid van de cellen. Experimenteel wordt duidelijk aangetoond, dat in vergelijking tot de magnetische roerstaaf mengmethode, de oscillatiemengmethode aanzienlijk minder schade aanbrengt aan de cellen. Een homogene celsuspensie is gedurende een nacht in stand gehouden in de microbioreactor tijdens oscillatie menging.

De karakteristieken van de microfluïde kanalen voor massa overdracht zijn verder onderzocht in hoofdstuk 4. Wanneer er twee vloeibare stromen samenkomen in een microkanaal met een diameter van circa 150 µm, zullen beide stromen een gedrag vertonen zoals een gelaagde stroom en zullen parallel naast elkaar stromen met een stabiele grenslaag ertussen. Bepaalde componenten hebben een concentratieverschil in deze twee stromen, zodat componenten overdragen worden van de ene stroom naar een andere via diffusie over de grenslaag. In dit hoofdstuk is de kwantitatieve overdracht van glucose tussen de twee gelijktijdige stromen berekend met CFD en experimenteel geverifieerd. Een microkanaal heeft een grote oppervlakte tot volume ratio, daarom zal binnen korte tijd een significante hoeveelheid glucose overdragen worden van de ene stroom naar de andere. De overdracht van glucose is gemeten op 2.4 - 11.9 nmol min<sup>-1</sup> bij een verblijftijd van 54 - 857 ms en een glucose concentratie in de toevoerstroom van 10.4 mM. Wanneer deze vorm van massatransport wordt toegepast voor fed-batch fermentatie in een 100  $\mu$ l micro bioreactor, kan een glucose toevoer van 0.26 tot 1.3 g  $L_{reactor}^{-1}$ h-1 bereikt worden, wat normaliter voldoende is om een industriële hoge biomassa concentratie fed-batch fermentatie uit te voeren. Dit microfluïde kanaal kan eveneens gebruikt worden voor selectieve productverwijdering.

De reden waarom bijproducten verwijderd moet worden is omdat ze een potentieel risico van productinhibitie vormen, met als gevolg een afname in micro-organisme activiteit. Een toegepaste ISPR methode kan dit risico vermijden door de productconcentratie laag te houden in de reactor. Hoofdstuk 5 beschrijft de implementatie van een geschikte ISPR methode in een microbioreactor. Melkzuur is geselecteerd als bijproduct met inhibitieeigenschappen. Extractie is gekozen als scheidingsmethode. Via doorvoering van een geselecteerde extractant (trioctylamine / decanol / dodecane) door een hydrofobe hol micromembraan, wordt melkzuur geëxtraheerd uit de water fase naar de organische fase, en daarmee verwijderd uit de microbioreactor. De holle microvezel dient ter isolatie van de micro-organismen van de organische fase. The extractiecapaciteit is berekend via een model en daarna experimenteel gevalideerd. Het hoge specifieke grensvlakoppervlak in het micro ISPR systeem (13.3×10<sup>3</sup> m<sup>2</sup> m<sup>-3</sup>) toont het voordeel van micro-extractie voor ISPR processen. Hoge ISPR verwijderingsnelheden (1.92e-6 mol l<sup>-1</sup> s<sup>-1</sup>) zijn experimenteel verkregen. Deze verwijderingsnelheden zijn van dezelfde ordegrootte als de melkzuur productiesnelheid in dierlijke celkweek (7.09e-7 to 3.7 e-5 mol l<sup>-1</sup> s<sup>-1</sup>).

De conclusie van dit proefschrift is dat de ontwikkeling van nieuwe micromengmethoden en mogelijke In Situ Production Removal (ISPR) methodes, heeft geleid tot een verbeterd concept voor een (fed-) batch microbioreactor platform voor langdurige hoge biomassa concentratie fermentaties en realisatie van een geïntegreerd microbioreactor platform dichterbij heeft gebracht. Echter, een gecombineerde microbioreactor (inclusief geïntegreerde sensor, ISPR en een van de nieuwe micromengmethodes) is vooralsnog niet experimenteel getest. Het proefschrift sluit af met een overzicht van de resterende uitdagingen voor daadwerkelijke implementatie tot een werkend microbioreactor platform in hoofdstuk 6.

#### Curriculum Vitae

Xiaonan Li was born on Oct. 31st, 1977 in BeiJing, The People's Republic of China. From 1991 to 1996 he attended the HuiWen Middle School in BeiJing, P. R. China. After completing secondary school, he did his undergraduate study at the Peking Univeristy, where he majored in Applied Chemistry and graduated with a B.Sc. degree in 2000. In Sept. 2000, he enrolled in the international Master of Science Program in Chemcial Engineering department with a specialization in Biotechnology from Deflt University of Technology (TU Delft), The Netherlands. In 2002, he obtained his M.Sc. degree in chemical engineering. He carried out his graduation project 'Modeling of the Crystallization of 6-Aminopencillanic acid' in the Bioseparation Technology (BST) group, Department of Biotechnology, TU Delft, under the supervision of Prof. Luuk van der Wielen. In september 2002, he joined the Designer in Bioprocess Engineering program, at TU Delft, The Netherlands. His final project was carried out at BST group, TU Delft, where he worked on the 'Designing and optimizing a mixing method for micro-bioreacor'. This project was supervised by Prof. Luuk van der Wielen and Dr. Marcel Ottens. He continued this research further for a PhD project (2004-2008), the results of which are presented in this thesis.

## List of Publications

Xiaonan.Li, L. A. M. van der Wielen, E.E. Krommenhoek, M. van Leeuwen, W.M. van Gulik, J.G.E. Gardeniers, J. J. Heijnen, A. van den Berg, Marcel Ottens (2008) *Application of direct fluid flow oscillations to improve mixing in micro bioreactors*, Accepted for publication in AICHE J.

Xiaonan.Li, L. A. M. van der Wielen, M. van Leeuwen, G. van der Steen, G.W.K. van Dedem, W.M. van Gulik, J.J. Heijnen, E.E. Krommenhoek, J.G.E. Gardeniers, A. van den Berg, Marcel Ottens (2008) *The use of recycle flows to improve mixing in micro bioreactors*, Chem. Eng. Sci. 3036-3046

M. van Leeuwen, Xiaonan.Li, E.E. Krommenhoek, W.M. van Gulik, J.G.E Gardeniers, M. Ottens, L. A. M. van der Wielen, J. J. Heijnen (2008) *Glucose feeding via micro hollow fiber*, Submitted for publication Biotechnology progress

Xiaonan.Li, Marcel Ottens, L. A. M. van der Wielen, G. van der Steen, G. W. K. van Dedem, M. van Leeuwen, W. M. van Gulik, J. J. Heijnen, J. G. E. Gardeniers, (2008) Microextraction for Lactic acid in micro-bioreactor, Submitted for publication

Juliana S. Ferreora. Adrie J. J. Straathof, Xiaonan Li, Marcel Ottens, Telma T. Franco, and Luuk A. M. van der Wielen, (2006), Solution Crystallization Kinetics of 6-Aminopenicillanic Acid, Ind. Eng. Chem. Res. Vol. 45, 6740-6744

Krommenhoek EE, Van Leeuwen M, Gardeniers JGE, Van Gulik WM, Van den Berg A, Li Xiaonan, Ottens M, Van der Wielen LAM and Heijnen JJ., (2007) Lab-scale fermentation tests of micro chip with integrated electrochemical sensors for pH, Temperature, dissolved oxygen concentration and viable biomass concentration. Biotechnol Bioeng 99 (4) 884-892

Krommenhoek EE, Gardeniers JGE, Bomer JG, Li X, Ottens M, Van der Wielen LAM, Van dedem GWK, Van Leeuwen M, Van Gulik WM, Heijnen JJ and Van den Berg A (2006) Monitoring of yeast cell concentration using a micromachined impedance sensor, Sens Actuators B Chem., 115 (1) 384-389

Krommenhoek EE, Gardeniers JGE, Bomer JG, Li X, Ottens M, Van der Wielen LAM, Van dedem GWK, Van Leeuwen M, Van Gulik WM, Heijnen JJ and Van den Berg A (2007) Integrated electrochemical sensor array for online monitoring of yeast fermentations, Anal. Chem., 79 (115) 5567-5573

#### POSTER PRESENTATIONS

Xiaonan Li, Marcel Ottens, Luuk van der Wielen, Design micro bioreactor mixing for biocatalyst screening in industrial fermentation, Presented at NPS-4 conference, Veldhoven, The Netherlands 2004

Xiaonan Li, Marcel Ottens, Luuk van der Wielen, Design and optimizing a novel mixing method for micro bioreactor, IBOS-2-Conference, Nunspeet, The Netherlands 2004

Xiaonan Li, Marcel Ottens, Luuk van der Wielen, Oscillation mixing study in the micro-bioreactor for biocatalyst screeening in industrial fermentation, Presented at AICHE 2005-Conference, Cincinnati, USA, 2005

Xiaonan Li, Marcel Ottens, Luuk van der Wielen, Micro bioreactor direct oscillation mixing for biocatalyst screening in industrial fermentation, Presented at NCCC VII, Leiden, The Netherlands, 2006

Xiaonan Li, Marcel Ottens, Luuk van der Wielen, Recycle flow mixing in micro-bioreactor. Presented at IBOS-4-Conference, Nunspeed, The Netherlands 2006 and Kluyver Center Symposium, Delft, The Netherlands, 2006

Xiaonan Li, Marcel Ottens, Luuk van der Wielen, Lactic acid in-situ product recovery (ISPR) in micro-bioreactor. Presented at IBOS-5-Conference, Nunspeed, The Netherlands 2007 and Kluyver Center Symposium, Delft, The Netherlands, 2007

#### ORAL PRESENTATIONS

Optimizing micro bioreactors mixing for biocatalyst screening in industrial fermentations Presented at NPS-5, Veldhoven, The Netherlands, 2005

Investigation on micromixing methods for micro-bioreactor platform, Presented at IBOS-3, Nunspeet, The Netherlands, 2005

Optimizing mixing in micro bioreactors for biocatalyst screening in industrial fermentations. Presented at NPS-6 Veldhoven, The Netherlands, 2006

Investigation lactic acid in-situ product recovery (ISPR) in micro-bioreactor, Presented at IBOS-5, Nunspeet, the Netherlands, 2007

# Acknowledgements

This research thesis compiles the results of a 4-years period of intense and challenging work. Many people have made their contribution (intellectual or / and emotional) to push toward the completion of this work. To all of them I am deeply and sincerely indebted.

My thank first goes to my promotor Prof. Luuk van der Wielen. I thank you Luuk for allowing me to work in this project freely, for giving the room for discussions, for all the opportunities you have offered me since I was a M.Sc. student and also for all the guidance, critical review, encouragement, feedback and so on towards completion of the thesis.

Next, I would like to acknowledge Dr. Marcel Ottens for the enormous amount of time you spent with me for daily supervision, guidance, critical thoughts, revision of manuscripts and all other things. Many chapters in this thesis would be less readable and less structured, were it not the effort of you. Many thanks Marcel for your suggestions while I was in the midst of a PhD quest. Having virtually unlimited and enlightening discussions with you helped me a lot in drawing up a better and challenging concept and in finalizing the contents of this thesis.

My gratitude is extended to all the industial partners. (Henk, Joep, Arthur, Jaap, Jan and Teun) for your continuous interest in the project and valuable discussions, comments, reviews, suggestions during the regular project meetings.

I also would like to express my thanks to the people from two other university groups, who also involved in this 'fed-batch on a chip' project, Prof. Han Gardeniers and Dr. Erik Krommenhoek from Twente university, Prof. Sef Hijnen, Prof. Gijs van Dedem, Dr. Walter van Gulik and Dr. Michiel van Leeuwen from TU Delft. I thank Michiel and Eric in particular for all the numerous instant discussions, brainstorming, exchange of ideas, sharing results and many other things.

Many helping hands have contributed to the experimental results presented in this thesis. Gert, thanks for the help on the electro-osmotic flow's set-up and measurement, although the result have not been included in this thesis. Stef,

thanks for the image analysis work and suggestion on dye selection, which were very important for chapter 2 and chapter 3. Max, thanks for your help with many analyses. Cor and Angie, thanks for your support with the HPLC measurement. Michiel and Dirk, thanks for your assistance for the Labview interface for recycle flow mixing experiments. Special thanks go to Joop and Arno van de Berg, for helping me design and make the first micro-reactor. Many thanks also go to all members of the workshop, thank you for your assistance, your work is the foundation of all my experiments.

Less scientifically related but not less important are the supporting services in the Kluyver lab. I would like to thank in particular Sjaark, Jos, Herman, Ginie, Wim, Robbert, Hans and Marcel, and also to our group secretaries, first Carla and later on Kawieta. Special thanks go also for Lies and Ger for all the help during TwAIO years and after that.

I would like to express my thanks to all my BST colleagues for their companion, coffee break discussions, scientific criticism, common quest for knowledge and fun. Special thanks go to those fellows, with whom I shared the room during all these years: Liang Wu, Hilal Taymaz, Frederik Aboka, Mervin, Pim, Martijn, Danielle, Evelyn, Marija, Arjen, Marjana, Maria, Esteban Freydell, Kedar, Tangir, Beckley, Cagri Efe, Arjan, Nahid, Carol, David, Adrie and Rob. These thanks are extended to the past and present BPT colleagues: Michiel, Zhen, Zheng, Andre, Sergio, Emrah, Penia, Roeland, Mlawule and Uly. It was indeed fun working with you.

I thank in particular Liang, Wenqian, Cagri, Esteban, Tony Zhou, Boudewijn and Zheng Zhao for the unlimited support, the encourangement, the smiles, motivations, and of course the great food and parties. Thank you. I was very lucky have you friends around. My thanks also to other friends: Song bo and Jan, Ling Lou, Edwin, Xue Qin, Susana, Tuan, Alfeno, Jun Yang, Beatrix, Yana and the list goes on, who made my life in Delft lively and enjoyable.

To Meily, ZhongXian, Rosman and Xujie thank you for all the support and interest during all these years, but especially *bedankt voor de gezelligheid*. I would like to express my gratefulness to Wei Siauw, my sister. Thanks to Weiwei and Jordi for helping me to translate the summary of this thesis into Dutch. I could not articulate how grateful I am to have you around anytime all the time. I can always count on you all, your presence and love have always

reminded me of how good life can be. Thank you so much for taking care of me all these years in the Netherlands.

Deep in my heart I thank my parents for their everyday support and trust in me. Lao ba, Lao ma, I learned the most valuable lesson from you: be responsible and work hard. I am fully indebted for all your blessings and tender care during the last three decades. Next I would like to thank my girlfriend, Shengbin Ma, for your support and understanding, for the days we have spend and will spend in our life.

Xiaonan Li Utrecht, Feb. 2009

